CRYSTAL STRUCTURE AND DEFECTS OF β-ALUMINA-RELATED HEXAGONAL ALUMINATES

（β－アルミナ関連六方晶アルミン酸化合物の
結晶構造と欠陥）

Nobuo IYI

（井伊伸夫）

1986

CONTENTS

ABBREVIATIONS

A	Angstrom.
APB	Anti-phase boundary.
B	Isotropic temperature factor.
$B_{eq.}$	Equivalent temperature factor.
CBED	Convergent beam electron diffraction.
E.s.d.	Estimated standard deviation.
$F_{c.}$	Calculated structure factor.
$F_{o.}$	Observed structure factor.
FZ	Floating zone.
I.T.	International Tables for X-Ray Crystallography.
NIRIM	National Institute for Research in Inorganic Materials.
SCFZ	Slow cooling floating zone.

BR	Beevers-Ross.
aBR	anti-Beevers-Ross.
mO	mid-Oxygen.

$$R = \Sigma||F_o| - |F_c|| \,/\, \Sigma|F_o|$$

$$wR = (\Sigma w(\Sigma|F_o| - |F_c|)^2 / \Sigma w|F_o|^2)^{1/2}.$$

$MoK\alpha$ = 0.71069 A.

1. GENERAL INTRODUCTION

In the present thesis, the crystal structure and defect nature of the hexagonal aluminates having a beta-alumina, magnetoplumbite, or related layer stucture are discussed mainly using X-ray single crystal data. "Hexaaluminates" has been commonly referred to as these kinds of hexagonal aluminates, so this term is used throughout this thesis only for convenience sake. Fig 1-1 depicts the arrangement of the atoms of beta-alumina and magnetoplumbite in a plane perpendicular to the a-axis. Beta-alumina and magnetoplumbite structures resemble each other. They consist of "spinel blocks" and "intermediate layers" stacking alternately to form a kind of layer structure as shown in the figure. Spinel blocks are composed of Al and O ions and have the same atomic arrangement as the spinel. Large cations are usually accommodated in the more spacious intermediate layer having a mirror plane symmetry. Hereafter we refer to it as "mirror plane." The major difference between structure types in the hexaaluminates is found in the mirror plane as depicted in Fig.1-2. In a magnetoplumbite structure, the mirror plane of a single unit cell contains a large cation, an Al ion, and three oxygen ions; in a beta-alumina structure, it contains only a large cation and an oxygen ion. As yet, several aluminates containing mono-, di- and trivalent cations have been reported to have beta-alumina or related layer structures. The hexa-aluminate containing monovalent Na ion is of a beta-alumina type and well-known as a prominent ionic conductor. Large divalent cations such as Ca and Sr are incorporated into hexaaluminates giving a magnetoplumbite structure with the general formula $MAl_{12}O_{19}$(M=large cation)(Kato & Saalfeld, 1968; Lindop et al., 1975).

Up to now, many investigations have been focused on the structure and nonstoichiometry of the beta-alumina compounds containing monovalent cation, such as Na, K, and Ag. The ionic conduction mechanism has been also discussed for these compounds due to the extreme mobility of the monovalent cations in the mirror plane. Beta-aluminas are usually expressed as $MAl_{11}O_{17}$ (where M=monovalent cation), but the mirror plane almost always accommodates more monovalent cations than unity per chemical formula. In reality, beta-aluminas are massively defective, and better expressed as "$M_{1+x}Al_{11.0}O_{17.0+x/2}$" with x-parameter indicating the amount of excess cations. It is known that x usually takes the value around 0.3 for the crystals grown by cooling the melt. The mechanism of accommodating excess cations in the mirror plane was revealed by Reidinger(1979), who showed the existence of unique defects which compensate extra positive charge owing to the excess cations. According to this mechanism, a pair of interstitial Al ions which migrated from spinel blocks by the Frenkel defect mechanism are bridged by an interstitial oxygen in the mirror plane with forming a kind of complex defect, which might be called "Reidinger defect"(Fig.1-3). It means that the interstitial oxygens do compensate the extra charge. The formula "$M_{1+x}Al_{11.0}O_{17+x/2}$" itself reflects this mechanism. The "Reidinger defect" mechanism was also confirmed by potential energy calculation by Wang(1980).

Such nonstoichiometric composition is not limited to the hexaaluminates containing monovalent cations. Though Ca and Sr hexaaluminates were shown to have ideal magnetoplumbite formulae $MAl_{12}O_{19}$, where M=Ca and Sr, the exact composition of hexaaluminates containing larger divalent cations such as Ba and Pb has not been clarified. Barium hexaaluminate was first reported by Toropov(1935). It has been accepted to have a

magnetoplumbite structure with the chemical formula $BaAl_{12}O_{19}$ for a long time until careful examinations on this material by Stevels (1980) and Haberey et al.(1980) threw doubt on this concept. Neither the structure nor the formula of "Ba hexaaluminate" was clarified until our works were published (Iyi et al.,1983, 1984a, 1985b). Moreover, the knowledge of the hexaaluminates containing large trivalent cations in the mirror plane, such as rare-earth elements, is extremely limited. After Roth & Hasko (1958) found the "beta-alumina"-like compound in the system La_2O_3-Al_2O_3 and tentatively denoted it as $La_2O_3 \cdot 11Al_2O_3$, the formula "$LnAl_{11}O_{18}$" has been used to express the phase of rare-earth hexaaluminates up to now. Only Stevels(1979), in the study of luminescence of the doped hexaaluminates, noticed the nonstoichiometric composition of lanthanum hexaaluminates and proposed the formula $(La_{1-x}O_x)Al_{11+2/3+5x/3}O_{19}$ (x=0.14, with narrow solid solution range) for non-doped lanthanum hexaaluminate on the basis of luminescence and X-ray powder diffraction data. But very little attention has been paid to his assumptions by other researchers. The composition of "beta-phase" was supposed to be $LnAl_{11}O_{18}$ (Morgan & Cirlin, 1982) or $Ln_2O_3 \cdot 11Al_2O_3$ on the basis of the phase study in the system Al_2O_3-Ln_2O_3(Ln: lanthanides)(e.g. Jantzen & Neuagaonkar, 1981). Such ambiguity is not confined to the composition; the crystal structures of these hexaaluminates containing large divalent and trivalent cations have not been clarified yet. It is very surprising that structure and composition of binary oxide compounds in such simple systems have not been analysed.

The reason for this situation can be attributed to the lack of single crystals of good quality. Indeed the composition can be determined by the powder sintering method, but the sintered specimens are so in-

homogeneous that very careful examinations are needed to draw a precise conclusion on the composition. As far as the author is aware, reliable works using the powder method was accomplished by only a few researchers such as Stevels(1979), Haberey et al.(1980), and Kimura et al.(1982) in the field of the hexaaluminates. The wet analysis of the single crystal of a given compound would offer the most reliable and decisive results. So, in this thesis, the composition was determined along these lines as far as possible. The structure could also be easily analysed if single crystals are available. The powder diffraction method is not suitable to clarify the detail of such a highly defective structure even if the Rietveld profile fitting method is applied(e.g. England et al.,1982). Some researchers discuss the structure of barium hexaaluminates phase II using the data obtained by the electron microscopy method(Zandbergen et al., 1984; Wagner & O'Keeffe, 1985). But, for such complex structures, the electron microscopy is not suitable to reveal the structure in detail, as they themselves admitted. It is useful only to clarify whether a given structure model is correct or not, together with the computer image-simulation method. Furthermore, even if X-ray single crystal data were collected, care must be taken in the refinement procedure. The structure analysis of the defect-rich hexaaluminates is very complicated and, furthermore interstitial ions are in general hard to be detected due to the low occupancy. Structure refinement only by the least-squares method may lead to a mistake. It is necessary to examine difference Fourier sections at each stage of the refinement process. The structural parameters of lanthanum hexaaluminate were determined by Gasperin et al.(1984) independent of us, but they failed to observe the interstitial Al which we recognized(Iyi et al., 1984b, c). It is probably because they

used the data for refinement without absorption correction and finished the structure analysis at the isotropic refinement with an R-factor of only about 0.06. Some refinements on beta-alumina compounds containing monovalent cations are not reliable because of the apparent mistakes such as negative temperature factors for some atoms and no absorption correction for flat crystals. As the cations are distributed among various sites in the mirror plane, a careful refinement is needed to obtain reliable parameters.

Purposes and Method of This Study

As mentioned above, there still remained the problems with respect to the structure and composition for hexaaluminate compounds. The aims of this study are;

(1) to clarify the effects of the large cation in the mirror plane upon the hexaaluminate structure, and

(2) to reveal the precise composition and the causes of the nonstoichiometry on the basis of the structural knowledge.

For these purposes, several hexaaluminates containing various cations with different valence and ionic radius were chosen and examined. The structure and composition of these hexaaluminates are revealed by using well-characterized single crystals which were grown mainly by the FZ method. The structure was revealed by using X-ray diffraction data obtained on a four-circle diffractometer. In reality, obtained parameters by the X-ray single crystal diffraction method are on the average structure; however, the present author take the position that we must not confine ourselves to reporting only the parameters, but that we should propose a structure model in order to understand the characteristics of

such defective compounds. In the present thesis, it is supposed that a defect structure is composed of several types of cells, and structure models based on this concept were presented for explanation of the structural parameters and occupation factors.

Contents of This Thesis

The present thesis is organized as follows:

In Chapter 2, the hexaaluminates containing trivalent rare-earth elements are studied. The composition and the structure are determined by X-ray single crystal data. By considering that the compound is made up of defective cells and non-defective cells(perfect cells), nonstoichiometric composition is explained. In Chapter 3, the hexaaluminates containing divalent cations are studied. These are Pb, and Ba hexaaluminates. Especially, two compounds, beta- and beta(II)-alumina are confirmed to exist for Ba hexaaluminate. Previously, they were referred to as phase I and phase II, respectively(Kimura et al., 1982). The structures of both compounds are elucidated. By the structure model considering defect and perfect cells, the nonstoichiometric composition of both compounds are explained. The structure determination of Mg-doped barium hexaaluminates are also included. Chapter 4 is focused on the hexaaluminates containing a large excess amount of monovalent cations. These are derived from the beta-aluminates containing divalent cations in the mirror plane by the ion exchange method and contain extremely high amount of excess cations in the mirror plane. On the basis of the occupational parameters of monovalent cations, the distribution of cations in the mirror plane is discussed. Final section of this chapter presents the results of energy calculation which are conducted to confirm some part of

these results. Chapter 5 deals with crystal chemistry of the hexaaluminates, in which the effects of the cation size, valence, and population on the structure type and mirror plane dimension are discussed.

The problems specific to each compound are described in the introduction part of each section.

Experimental Procedure and Nomenclature

The FZ apparatus was of a SC-7 type (Nichiden Kikai Co., Ltd.), and its heat source was a xenon arc lamp. The atmosphere during the growth was nitrogen to prevent the bubble formation in the molten zone due to the the same reason as indicated in the growth of some silicates (Iyi & Shindo, 1979).

The automatic four-circle diffractometer is an AFC-3 model(Rigaku Denki Co. Ltd.), and MoKα radiation (λ =0.71069 A) was used for data collection. For the least-squares refinement, a modified RSFLS-4 program (UNICS), which was originally written by Sakurai et al.(1967), was used. The Fourier syntheses were accomplished by RSSFR-5 program (UNICS) written by Sakurai(1967). Secondary extinction corrections according to Becker & Coppens(1974) and Coppens & Hamilton (1970) were incorporated in the RSFLS-5 program. Absorption corrections were according to Busing & Levy's algorism(1957).

The nomenclature of the cation sites in the mirror plane was taken from that of Peters et al.(1971), but in wider sense. As the real positions which cations occupy shift from the ideal BR (2/3,1/3,1/4), mO(5/6,2/3,1/4), and aBR(0,0,1/4) sites, it would be better to redefine them to cover a wider region. The BR site would be better to be defined as the site near (2/3,1/3,1/4) which cannot be occupied at the

same time with the symmetrical equivalent positions or mO cations in the same single mirror plane. In the similar way, the mO site can be defined as the site near (5/6,2/3,1/4) which is able to coexist with the symmetrical equivalents or other mO cations in the same single mirror plane. The aBR site is (0,0,1/4). Naturally the boundary between the BR and mO sites varies according to the radius of the cation in the mirror plane. In the present thesis, the word "cation" means the large cation in the mirror plane situated at the BR, mO, or aBR sites unless otherwise stated.

The usage of nomenclature for the atomic positions such as Al(1) and O(3) is consistent throughout the thesis. These atomic positions are shown in Fig.1-5.

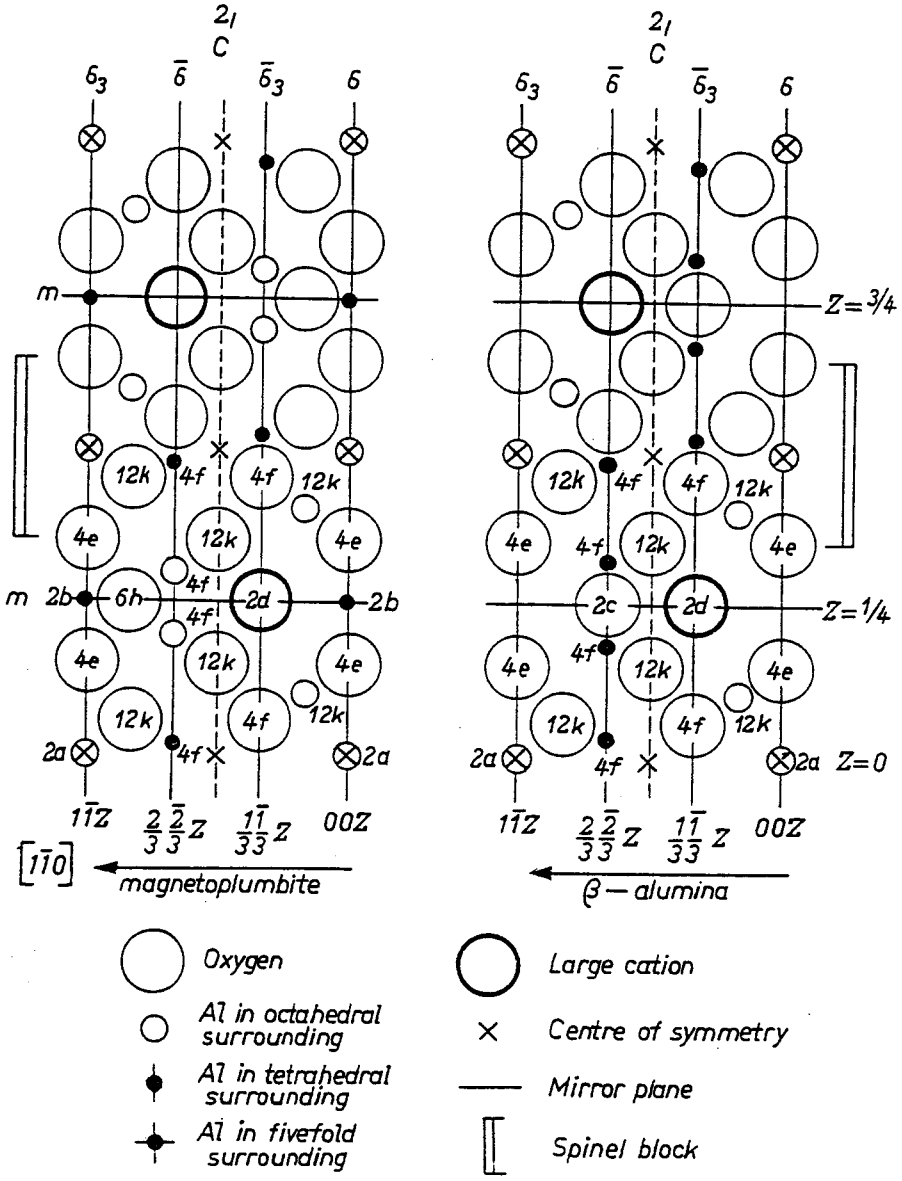

Fig.1-1. Projection on [1$\bar{1}$0] plane in beta-alumina and magnetoplumbite structures showing the arrangement of atoms. (Stevels & Schrama-de Pauw, 1976).

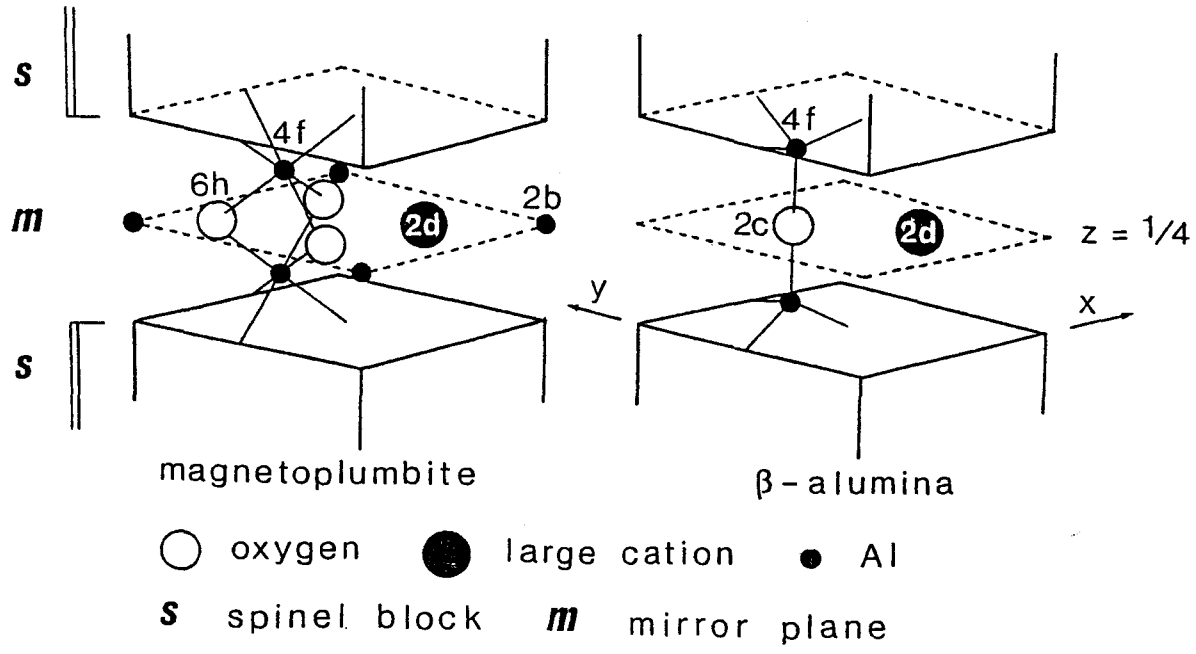

Fig.1-2. Schematic representation of a part near the mirror plane (z=0.25) in the structure of the (a) magnetoplumbite type and (b) beta-alumina type.

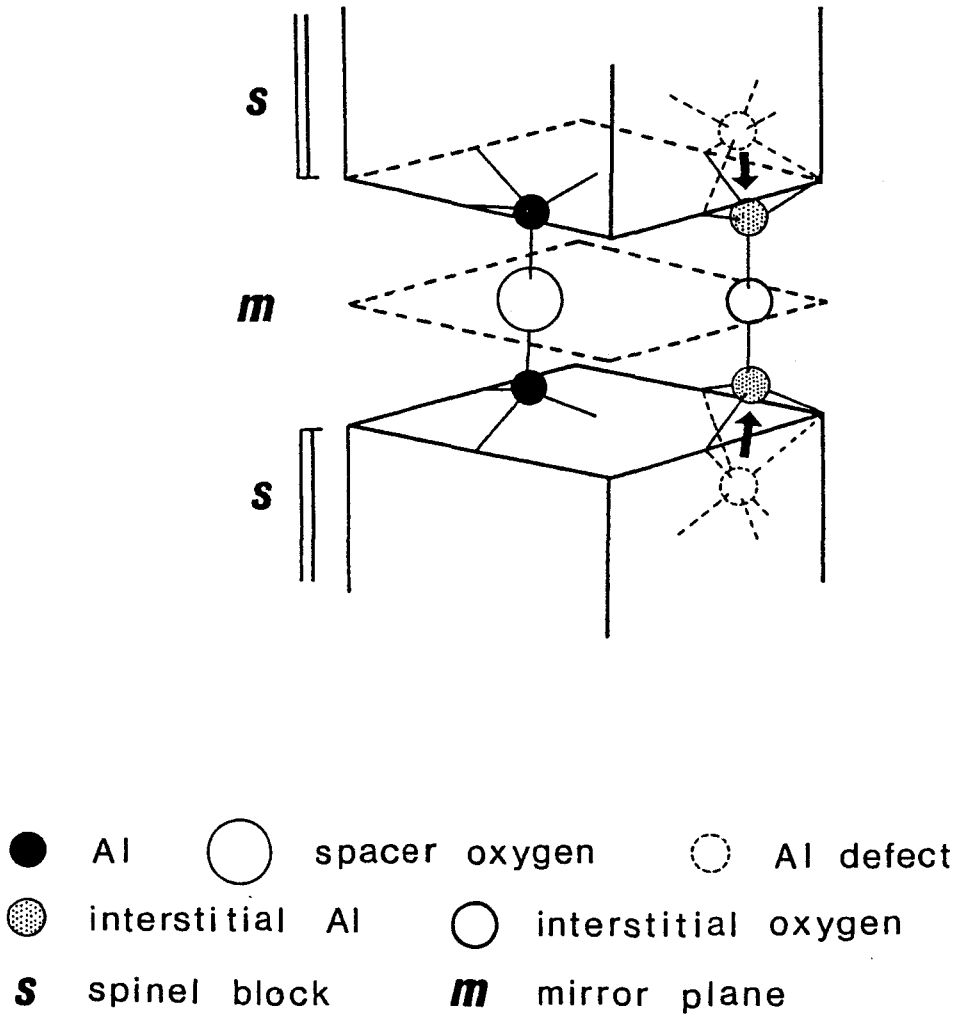

Fig.1-3. The Reidinger defect. The bold arrows indicate the migration of Al ions after the Frenkel defect mechanism.

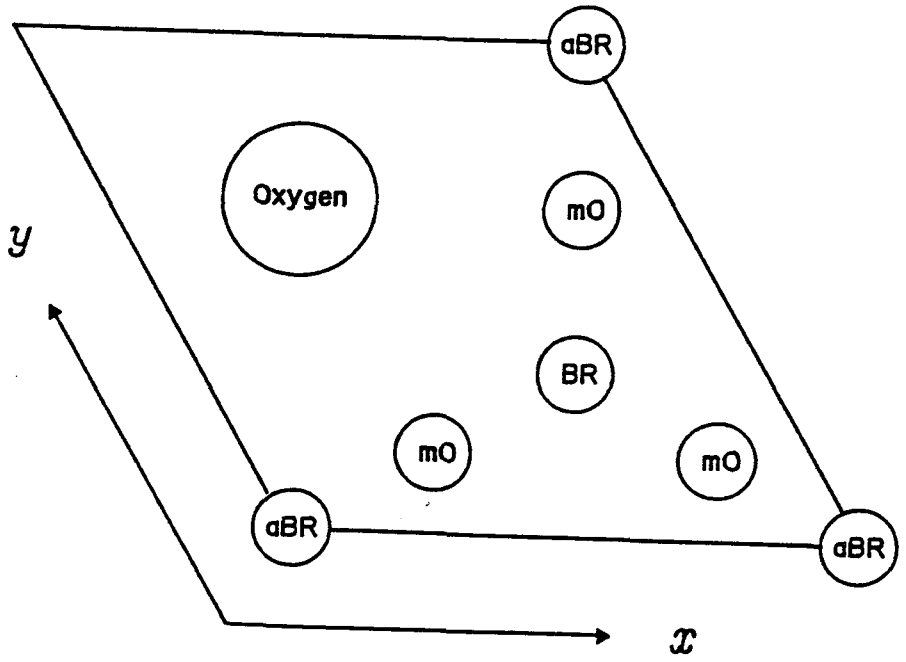

Fig.1-4. The mirror plane depicting the large various cation sites. BR = Beevers-Ross site, mO = mid-Oxygen site, aBR = anti-Beevers-Ross site.

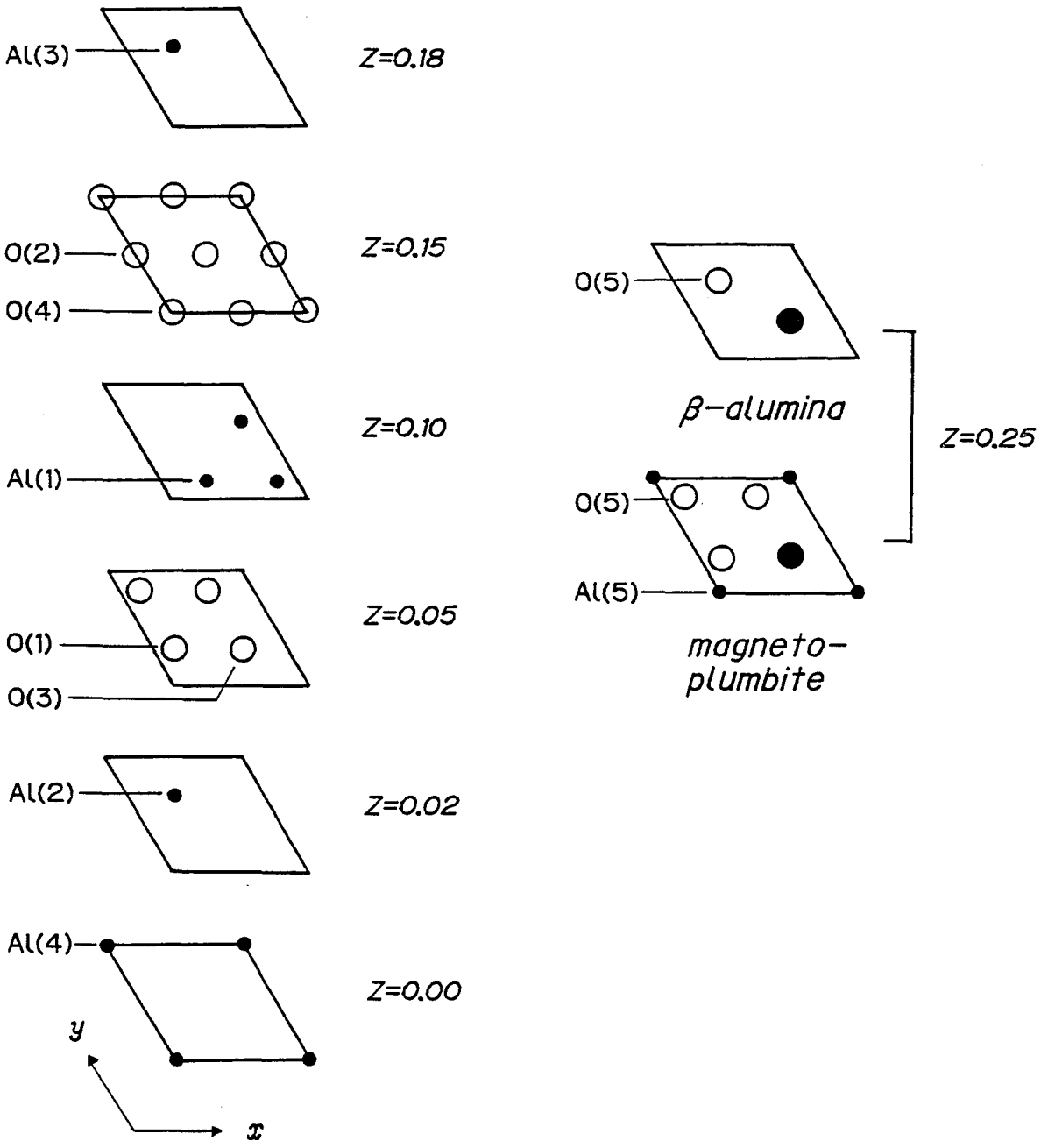

Fig.1-5. Nomenclature of the atomic positions in beta-alumina and magnetoplumbite structures.

2 HEXAALUMINATES CONTAINING LARGE TRIVALENT CATIONS

2-1 Introduction

In the phase investigation of the system La_2O_3-Al_2O_3, a "beta-alumina-type compound" ($La_2O_3 \cdot 11Al_2O_3$) was first recognized by Roth & Hasko(1958). Since then, several investigations were published on the hexaaluminates containing various rare-earth elements. Up to now, the existence of the "beta-alumina-type compound" containing a trivalent rare-earth elements has been recognized for the elements with large ionic radii such as La, Ce^{3+}, and Pr; on the other hand, no such phase is considered to exist for the elements with small ionic radii such as Gd, Tb, and Yb (Toropov et al. 1972). However, it is still a matter of controversy that there are such phases for the elements of intermediate ionic size, e.g., Nd, Sm, and Eu^{3+} (Liebertz, 1984; Mizuno et al., 1977a, 1977b). First of all, preliminary studies were conducted on the solidification of melts with the composition $Ln_2O_3 \cdot 11Al_2O_3$ (Ln = La, Nd, Sm, and Eu) in the FZ apparatus in order to clarify whether there is such a phase for each element. In the solidified specimens, a "beta-alumina-type" phase was detected for Ln= La, Nd, but not for Ln=Sm, Eu, by using the X-ray powder diffraction method. This is in accordance with the results of the phase investigations by Mizuno et al.(1974,1975,1977a,1977b). So, it was presumed that Nd hexaaluminate was the hexaaluminate containing the smallest rare-earth ion and that the phase exists for the rare-earth cations in the range from La to Nd.

Besides the existence of the "beta-alumina phase," there are two problems on these hexaaluminates; composition and structure. Roth & Hasko

(1958) supposed that the "beta-phase" exists in the composition near Al/La = 11.0. Other works on the phase study of La_2O_3-Al_2O_3 lead to nearly the same conclusion (Rolin & Thanh, (1965); Fritsche & Tensmeyer, (1967)). However, Stevel(1978) established the composition range as Al/La = 13.07 to 13.89. Recently, Dexpert-Ghys et al.(1976, 1982) proposed the solid solution range from 11.0 to 14.0 on the basis of their X-ray powder diffraction data and structure model. Thus the composition and its range still remain unestablished.

Not only the composition but also the structural knowledge of these hexaaluminates is extremely limited. Generally, they are accepted as having a beta-alumina structure on the basis of the composition Al/La=11.0 (e.g. Morgan & Cirlin, 1982). Stevels & Verstegen(1976) considered, for the first time, lanthanum hexaaluminate to have the magnetoplumbite structure and, later, mainly based on luminescence data Stevels(1979) constructed the structure model in which excess oxygen enters into the BR site instead of a large cation to form 6-coordinated interstitial Al. On the other hand, using powder diffraction and fluorescence data, Dexpert-Ghys et al.(1982) proposed that this compound was composed of beta-alumina-type and magnetoplumbite-type unit cells, the ratio of which depended on the composition. A refinement of structure using single crystal X-ray diffraction data was accomplished on the related compound $LaMgAl_{11}O_{19}$ by Kahn et al.(1981). The result showed this Mg-substituted hexaaluminate to be of the magnetoplumbite structure. As Mg^{2+} ions are substituted for Al^{3+} ions in the spinel block to attain charge neutrality in the case of $LaMgAl_{11}O_{19}$, the problem of nonstoichiometry or charge compensation for the nondoped hexaaluminates that contain trivalent cations in the mirror plane still remains unsolved. Whatever the composi-

tion and structure may be, the hexaaluminates having trivalent cations in the mirror plane cannot be formed without containing defects in their structures.

In section 2-2, the crystal structure determination of nonsubstituted lanthanum hexaaluminate using X-ray single crystal diffraction data is described, and a possible structure model explaining the nonstoichiometry of this compound is proposed(Iyi et al., 1984b). At the same time that our work was published, Gasperin et al.(1984) reported the structure of La hexaaluminate and its derivatives independently. However, they only reported the parameters obtained by isotropic refinement and clarified neither the composition nor the causes of the La-deficiency. Section 2-3 deals with the structure of Nd hexaaluminate (Iyi et al., 1984c) for comparison with La hexaaluminate.

2-2 Crystal Structure of Lanthanum Hexaaluminate

2-2-1 Experimental

Before conducting the single-crystal growth, the melting nature of La hexaaluminate was examined. The molten zone with the composition of $La_2O_3 \cdot 11Al_2O_3$ was made between sintered rods in the FZ apparatus with a xenon arc lamp as the heat source, and the rods were pulled apart gradually with slow cooling according to the SCFZ method (Shindo, 1980). A longitudinal section of the solidified specimen was examined by EPMA, which revealed successive segregation of Al_2O_3, La hexaaluminate, and eutectic lamellae composed of La hexaaluminate and $LaAlO_3$. This fact indicates incongruent melting nature of La hexaaluminate, which is in accordance with the result of Mizuno et al.(1974).

The single crystal was grown by the FZ method using a xenon arc lamp as the heat source. The growth rate was 1.5 mm/hr and nitrogen was used as the atmosphere during growth. The molar ratio Al/La of the grown crystal was revealed to be always near 13.6 by EPMA even if the starting material was of composition Al_2O_3/La_2O_3 = 11.0, so the composition with the molar ratio of 13.6 was used as starting material. The grown boule was 3 - 4 mm in diameter and 15 mm in length. It was, for the most part, clear and transparent, but still contained small amounts of inclusions besides large and tiny cracks. From clear part of the boule several specimens were taken, which were examined by Laue and precession methods. The space group was determined to be $P6_3/mmc$ and superstructure reflections were not detected. A crystal measuring approximately 0.09 x 0.06 x 0.04 mm was used for data collection on an automatic four circle diffractometer with graphite-monochromatized MoKα radiation. Reflections $\underline{hkl}$, $h \geq k \geq 0$, and $l \geq 0$, were measured to a maximum 2θ of 115°. A set of three standard reflections (107), (220) and (00,10) was measured every 100 reflections. After Lorenz polarization and absorption corrections, the intensities of 290 non-zero unique reflections were obtained. As the linear absorption coefficient for the specimen was μ = 43.6 cm^{-1}, the X-ray absorption correction was applied to. The scattering factors for the neutral atoms were taken from the I.T.(Vol.IV). The lattice parameters were refined using 20 2θ-data collected on the four-cicle diffractometer. The type I isotropic correction was applied for the secondary-extinction correction. The crystallographic data are shown in Table 2-1, in which the density of the specimen was determined by the method of Archimedes. The molar ratio Al/La was determined by means of EPMA using Al_2O_3 and LaB_6 as the standard material.

2-2-2 Chemical Formula

The result of EPMA showed that the molar ratio Al/La of the grown crystal was about 13.6. However, even with the composition of Al_2O_3/La_2O_3 = 13.6 as the starting materials, the grown boules still contained a small amount of $LaAlO_3$ inclusions. The inclusion-free part was selected and examined by the wet chemical analysis (chelatometry titration method). As a result, Al/La molar ratio of 14.4(3) was obtained. The result of EPMA may be less reliable probably due to inappropriate conditions of measurement and/or of standard materials. From data of density, wet chemical analysis, and cell volume, the chemical formula of lanthanum hexaaluminate used for the present study was deduced to be $La_{0.827}Al_{11.9}O_{19.09}$ as shown in Table 2-1. The composition range of La hexaaluminate was examined using the longitudinal section of the specimen obtained by SCFZ method(Shindo, 1980). EPMA showed the solid solution range from about 13.5 to 14.4 when lanthanum hexaaluminate which was revealed to be Al/La=14.4 by wet chemical analysis was used as the standard.

2-2-3 Refinement

At first, Fourier and difference Fourier syntheses, which corresponded to an R-value of 0.286, were carried out using the positional parameters of $LaMgAl_{11}O_{19}$ (Kahn et al., 1981). It was revealed that the structure of lanthanum hexaaluminate was essentially of a magnetoplumbite type and that the occupation factors of La at the 2d site (2/3,1/3,1/4) and Al at the 2b site (0,0,1/4) were less than unity for each site as can be supposed from the chemical formula. The refinement using general isotropic temperature factor, the occupancy of La(at 2d) and Al(at 2b),

and the positional parameters as variable parameters yielded an R-value of 0.169. The difference electron map at this stage indicated a slight displacement of the La ion from the three-fold axis (2d site) to the 6h site. When the La ion was split in the 6h site in the refinement, the R-value dropped to 0.118. However, electron density difference was still observed around the large cation site in the difference Fourier section at z=1/4. This is probably because La ions are distributed among various sites around the BR site. So, in the next step, La was placed at the 2d site in addition to the 6h site and the refinement was tried again. The resulting R-value was 0.093. When individual isotropic temperature factors were introduced, the refinement converged at R=0.079 and wR=0.096, with unit weight. The result showed that the isotropic temperature factor of Al(5) at the 2b site increased anomalously to 2.2 as compared to 0.08 - 0.36 for the other Al ions. The difference Fourier sections corresponding to R=0.093 indicated an elongated electron density from the 2b site in the c-direction. From these features, we assumed that Al(5) was moved off the mirror plane into 4e sites(0,0,1/4+d) and split with 50% occupancy for each site. The refinement with Al(5) at the 4e site gave an R-value of 0.071 and a reasonable isotropic temperature factor of 0.57 for Al(5). Further refinement introducing individual isotropic temperature factors and secondary extinction corrections gave R=0.049 and wR=0.053 with unit weight. The difference Fourier maps at this stage still indicated a small amount of additional electron density (about 2 eA^{-3}) at (x, 2x, 0.19) and (x, 2x, 0.18) sections with x=0.83, which we attributed to interstitial Al, as was found in the other hexaaluminates having a beta-alumina structure (Roth et al., 1977). The refinement incorporating interstitial Al as Al(6) yielded an R-value of 0.043 (wR=0.045) when individual

isotropic temperature factors were used. Here the common temperature factor of 0.47 was used for Al(6) and this temperature factor was fixed during the refinement. In addition, the occupancy of Al(1) was varied. At this stage all occupation factors were varied while other parameters being fixed. However, the occupation factors of all sites including oxygen sites showed no sign of reduction. Anisotropic refinements, except the temperature factor of Al(6), converged quickly to give a final R-value of 0.039 (wR=0.042). The final difference synthesis showed random peaks and depressions not exceeding the largest amplitude of $\pm$ 1.0 eA^{-3}. The g-value for the secondary extinction correction was 5.1(6) x 10^{3}. The final values of the positional parameters are shown in Table 2-2. The inter-atomic distances and bond angles are presented in Table 2-3 and 2-4, respectively.

2-2-4 Discussion

The refined parameters of lanthanum hexaaluminate correspond to a magnetoplumbite structure. Dexpert-Ghys *et al.*(1982) considered the structure to be made up of a mixture of beta-alumina-like and magneto-plumbite-like unit cells, the ratio of which depends on the composition. In the present study, difference Fourier maps at various stages did not give any indications of the additional electron density at the 2c site (1/3,2/3,1/4) which could be expected if there were beta-alumina-like cells. The final synthesis showed a difference electron density of about -0.5 eA^{-3} at the 2c site. Thus, there is no possibility for beta-alumina-like cells to exist in the present specimen.

An interesting feature in the refined structure is the coordination of the Al(5) ions. For other hexaaluminates with magnetoplumbite struc-

ture, this Al ion is known to be situated at the 2b (0, 0, 1/4) site and 5-coordinated. In the course of the refinement, the isotropic temperature factor of Al(5) at the 2b site became anomalously large as mentioned in the preceeding section. The difference Fourier map at that stage also indicated an elongated electron density in the c-direction. When Al(5) was split into 4e sites (0, 0, 0.24) with 50% occupation for each, the R-value dropped significantly in the subsequent refinements, finally giving a value of z=0.240 with a reasonable isotropic temperature factor of 0.57. Accordingly, Al(5) was split and placed into the 4e sites in the subsequent refinements. Al(5) can thus be considered as "distorted 4-coordinated". In addition to the above described treatment, a refinement was tried on the assumption that the Al ions were distributed among the 4e and 2b sites. The occupation ratio Al(4e)/Al(2b) of 4.0 was obtained as the result. This model was not, however, adopted in the further refinement because no improvement of the R-value could be seen. In other hexaaluminates and hexaferrite of magnetoplumbite type, strong anisotropy of Al(5) or Fe(5) was observed and discussed(e.g., Obradors et al., 1985).

One of the interesting problems on lanthanum hexaaluminate is the cause of nonstoichiometry or its charge compensation mechanism. As La and Al ions have the same +3 charge, the occupation factor of La and Al ions cannot be fixed, a priori. Thus, structure model must be sought to explain the nonstoichiometric nature of the composition. In the structure of beta-aluminas containing monovalent cations, part of Al(1) was supposed to be migrated in a pair to form interstitial Al ions which were bridged by an interstitial oxygen in the mirror plane(Roth et al.,1977). Similar interstitial Al ions could be detected in lanthanum hexaaluminate. The difference Fourier map corresponding to an R-value of 0.049 showed a

small amount of excess electron density as described in the refinement section. To assure that an interstitial Al ion is formed by the same Frenkel defect mechanism as was found in beta-aluminas, the occupation factors of all Al ions including interstitial Al were varied with the scale factor being fixed. As a result only the occupation factor of Al(1) decreased beyond the e.s.d. When the interstitial Al was incorporated as Al(6) with occupancy of Al(1) being varied, a significant reduction of the R-value could be observed and the defect number of Al(1) could be concluded to be almost equal to the number of Al(6) in a unit cell within experimental uncertainty. Accordingly it was postulated that interstitial Al ions were migrated from Al(1) according to the Frenkel defect mechanism. To examine whether there are other defects, all occupation factors were varied with the other parameters being fixed, but no reduction of occupancy was observed. So, the interstitial Al ions were supposed to be the clue to understand the nonstoichiometry of the non-doped lanthanum hexaaluminate.

For the coordination of interstitial Al, there appear to be two possibilities. First, a defect of La takes place to avoid the cation-cation interaction between La and interstitial Al(6) (about 2.1 A) and the large cation site (BR site) becomes vacant. In this case an interstitial Al square piramid is formed (Fig.2-1a). The defect structure of this type is referred to as "vacancy model" in the present thesis. Second, a La ion at the BR site is replaced by an interstitial oxygen and an interstitial Al octahedron is formed. This model resembles that of Stevels(1979). This model is referred to as "Oi model." As the existence of interstitial O cannot be determined directly by X-ray diffraction method owing to the very large difference in the scattering power between

La and oxygen, both models are to be considered in the following discussion.

Besides the coordination of interstitial Al, we assumed two types of Al_i - Al_i(i: interstitial) relation depending on whether interstitial Al ions are migrated in a pair or not as shown in Fig.2-1. According to Type 1 (Fig.2-1a), interstitial Al ions are formed singly and an interstitial Al polyhedron (Al octahedron in "Oi model," and Al square piramid in "vacancy model") shares an edge with an Al(5) tetrahedron. In this case, for charge compensation, the defects of Al(5) are only randomly distributed among the Al(5) ions which do not share edges with interstitial Al polyhedra. On the other hand, interstitial Al ions in a pair form the bridge between two spinel blocks in type 2 (Fig.2-1b). In this case the Al(5) site in the vicinity of interstitial Al ions would be vacant because an Al(5) tetrahedron would avoid sharing a face with an Al(6) polyhedron. Consequently simultaneous defects of La and Al(5) would occur by a pairwise migration of interstitial Al. The result of refinement shows that the number of La per unit cell is almost equal to that of Al(5), and that the number of Al(6) per unit cell is twice that of the La defects.(Table 2-2). These can be better explained by the interstitial Al formation of the type 2, so the type 2 structure, in which interstitial Al ions exist in a pair, was chosen for the subsequent considerations, though more evidences would be needed to confirm this defect model.

As discussed above, interstitial Al(6) ions cannot coexist with La and Al(5) in the same mirror plane of a single unit cell. On the basis of these considerations, we assumed two types of half unit cell having a spinel block and a mirror plane as the main constituent of lanthanum hexaaluminate, as shown in Figs.2-2a and b: One contains a La ion and has

the composition of "$LaAl_{12}O_{19}$" with the charge +1; (a) the other contains, in the case of "vacancy model," La and Al(5) defect due to interstitial Al(6), with composition of "$Al_{11}O_{19}$" having charge -5, and (b) in the case of "Oi model," the other contains an interstitial oxygen in addition, with composition of "$OAl_{11}O_{19}$" having the charge -7. In "vacancy model," the ratio of the half unit cells should be 5 to 1 in order to attain the charge balance and the resulting chemical formula would be $La_{0.833}Al_{11.833}O_{19.0}$, where the molar ratio of Al/La is 14.2. On the other hand, in "Oi model," the ratio should be 7 to 1 and $La_{0.875}Al_{11.875}O_{19.125}$, where Al/La = 13.57, can be obtained as the formula. The chemical formulas and the number of atoms in a unit cell at La, Al(1), Al(5), and Al(6) sites for two models are presented in Table 2-5 together with the result of the final refinement for comparison.

In conclusion, because the results of the refinement and chemical analysis are more consistent with the "vacancy model" than the "Oi model," the structure model based on the "vacancy model" is preferable for explaining the nonstoichiometry of lanthanum hexaaluminate. The mechanism of narrow solid solution range still remains unclarified.

2-3 Crystal Structure of Neodymium Hexaaluminate

In the previous section 2-2, La hexaaluminate ($La_{0.827}Al_{11.9}O_{19.09}$) was revealed to have a magnetoplumbite structure with the Frenkel defects of Al ions. Here, Nd hexaaluminate, containing a smaller rare-earth element, is compared with the hexaaluminate containing the largest rare-earth ion La^{+3} by using single-crystal X-ray structure data.

2-3-1 Experimental and Results

Before conducting the single-crystal growth, melting nature of Nd hexaaluminate was examined. A molten zone with composition of $Nd_2O_3 \cdot 11Al_2O_3$ was made between sintered rods in the FZ apparatus with a xenon arc lamp as the heat source, and the rods were pulled apart gradually with slow cooling according to the SCFZ method (Shindo, 1980). A longitudinal section of the solidified specimen was examined by EPMA, which revealed successive segregation of Al_2O_3, Nd hexaaluminate, and eutectic lamellae composed of Nd hexaaluminate and $NdAlO_3$. This fact indicates the incongruent melting nature of Nd hexaaluminate, which is in agreement with the result of Mizuno et al.(1977).

The single crystal growth of Nd hexaaluminate by the FZ method was not very successful. The boule still contained small amount of Al_2O_3 and $NdAlO_3$ besides the single-crystal grain of Nd hexaaluminate. The molar ratio of Al/Nd in the clear crystalline part (pale purple) was determined by EPMA to be 13.3. Several specimens from these boules were examined by Laue and precession methods. The structure belongs to the hexagonal space group $P6_3/mmc$. The electron diffraction patterns showed no sign of superstructure. Using a 0.11 x 0.07 x 0.07 mm^3 crystal, intensity data were collected on an automatic four-circle diffractometer using graphite monochromatized MoKα radiation. The final set of 422 non-zero independent reflections below $2\theta = 115^o$ were corrected for Lorenz polarization and absorption effects. The neutral scattering factors were taken from the I.T.(Vol.IV). The lattice parameters were a=5.553(2)A, and c=21.990(7)A. The structural refinement procedure was almost the same as that of La hexaaluminate. The refinement without an extinction correction met with failure. When an isotropic type I secondary extinction

correction was applied, the refinement with anisotropic temperature factors was accomplished successfully, yielding R=0.046 and wR=0.058, where w=1.0. As anisotropy of extinction was observed, the anisotropic refinement incorporating a constrained anisotropic extinction correction was accomplished to give a final R-value of 0.044 (wR=0.047). The difference Fourier synthesis at this stage is practically featureless with a minimum of -1.4 eA^{-3} at (0,0,0.03). The other peaks or depressions are below 1.0 eA^{-3} in amplitude. The final parameters are given in Table 2-6. The bond lengths and angles are presented in Tables 2-7 and 8, respectively.

2-3-2 Discussion

The final parameters correspond to a magnetoplumbite structure as in the case of La hexaaluminate. Furthermore, the interstitial Al ion as described in La hexaaluminate was also detected in the difference Fourier sections at (x, 2x, z) with x=0.83 and z=0.18, 0.19. It was assigned as Al(6) in the refinement. In the previous section 2-2, the structure of La hexaaluminate was assumed to be mainly made up of two types of half unit cells with dimension 1/2 c: one has a La ion and contains no defects, the other has an interstitial Al(6) migrated from Al(1), a vacancy at the BR site instead of a La ion, and a defect of Al(5) at the 4e site. The former has the composition of "$LaAl_{12}O_{19}$", and the latter "$Al_{11}O_{19}$". These nonneutral half cells were supposed to cause the nonstoichiometry of La hexaaluminate. As shown in Table 2-9, the occupancy of Nd hexaaluminate is quite similar to that of La hexaaluminate, which leads to the conclusion that the mechanism of nonstoichiometry in Nd hexaaluminate is the same as that of La hexaaluminate.

Formula	:	$La_{0.827}Al_{11.9}O_{19.09}$
Symmetry	:	hexagonal
Space group	:	$P6_3/mmc$
a	=	5.561(2) Å
c	=	22.07(1) Å
V	=	591.0(4) $Å^3$
Z	=	2
D_{obs}	=	4.17 gcm^{-3}

Table 2-1. Crystallographic data of La hexaaluminate.

THE POSITIONAL AND THERMAL PARAMETERS[α]

	Position	Number per unit cell	x	z	β11x10^4	β22x10^4	β33x10^5	β23x10^5	B
La(1)	2(d)	0.98(21)	2/3	1/4	64(51)	β11	23(5)	0	
La(2)	6(h)	0.69(21)	0.718(7)	1/4	100(48)	115(139)	37(10)	0	
Al(1)	12(k)	11.0(2)	0.8310(4)	0.10772(8)	47(8)	50(11)	18(3)	-11(26)	
Al(2)	4(f)	4	1/3	0.0271(2)	59(11)	β11	17(5)	0	
Al(3)	4(f)	4	1/3	0.1899(2)	52(11)	β11	16(5)	0	
Al(4)	2(a)	2	0	0	34(14)	β11	14(7)	0	
Al(5)	4(e)	1.70(7)	0	0.2389(4)	58(29)	β11	51(21)	0	
Al(6)	12(k)	0.58(8)	0.839(7)	0.186(2)					0.47
O(1)	12(k)	12	0.1561(7)	0.0518(2)	86(17)	49(25)	26(5)	39(45)	
O(2)	12(k)	12	0.5023(7)	0.1501(2)	51(15)	69(22)	20(5)	53(44)	
O(3)	4(f)	4	2/3	0.0553(4)	57(26)	β11	47(14)	0	
O(4)	4(e)	4	0	0.1481(4)	29(23)	β11	36(14)	0	
O(5)	6(h)	6	0.178(1)	1/4	116(26)	126(46)	22(8)	0	

[α] The thermal parameters are of the form : $\exp[-(h^2\beta 11 + k^2\beta 22 + l^2\beta 33 + 2hk\beta 12 + 2hl\beta 13 + 2kl\beta 23)]$.
$\beta 12 = 1/2\ \beta 22$; $\beta 13 = 1/2\ \beta 23$

Table 2-2. The positional and thermal parameters of La hexaaluminate.

	Number of bonds	distance (Å)
Octahedral coordination		
Al(1) - O(1)	2	1.996(6)
- O(2)	2	1.839(6)
- O(3)	1	1.960(6)
- O(4)	1	1.856(6)
Al(3) - O(2)	3	1.850(7)
- O(5)	3	2.000(8)
Al(4) - O(1)	6	1.889(6)
Tetrahedral coordination		
Al(2) - O(1)	3	1.792(7)
- O(3)	1	1.819(10)
Polyhedron 5-coordinated		
Al(5) - O(4)	1	2.004(13)
- O(4)'	1	2.494(13)
- O(5)	3	1.732(10)
Al(6) - O(2)	2	1.81(4)
- O(4)	1	1.76(2)
- O(5)	2	2.16(4)
Polyhedron 12-coordinated		
La(1) - O(2)	6	2.714(5)
- O(5)	6	2.783(8)

Table 2-3. Interatomic distances of La hexaaluminate.

	Bond angles (°)
Octahedral coordination	
O(1) - Al(1) - O(1)'	81.43(37)
O(1) - Al(1) - O(2)	90.97(29)
O(1) - Al(1) - O(3)	89.41(25)
O(1) - Al(1) - O(4)	84.95(28)
O(2) - Al(1) - O(3)	87.30(31)
O(2) - Al(1) - O(4)	97.64(25)
O(2) - Al(3) - O(2)'	99.30(25)
O(2) - Al(3) - O(5)	89.19(30)
O(5) - Al(3) - O(5)'	80.79(31)
O(1) - Al(4) - O(1)'	87.16(24)
O(1) - Al(4) - O(1)"	92.84(24)
Tetrahedral coordination	
O(1) - Al(2) - O(1)'	111.17(19)
O(1) - Al(2) - O(3)	107.71(20)
Polyhedron 5-coordinated	
O(5) - Al(5) - O(4)	98.13(29)
O(5) - Al(5)'- O(4)	81.87(29)
O(5) - Al(5) - O(5)'	118.03(14)
O(2) - Al(6) - O(4)	102.4(20)
O(2) - Al(6) - O(5)	85.4(16)
O(4) - Al(6) - O(5)	91.6(10)

Table 2-4. Bond angles of La hexaaluminate.

	Tne number of atoms per unit cell				Al/La (in mole)	Chemical formula
	La	Al(1)	Al(5)	Al(6)		
Result of refinement	1.67	11.0(2)	1.70(7)	0.58(8)	13.9(4)	$La_{0.835}Al_{11.64}O_{19.0}$ [d]
"vacancy model"	1.667	11.333	1.667	0.667	14.2	$La_{0.833}Al_{11.833}O_{19.0}$
" O_i model "	1.750	11.500	1.750	0.500	13.6	$La_{0.875}Al_{11.875}O_{19.125}$
Chemical analysis					14.4	$La_{0.827}Al_{11.9}O_{19.09}$

[d] Charge balance is not attained.

Table 2-5. Comparison of the site occupancy and formula for La hexaaluminate.

	Position	Number per unit cell	x	z	$\beta 11 \times 10^4$	$\beta 22 \times 10^4$	$\beta 33 \times 10^5$	$\beta 23 \times 10^5$	B
Nd(1)	2(d)	1.02(5)	2/3	1/4	86(16)	β11	28(2)	0	
Nd(2)	6(h)	0.63(5)	0.728(2)	1/4	47(20)	128(54)	15(4)	0	
Al(1)	12(k)	11.1(1)	0.8311(3)	0.10808(6)	30(6)	14(8)	18(2)	6(17)	
Al(2)	4(f)	4	1/3	0.0268(1)	33(7)	β11	14(3)	0	
Al(3)	4(f)	4	1/3	0.1902(1)	33(8)	β11	11(3)	0	
Al(4)	2(a)	2	0	0	37(11)	β11	13(5)	0	
Al(5)	4(e)	1.62(6)	0	0.2396(4)	56(24)	β11	45(15)	0	
Al(6)	12(k)	0.70(7)	0.847(5)	0.185(1)					0.51
O(1)	12(k)	12	0.1559(6)	0.0523(2)	59(12)	60(18)	31(4)	-25(31)	
O(2)	12(k)	12	0.5046(6)	0.1507(2)	36(11)	29(16)	24(4)	- 3(30)	
O(3)	4(f)	4	2/3	0.0548(3)	31(15)	β11	21(7)	0	
O(4)	4(e)	4	0	0.1488(3)	22(16)	β11	30(9)	0	
O(5)	6(h)	6	0.1809(9)	1/4	158(23)	48(31)	31(6)	0	

[a] The thermal parameters are of the form : $\exp[-(\underline{h}^2\beta 11 + \underline{k}^2\beta 22 + \underline{l}^2\beta 33 + 2\underline{h}\underline{k}\beta 12 + 2\underline{h}\underline{l}\beta 13 + 2\underline{k}\underline{l}\beta 23)]$.

$\beta 12 = 1/2\ \beta 22$; $\beta 13 = 1/2\ \beta 23$

Table 2-6. The positional and thermal parameters of Nd hexaaluminate.

INTERATOMIC DISTANCES

	Number of bonds	Distance (A)
	Octahedral coordination	
Al(1) - O(1)	2	1.989(6)
- O(2)	2	1.829(4)
- O(3)	1	1.968(5)
- O(4)	1	1.855(4)
Al(3) - O(2)	3	1.862(6)
- O(5)	3	1.969(7)
Al(4) - O(1)	6	1.890(5)
	Tetrahedral coordination	
Al(2) - O(1)	3	1.796(6)
- O(3)	1	1.794(7)
	Polyhedron 5-coordinated	
Al(5) - O(4)	1	1.997(11)
- O(4)'	1	2.454(11)
- O(5)	3	1.755(9)
Al(6) - O(2)	2	1.82(5)
- O(4)	1	1.67(4)
- O(5)	2	2.16(4)
	Polyhedron 12-coordinated	
Nd(1) - O(2)	6	2.683(5)
- O(5)	6	2.780(7)

Table 2-7. Interatomic distances of Nd hexaaluminate.

BOND ANGLES

	Bond angles (°)
Octahedral coordination	
O(1) - Al(1) - O(1)'	81.52(32)
- O(2)	91.55(25)
- O(3)	89.21(21)
- O(4)	84.98(26)
O(2) - Al(1) - O(3)	87.28(17)
- O(4)	97.86(19)
O(2) - Al(3) - O(2)'	100.00(20)
- O(5)	88.98(27)
O(5) - Al(3) - O(5)'	80.29(26)
O(1) - Al(4) - O(1)'	86.81(22)
- O(1)"	93.19(22)
Tetrahedral coordination	
O(1) - Al(2) - O(1)'	110.72(15)
- O(3)	108.19(16)
Polyhedron 5-coordinated	
O(5) - Al(5) - O(4)	97.49(29)
- O(4)'	82.51(29)
- O(5)'	118.33(13)
O(2) - Al(6) - O(4)	105.4(13)
- O(5)	84.4(14)
O(4) - Al(6) - O(5)	94.0(25)

Table 2-8. Bond angles of Nd hexaaluminate.

Atom	Position	Number per unit cell	
		La-hexAl_2O_3	Nd-hexAl_2O_3
M(1)	2(d)	0.98(21)	1.02(5)
M(2)	6(h)	0.69(21)	0.63(5)
Al(1)	12(k)	11.0(2)	11.1(1)
Al(5)	4(e)	1.70(7)	1.62(6)
Al(6)	12(k)	0.58(8)	0.70(7)

Table 2-9. Comparison of the site occupancy between Nd hexaaluminate and La hexaaluminate.

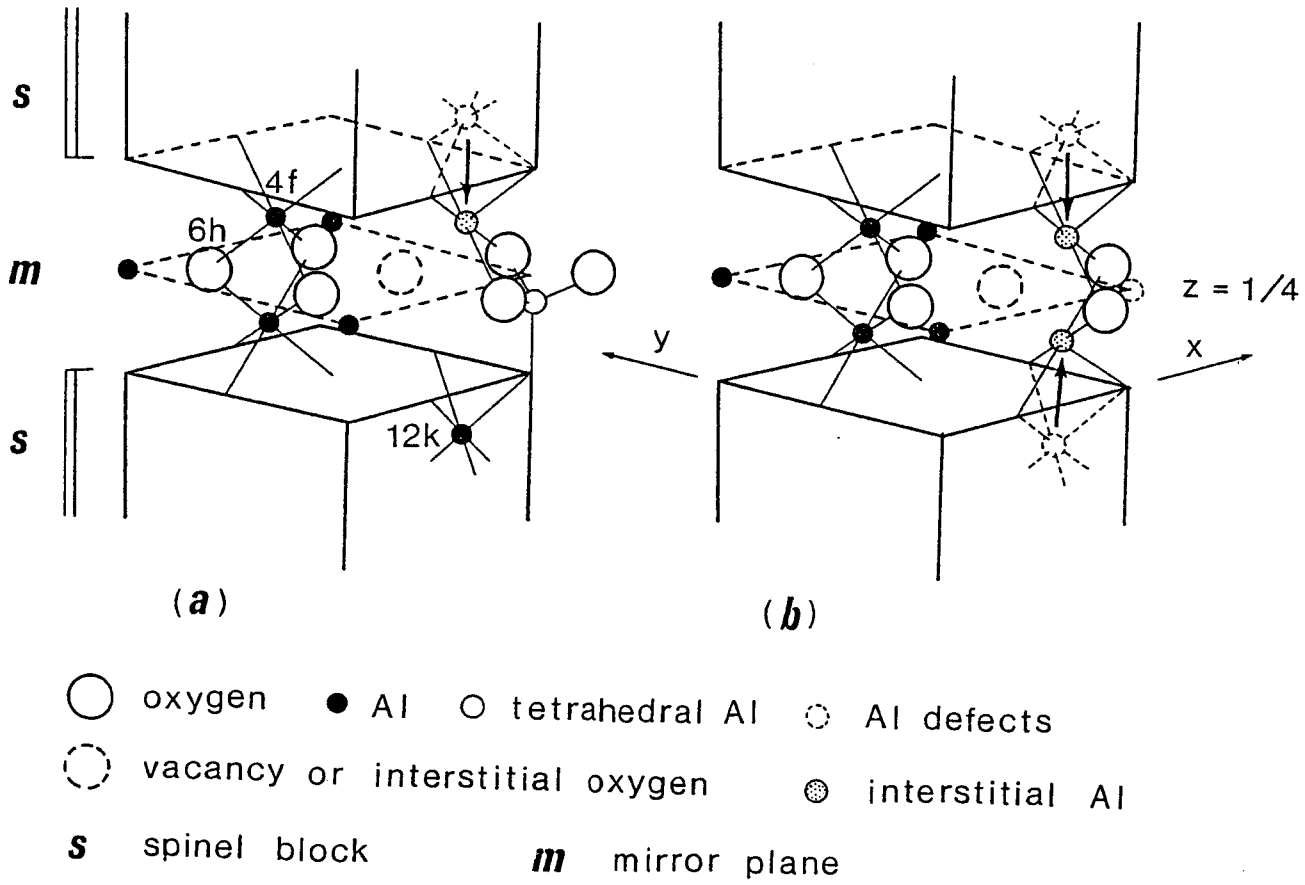

Fig.2-1. Two possible types of interrelation between interstitial Al ions in La hexaaluminate. (a) Type 1: interstitial Al ions are formed singly and bonded to Al tetrahedra. (b) Type 2: interstitial Al ions due to Frenkel defect occur in a pair to bridge the spinel blocks. The bold arrows indicate the shift of Al ions and the large cation site is vacant or filled with an interstitial oxygen.

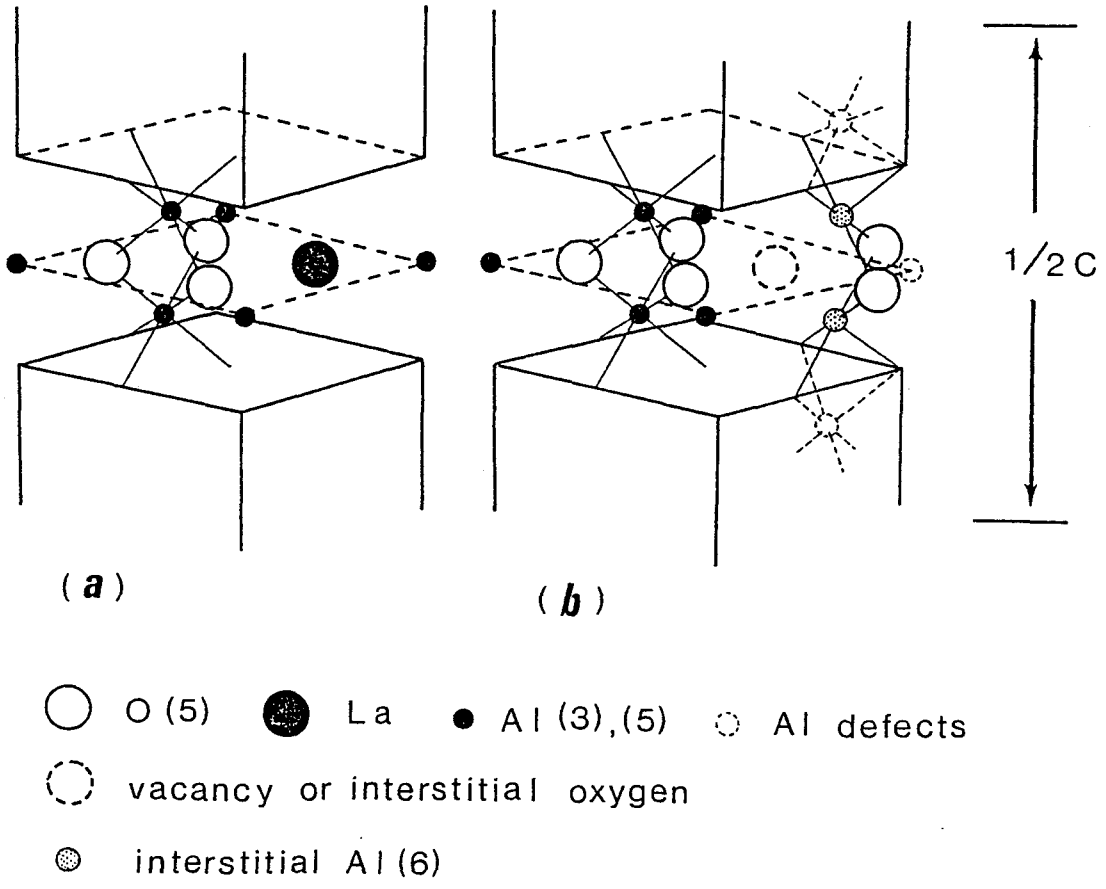

Fig.2-2. Two kinds of half unit cells supposed to constitute La hexaaluminate. (a) Half unit cell containing a large cation La^{3+} in the mirror plane. (b) Half unit cell containing interstitial Al ions . In this case, the large cation site is vacant or filled with an interstitial O ion.

3. HEXAALUMINATES CONTAINING LARGE DIVALENT CATIONS

3-1 Introduction

The hexagonal aluminates containing divalent cations such as Ca and Sr were revealed to have a magnetoplumbite structure with a formula $MAl_{12}O_{19}$, where M = Ca, Sr, by the X-ray structure analysis (Kato & Saalfeld, 1968; Lindop et al., 1975). Only a few reports were published on those containing larger divalent cations such as Pb and Ba, and the detail of the structure is still unknown. As for Pb ion, only X-ray powder diffraction data and electron diffraction data have published on Pb hexaaluminate (Comer et al.,1967). Judging from its chemical composition they determined, it appears that its structure is of a magnetoplumbite type.

On the other hand, barium hexaaluminate has more complex problems. "Barium hexaaluminate" was first described by Toropov(1935) as having an ideal formula $BaO \cdot 6Al_2O_3$ or $BaAl_{12}O_{19}$, and has been considered to be a single compound with the magnetoplumbite structure(e.g. Wyckoff, 1965), similar to other hexaaluminates containing divalent cations. Recently, however, data contradictory to these concepts began to be published by several researchers. Haberey et al.(1977) reported for the first time the existence of two distinct phases having compositions close to that of so-called barium hexaaluminate, and expressed them as $BaO \cdot 4.6Al_2O_3$ and $BaO \cdot 6.6Al_2O_3$. Kimura et al.(1982) confirmed their results and referred to Ba-poor ($0.82BaO \cdot 6Al_2O_3$) and Ba-rich ($1.32BaO \cdot 6Al_2O_3$) phases as phase I and phase II, respectively(Fig.3-1). On the other hand, Stevels (1978), who did not distinguish phase I and phase II, introduced the

formula $Ba_{1-x}Al_{10+2/3+4x/3}O_{17+x}$($-0.2 \leq x \leq 0.35$), the composition of which covers the range from phase I to phase II. Other formulae postulated were as follows: Mateika and Lauden(1979) used $Ba_{1-x}Al_{12+2x/3}O_{19}$ as the formula ($0.1 \leq x \leq 0.19$) for phase I, and Bartels et al.(1979) introduced $BaAl_{11}O_{17.5}$ and $BaAl_{12}O_{19}$ for two phases. These formulae were deduced only from hypothetical structural models. The discrepancies seem to have been caused by the lack of crystallographic data for the compounds. Morgan & Shaw(1983) and Yamamoto & O'Keeffe(1984) also observed the two phase by electron microscope, but they did not clarified the formulae.

Neither the formulae nor the structures and symmetries are as yet established. The symmetry of "barium hexaaluminate" was generally accepted as hexagonal, but Haberey et al.(1977) suggested that phase I exibited monoclinic (pseudo-hexagonal) symmetry. On the other hand, Stevels(1978) suggested the presence of a superstructure in $Ba_{1-x}Al_{10+2/3+4x/3}O_{17+x}$. They assumed the superstructure to have a volume threefold that of a magnetoplumbite type subcell, but the relation between the superstructure and the subcell was not made clear.

In section 3-2, the structure of Pb hexaaluminate is shown to be a magnetoplumbite type. Section 3-3 deals with the crystallographic data of barium hexaaluminate phase I and phase II, which are presented to show the existence of two distinct compounds; phase I and phase II. The crystal structure of barium hexaaluminate phase I and phase II are described in sections 3-4 and 3-5, respectively. The final section of this chapter contains structural parameters of Mg-doped barium hexaaluminate, ideally having the formula $BaMgAl_{10}O_{17}$, which was revealed to have a beta-alumina structure as Stevels & Verstegen(1976) have predicted.

3-2 Crystal Structure of Lead Hexaaluminate

3-2-1 Refinement and Results

The single crystals were grown by the flux evapolation method (Takekawa, 1984), in which PbO was evapolated from PbO-Al_2O_3 mixture at 1300 ℃ for two days. They were very brittle and the crystallinity was not good. Among them, some specimens were chosen, and a crystal of good shape and quality was selected. The precession photographs revealed that the structure belongs to the hexagonal space group $P6_3/mmc$, and showed no sign of superstructure. Using a 0.16 x 0.16 x 0.06 mm^3 crystal, intensity data were collected on the automatic four-circle diffractometer using graphite monochromatized MoK radiation. The final set of 546 non-zero independent reflections below $2\theta = 120°$ were corrected for Lorenz polarization and absorption effects. Since the linear absorption coefficient was as large as μ =156 cm^{-1}, absorption corrections were applied. The neutral scattering factors were taken from the I.T.(Vol.IV). The lattice parameters were determined to be a = 5.5711(3)A, and c = 22.045(2)A by using 2θ-data collected on the four-circle diffractometer.

The refinement was not successful due to large absorption effect, but an anisotropic refinement gave a final R-value of 0.043 (wR=0.054, w=1.0). The difference Fourier synthesis at this stage showed peaks and depressions in the range of -2 to +8 eA^{-3}. The final parameters are given in Table 3-1. The bond lengths are presented in Table 3-2, and the angles are in Table 3-3. The obtained parameters clearly shows the structure to be of a magnetoplumbite type.

3-3 Crystallography of Barium Hexaaluminate phase I and II

3-3-1 Experimental

Phase I. Phase I was grown by the FZ method at a rate of 1 mm/hr using a xenon arc lamp as the heat source. Air was chosen for the atmosphere during growth and a heat reservoir made of alumina was used in the same manner as already reported by Kitamura et al.(1982). The starting materials were $BaCO_3$ and Al_2O_3 (0.85 : 6.0 in molar ratio), which were mixed and sintered in an usual manner. The grown crystal was 7 mm in diameter and 5 cm in length. It was for the most part transparent and clear without visual imperfections, except for some cracks, of which clear parts without inclusions were selected and examined.

Phase II. For the growth of phase II, the $PbO-PbF_2$ flux (1:1 in molar ratio) was chosen as a solvent. The flux containing a proper amount of raw material was heated to 1200°C and cooled to 700 °C at a constant rate. After such treatment, tiny columnar crystals up to 0.2 x 0.2 x 0.3 mm were obtained, which were clear and transparent but contained small particle-like inclusions near one end of the crystal. Crystalline parts containing inclusions were cut off with a razor blade, and the remaining clear crystals without visual imperfections were used for the examination. In this section 3-3, the specimen thus prepared is referred to as BaPb-phase II.

Flux-free phase II was obtained by the FZ method using $BaCO_3$ and Al_2O_3 (3.12 : 6.0 in molar ratio) as starting materials. The boule so obtained was a mixture of $BaAl_2O_4$ and phase II, the grain size of which was about 20 μ or less. This specimen is referred to as Ba-phase II in this section.

Electron diffraction patterns were taken by a high voltage electron microscope (Hitachi-1250), operated at an accelerating voltage of 1 MV.

The powder X-ray diffraction measurements were carried out by a Phillips diffractometer using aluminum powder (#300) as the internal standard material, and lattice parameters were calculated by the least-squares computer program. The precession photographs were taken by using 40 kV x 20 mA MoKα radiation. The density of phase I was measured by the method of Archimedes. For BaPb-phase II, the density was measured by the flotation method using a heavy aqueous solution of a mixture of thallous formate and malonate, the density of which was determined separately. By means of EPMA, the chemical compositions of the specimens were determined, using Al_2O_3, $BaAl_2O_4$, and $PbTiO_3$ crystals as standards for Al, Ba, and Pb, respectively.

The growth conditions of barium hexaaluminate are reported by Takekawa in the NIRIM report(1983).

3-3-2 Result and Discussion

Phase I. Figures 3-2a, b, and c show electron diffraction patterns taken on FZ-grown crystal fragments, in which the incident electron beam was normal to the (001),(100), and (110) planes, respectively. By tilting the crystal around the c-axis to avoid the forbidden reflections due to multiple diffraction, the extinction rule of phase I was obtained, which was consistent with the results of X-ray precession photographs. The crystal has hexagonal symmetry and the systematic absent reflections were $\underline{l}=2n+1$ (n; integer) for $00\underline{l}$ and $\underline{hhl}$. The possible space groups are therefore $P\bar{6}2c$, $P6_3mc$ and $P6_3/mmc$. Since phase I has a structure similar to beta-alumina or magnetoplumbite, it is reasonable to assume that the space group of phase I is $P6_3/mmc$. The lattice parameters were refined by X-ray powder diffractions giving a = 5.587A and c = 22.72 A.

The density of the phase I crystal was 3.657 g/cm^3 and the molar ratio of Al/Ba, determined by wet chemical analyais, was 14.7. The formula of phase I was, therefore, calculated to be $Ba_{0.75}Al_{11.0}O_{17.25}$, with molar units Z=2. The formula of phase I thus obtained suggests a closer relation to the beta-alumina ($M^{1+}Al_{11}O_{17}$) structure than the magnetoplumbite ($M^{2+}Al_{12}O_{19}$), and implies that the large amount of Ba-deficiency as well as interstitial oxygen, which achieve the charge balance, are formed.

The results of Haberey et al.(1977) are different from ours both as to diffraction data and as to the space group. They observed l=2n+1 (n;integer) reflections for hhl; e.g., 005, 009, and 00.15, by precession photograph and proposed that the symmetry was monoclinic (pseudohexagonal) on the basis of the intensity distribution which was incompatible with hexagonal symmetry. This discrepancy is probably due to their method of sample preparation. They prepared the sample for X-ray diffraction by cooling the melt of phase I composition. As reported by Kimura et al. (1982), phase I melts incongruently, so the solidification of the melt having phase I composition leads to a mixture of Al_2O_3, phase I, $BaAl_2O_4$, and phase II, which derives from the solid state reaction of phase I and $BaAl_2O_4$. The sample, which Haberey et al.(1977) selected as a specimen for X-ray diffraction, could have been such a mixed or inhomogeneous crystal.

Phase II. Ba-phase II and BaPb-phase II yielded the same electron diffraction and X-ray powder diffraction patterns. The BaPb-phase II crystals contained Pb ions, and the molar ratio of Ba:Pb:Al was determined to be 1.0:0.25:11.2 by EPMA. On the other hand, the molar ratio of Ba:Al for Ba-phase II was 1.0:8.8-8.9. These data indicate that Pb^{2+} sub-

situtes for 20% of Ba^{2+}; these two specimens were confirmed to have the same structure. The density, measured for BaPb-phase II, ranged from 3.88 to 3.89g/cm^3, which were averaged to give 3.884g/cm^3. The lattice parameters of Ba-phase II and BaPb-phase II were determined by X-ray powder diffraction to be a=5.601 A, c=22.91 A and a=5.600 A, c=22.91 A, respectively. The formula for the BaPb-phase II then, is calulated to be $(Ba_{0.80}Pb_{0.20})_{2.34}Al_{21.0}O_{33.84}$. Since the molar ratio of(Ba + Pb)/Al for the BaPb-phase II and that of Ba/Al for the Ba-phase II are almost equal, the formula of the Ba-phase II can be written as $Ba_{2.34}Al_{21.0}O_{33.84}$. The crystallographic data of Ba-phase II are listed in Table 3-4.

Figure 3-3 shows the electron diffraction patterns of Ba-phase II. The indexed spots are the fundamental reflections of the beta-aluminta type subcell. In the diffraction pattern (a), taken with the incident electron beam normal to the (001) plane, some weak extra spots are observed. They are situated at $\underline{h}=m/3$ and $\underline{k}=n/3$, where m and n are integers. In the diffraction pattern (b), taken with the incident beam normal to the (100) plane, continuous extra reflections elongated along the c^* direction are also observed, while in (c), taken normal to the (110) plane, no extra spots are present. Such streaks were generally observed for the specimens of phase II. The diffuse reflections also appear in the powder diffraction patterns as broad reflections in the range of 28 to 31° for 2θ values. These results suggest the presence of an $a\sqrt{3}$ x $a\sqrt{3}$ superstructure. The lattice relationships between the beta-alumina-type subcell and the supercell are $A_1=a_1-a_2$, $A_2=a_1+2a_2$, and $C=nc_0$(n;integer), where A_1, A_2, and C are lattice vectors for the supercell, and a_1, a_2, and c_0, for the subcell.(Fig.3-4). The c axis length of the supercell is not well defined because the extra reflections are

elongated along the c^* direction as continuous streaks. If the c axis length is equal to the subcell, the superstructure cell volume will be threefold that of the subcell, as reported by Stevels (1978).

In addition to the presence of a superstructure, it should be pointed out that the fundamental odd number reflections such as $\underline{l}$=2n+1 (n;integers) for 00$\underline{l}$ and $\underline{hhl}$ are present, as observed in Fig.3-3b and c. This was also confirmed by the X-ray precession photographs. As a $\bar{6}$ axis was observed by means of the convergent beam electron diffraction(CBED) (Bando, 1984), the reasonable space group is $P\bar{6}$ or $P\bar{6}m2$. A discussion is also given in the section 3-5. An interesting imperfection in phase II crystals was observed by the 1-MV electron microscope. Figure 3-5 shows an electron micrograph of the phase II crystal from a very thin part of the crystal region. The incident electron beam was parallel to the [100] direction of the subcell. It is clear that the crystal is not perfect and there appeares to be "anti-phase boundaries(APB)" with the displacement vector of 1/2c. The size of antiphase domains varies from specimen to specimen. The problem of "APB" defect is to be treated in detail in the section 3-5.

3-4 Crystal Structure of Barium Hexaaluminate Phase I

Barium hexaaluminate phase I and phase II were shown to have the composition of $Ba_{0.75}Al_{11.0}O_{17.25}$ and $Ba_{2.34}Al_{21.0}O_{33.83}$, respectively. It was also suggested on the basis of the electron diffraction and crystallographic data that these were essentially of a beta-alumina structure. As yet, no refinement of the crystal structure has been made, so the detailed structure and the charge compensation mechanism for nonstoichio-

metry are not clearly determined.

In this section, the structure determination of barium hexaaluminate phase I by using the single-crystal X-ray reflection data is described and a charge compensation mechanism for nonstoichiometry is proposed on the basis of the refined parameters. After our work(Iyi et al., 1984) was published, van Berkel et al.(1984) reported the crystal structure of this compound independently. Their results and structure model are essentially the same as ours.

3-4-1 Experimental

Several spherical specimens were prepared from the single crystal which was grown by the FZ method. After examination by precession photographs, a spherical specimen of radius 92 um was used for the data collection. The intensities were measured below 2θ=120°, using the computer-controlled four-circle diffractometer with monochromated MoKα radiation. A set of standard reflections (107), (220), and (00,10) was measured every 50 reflections. The 836 independent non-zero reflections were corrected for Lorenz-polarization effects. The absorption factor for the chosen sample was uR = 0.335, and the data were corrected for this effect. Atomic scattering factors were taken from the I.T.(Vol. IV) and the values for the anomalous dispersion corrections for Ba were from the same reference (Vol. III). The lattice parameters are refined using 2θ-data of 20 reflections collected on the four-circle diffractometer. The refined lattice parameters are slightly diferent from those obtained by using powder diffraction data. Crystallographic data are shown in Table 3-5.

3-4-2 Refinement

In the section 3-3, barium hexaaluminate phase I was considered to be of a beta-alumina structure. For Fourier and difference Fourier syntheses, the positional parameters of Al(1)to Al(4) and O(1)to O(5) were chosen from the structure of K beta-alumina (Collin et al.,1977), and the Ba ion was placed in the ideal BR site. The Fourier sections, which corresponded to an R-value=0.318, revealed that main electron density differeces occurred in the mirror plane (z=0.25). The barium site was only partially occupied as anticipated from the formula $Ba_{0.75}Al_{11.0}O_{17.25}$. No unusual electron density variations were observed in the spinel block. Refinements were attempted on the occupation factor of Ba in addition to the general temperature factor and positional parameters, which led to the convergence with an R-value=0.157. In the subsequnet refinement individual isotropic temperature factors were introduced. At this stage an R-factor of 0.135 was obtained, but the isotropic temperature factor of oxygen at the 2c site (1/3, 2/3, 1/4) in the mirror plane increased anomalously to 2.0 as compared to 0.2-0.4 for the oxygen ions at other sites. Further refinements based on this simple beta-alumina model in which the Ba ion partially occupies the BR site turned out to be unsatisfactory.

Subsequent difference Fourier maps using the paramenters corresponding to an R-value of 0.135 revealed that the electron density distribution of Ba and oxygen in the mirror plane was distorted and triangular. After splitting the Ba and oxygen sites into 6h, the next refinement of general temperature factor, positional parameters, and the occupation factors of ions in the mirror plane resulted in an R-value of 0.083. Difference Fourier sections suggested additional electron density at the 2c site (z=0.25) and the 12k site near z=0.18. Electron density around

the 2c site could not be accounted for only by oxygen at the 6h site. The oxygen in the mirror plane would be probably distributed between the 2c and 6h sites. On the other hand, the atom occupying the 12k site near z=0.18 would be interstitial Al. The existence of interstitial Al was already reported in some beta-alumina compounds by Roth et al.(1977) and Collin et al.(1977). In the next refinement, occupation factors of Al(1), interstitial Al(5), O(5) at the 2c site, and O(6) at the 6h site were treated as additional variables. With a type I isotropic secondary extinction correction and individual isotropic temperature factors, the R-factor dropped to 0.043. Subsequent anisotropic refinements led to R=0.026 and wR=0.031, with unit weights. At this stage the difference Fourier synthesis still showed small amount of excess electron density (2.2 eA^{-3}) at the 6h site (x,2x,1/4) with x=0.88. This was assumed to be due to the interstitial oxygen as was already found in M^{+1} beta-alumina. With the interstitial oxygen as O(7), the last refinement with anomalous dispersion corrections yielded final R=0.023 and wR=0.027, with unit weights. The g-value for the secondary extinction was $1.36(6)x10^{4}$. Final difference electron maps showed random peaks and depression, not exceeding the maximum amplitued of +1 eA^{-3}. These final values of the positional and thermal parameters are given in Table 3-6. The interatomic distances and bound angles are presented in Tables 3-7 and 3-8, respectively.

3-4-3 Discussion

The refined parameters of barium hexaaluminate phase I completely corresponds to a beta-alumina structure in accordance with our assumption in the previous section. Accordingly, from the structural point of view, barium hexaaluminate phase I should be referred to as "barium beta-

alumina." The reason for the beta-alumina structure in the case of this hexaaluminate with Ba^{2+} ions, contrary to the other hexaaluminates containing divalent cations in the mirror plane, is probably because the configuration of the intermediate layer in a beta-alumina structure affords the more space for the larger Ba ion (compared with other divalent ions) than that in a magnetoplumbite structure, as pointed out by Stevels et al.(1976).

It is well-known that, in M^{+1} beta-aluminas (e.g., Collin et al., 1977), the monovalent cation distributes among the BR, aBR, and mO sites, with the ratio of distribution depending on the species of the large cation. In the case of barium beta-alumina, however, no significant electron density attributable to the Ba ion was detected at the aBR and mO sites. The Ba ion was found to be confined to the area near the BR site (Fig.3-6a).

Another point to be noted is the charge compensation mechanism for nonstoichiometry in this beta-alumina containing a divalent cation of Ba^{2+}. Difference Fourier maps clearly indicate additional maxima at the 12k site near z=0.18. The electron density section at z=0.177 after refinement is shown in Fig.3-6b. This site is consistent with the interstitial Al site as pointed out by Roth et al.(1977). The observed site occupancy of interstitial Al(5) is almost equal to the lack of Al(1), which suggests that the Frenkel defect mechanism proposed by Roth et al.(14) and Collin et al.(11) does operate in barium beta-alumina. Furthermore, the difference Fourier at R=0.026 showed small amounts of additional electron density at the 6h site(x, 2x, 1/4) with x=0.88. These were attributed to the interstitial oxygen bridging a pair of interstitial Al ions as already reported in M^{+1} beta-alumina. In fact, the

incorporation of interstitial oxygen as O(7) in the refinement resulted in the significant reduction of the R-factor, and after refinement the number of interstitial Al(5) per unit cell turned out to be nearly twice that of interstitial O(7). These results support the existence of intersitial oxygen in the mirror plane and are well consistent with the defect mechanism in which an interstitial oxygen bridges a pair of interstitial Al, as shown in Fig.3-7b. According to this defect mechanism, the Al ions do not directly participate in charge compensation because the number of Al ions in a unit cell does not change. It is the interstitial oxygens that compensate the extra charge due to Ba ions.

On the basis of the atomic parameters and supposed defect mechanism, a possible structure model for barium beta-alumina can be proposed. A Ba ion is located near the BR site and an interstitial oxygen is placed near the mO site. Simultaneous occupation by an interstitial oxygen and a barium ion in the same mirror plane of a single cell is, however, unacceptable owing to the large ionic radii of both atoms compared with the distance of 2.0 A between the Ba and O(7) sites. Accordingly two kinds of half unit cells with 1/2c dimension, each of which contains one mirror plane and one spinel block, can be supposed as shown in Figs.3-7a and b; one contains a barium ion and has the composition of "$BaAl_{11}O_{17}$" with a charge of +1, and the other contains an interstitial oxygen with the defect of barium ion in the mirror plane due to Reidinger defect of Al ions, the composition of which is "$OAl_{11}O_{17}$" with a charge of -3. To attain charge neutrality as a whole, the molar ratio of these two types of half cell should be 3 to 1. Furthermore, lack of superstructure reflections suggests random distribution of the two kinds of half unit cell throughout a crystal. Thus the formula of barium beta-alumina would be

necessarily $Ba_{0.75}Al_{11.0}O_{17.25}$. According to this structure model, it follows that the number per unit cell of Ba, Al(1), Al(5), and O(7) are 1.5, 11.0, 1.0, and 0.5, respectively. These values are consistent with the results obtained by X-ray structure analysis (Table 3-6). The obtained formula is also supported by the wet chemical analysis.

3-5 Crystal Structure of Barium Lead Hexaaluminate Phase II

From the chemical formula, electron diffraction data, and the presence of an $a\sqrt{3}$ x $a\sqrt{3}$ superstructure, it was presumed that barium hexaaluminate phase II, referred to as barium beta(II)-alumina, would have a beta-alumina-like structure with space group symmetry $P\bar{6}$ or $P\bar{6}m2$. A preliminary structure model, in which the mirror planes alternately consist of a fully occupied Ba-O layer and an excess Ba-O layer, was proposed by us (Iyi et al.,1983). Later Zandvergen et al.(1984) found "$1.31BaO{\cdot}6Ga_2O_3$" to have a similar structure by electron microscopic observation and elaborated our model by considering plausible defect mechanisms. But they presented no definite evidence for the model. Though Morgan & Shaw(1983) and Yamamoto & O'Keeffe(1984) also observed $a\sqrt{3}$ x $a\sqrt{3}$ superstructure for barium beta(II)-alumina, they clarified neither the chemical formula nor the basic structure type.

To clarify the crystal structure, it is desirable to obtain single crystals. For barium beta-alumina, single crystals were grown by the floating zone(FZ) method. Though single crystals of barium beta(II)-alumina were not obtained by the same method, single crystal growth of isostructural barium lead beta(II)-alumina was achieved from $PbO-PbF_2$

flux. About 20% of Ba was substituted by Pb ions in the yielded crystals.

The present section deals with the crystal structure of barium lead beta(II)-alumina revealed by X-ray single crystal diffraction; furthermore, the charge compensation mechanism, the causes of the superstructure, and the "APB" defect of barium beta(II)-alumina are discussed on the basis of the refined parameters.

3-5-1 Experimental

The specimens used for our structural investigation were taken from flux-grown crystals of barium lead beta(II)-alumina. PbO-PbF_2(1:1 in molar ratio) was used as the solvent and the crystal growth was accomplished under conditions already described. The chemical formula of the resulting crystal was found to be $(Ba_{0.8}Pb_{0.2})_{2.34}Al_{21.0}O_{33.84}$ by using EPMA data, lattice parameters, and density. Electron microscopy showed that large crystals had a tendency to contain defects of "antiphase boundary(APB)" with displacement vector 1/2c, which will be discussed in the final section. These crystals were examined also by the precession photographs using MoKα radiation. Diffuseness perpendicular to c^*-axis around (00$\underline{l}$) spots (where $\underline{l}$=odd) was observed for several large crystals of 0.2mm order, which may be due to "APB" defects. To avoid the "APB defects," smaller crystals were chosen, and furthermore, a specimen with clear (00$\underline{l}$) (where $\underline{l}$=odd) spots was selected for X-ray diffraction data collection. The selected hexagonal prism crystal was of dimension 0.05 x 0.05 x 0.08 mm. A preliminary study of Bando(1984) using the convergent beam electron diffraction (CBED) method indicated the presence of $\bar{6}$ axis, and suggested still two possibilities, either $P\bar{6}$ or $P\bar{6}m2$. So we accomplished the refinement, at first, by assuming $P\bar{6}$ symmetry, and then $P\bar{6}m2$.

The intensities were measured only on the Bragg reflections below $2\theta=120°$, using a computer-controlled four-circle diffractometer with monochromated MoKα radiation. A set of (220),(114) and (205) reflections was measured every 50 reflections as standard. The 596 independent nonzero reflections were collected, and successively subjected to the Lorenz-polarization and absorption corrections. X-ray absorption corrections were conducted using the linear absorption coefficient of μ= 71.6 cm^{-1}. Scattering factors were taken from the I.T.(Vol.IV)(1974) for neutral atoms. The lattice parameters were refined using 2θ-data of 19 reflections measured on the four-circle diffractometer. For the similarity to a beta-alumina structure, the nomenclature of the cation sites in the mirror plane is after that of Peters et al.(1971). The crystallographic data are shown in Table 3-9.

3-5-2 Refinement

At first, the Fourier and difference Fourier syntheses were accomplished using centro-symmetrical beta-alumina model with full occupancy of Ba at the BR site because of the similarity of barium lead beta(II)-alumina to a beta-alumina structure. The positional parameters were chosen from those of barium beta-alumina. Coordinates were adjusted to space group $P\bar{6}$ by moving the z=0.25 mirror plane of $P6_3/mmc$ to z=0.0. R-value was 0.287 at this stage. Because the starting model is centro-symmetrical, the resulting Fourier maps were also overlapped with their centro-symmetrical counterparts. These maps showed additional electron densities at (2/3,1/3,0.24) and (0.8,0.2,0.07) and their centro-symmetrical positions. Furthermore, defects of Ba(1) at z=0.0 and Ba(2) at z=0.5 were indicated. As previously described, electron microscopy revealed the non-

equivalency of Ba-O layers at z=0.0 and at z=0.5, so the starting model was modified by decreasing the occupancy of Ba(1) at z=0.0. By this treatment, the model lost centrosymmetry and successive Fourier syntheses indicated the addition of atoms at (2/3,1/3,0.24) and (0.85,0.15,0.07) more clearly. We assumed the former to be an inside-spinel Ba(and/or Pb) ion and the latter to be an interstitial Al ion as was found in barium beta-alumina. In addition, Al(1) at z=0.15 showed a little deficiency. Using an overall temperature factor, the refinement was accomplished on the modified model, with reduction of an R-value to 0.141. At this stage, difference Fourier maps still indicated another additional electron density at (2/3,1/3,0.22), which we supposed to be another inside-spinel large cation site. So we placed a Ba ion at this site with little occupancy in the next refinement. The R-value dropped to 0.101. The difference Fourier synthesis at the R-value of 0.101 still pointed out a small shift from the theoretical position of Ba(1) and Ba(2). The simultaneous change of coordinations and occupancies of Ba(1) and Ba(2) with other parameters met with failure in the least-squares refinement because of the high correlations between these parameters. So, the refinement was attempted by changing only one or two of the parameters at the same time, while the other parameters remained fixed. After the addition of O(11), which is bonded to the interstitial Al ion pair after the Reidinger defect mechanism, individual isotropic temperature factors were introduced. Because the difference Fourier maps still indicated the split of Al(5), O(9) and O(10) atoms, the refinement with these splitting atoms was further conducted step by step. Finally, all parameters were varied simultaneously with an R-value of 0.036 (wR= 0.040, w=1.0). At this stage, an elongated electron density just below O(3) at z=0.108 was

observed in the difference Fourier map, which we attributed to a partial shift of O(3). After the addition of O(12) at the site just below O(3), the final refinement with varying all parameters converged to R=0.030(wR=0.034, w=1.0). The final difference Fourier maps showed ramdom peaks and depressions not exceeding the range of - 1.1 to + 0.7 eA^{-3}. Anisotropic refinement was not attempted because there would be too many parameters compared with the number of observed diffraction data. Since the specimen contains about 20% Pb replacing Ba, the Pb ion should be included in the refinement procedure. For the reason to be described in the next section, Ba(4) was assumed to be the site where a large amount of Pb was concentrated. After changing Ba(4) into Pb, the refinement gave a total number of Ba and Pb as 2.27, which is in good agreement with the value of 2.34 deduced from EPMA data, lattice parameters, and density. The R-value did not change after these treatments.

As previously mentioned, there is another possibility of having space group symmetry $P\bar{6}m2$. The intensities hkl and khl were observed to have almost the same value, and, furthermore, the result of $P\bar{6}$ refinement showed that the y-coordinates were almost twice those of x. These facts indicate the space group $P\bar{6}m2$, of higher symmetry. The isotropic refinement using 432 independent reflections resulted in R=0.030 (wR=0.033, w=1.0) when adopting $P\bar{6}m2$ symmetry. No significant change in the coordinates and occupancies was observed, and also the R-value remained almost unchanged. Accordingly we adopted $P\bar{6}m2$ as the space group symmetry for barium beta(II)-alumina as well as barium lead beta(II)-alumina.

The atomic coordinates are shown in Table 3-10. Tables 3-11 and -12 contain the interatomic distances and the bond angles, respectively.

3-5-3 Discussion

In the previous section, the structure of barium beta(II)-alumina was supposed to be essentially of a beta-alumina type on the basis of the chemical formula $Ba_{2.34}Al_{21.0}O_{33.84}$. And, in the preliminary paper(Iyi et al.,1983), it was assumed that an "excess Ba-O layer" containing 1.33 Ba per mirror plane and a "fully occupied Ba-O layer" containing 1.0 Ba would stack alternately, each separated by a spinel block. The model of Zandvergen et al.(1984) is essentially a variation of this model, though a more elaborate one. Indeed the refined parameters clearly indicate isostructural barium lead beta(II)-alumina to be of a beta-alumina structure, but the number of Ba ions in a mirror plane per single unit cell does not exceed 1.0, which invalidates the concept of "excess Ba-O layer." Instead, there are two types of mirror planes; i.e. a defect Ba-O layer (z=0.0) and a fully occupied Ba-O layer(z=0.5). The latter layer contains no defects or interstitials in its neighborhood. These layers stack alternately being separated by a spinel block. Furthermore, excess Ba(Pb) ions were found inside the spinel blocks. The existence of "inside-spinel" sites seems to be very different from most other beta-alumina compounds. Only a few cases of inside-spinel sites occupied by a large cation have been reported(Roth, 1975; Anderson, 1981). For the beta-gallate system, it was observed that excess Na^+ in sodium beta-gallate substitutes for Ga^{3+} inside the spinel block, forming Na^+ tetrahedrons(Anderson, 1981). But this may not be the case with barium beta(II)-alumina or barium lead beta(II)-alumina as the radius of the Ba^{2+} ion(1.36A) or the Pb ion(1.18A)(Shannon & Prewitt, 1969) is very large compared with that of the Al^{3+} ion (0.53A) in the spinel block. So a different mechanism might operate in this case. The peculiar defects of

barium beta(II)-alumina described below afford a clue to the inside-spinel site formation.

In barium beta-alumina, interstitial Al and oxygen ions due to the Reidinger defects were observed. The same interstitial Al ion at z=0.07 and oxygen ion in the z=0.0 mirror plane were found. The fact that the number of atoms per unit cell of interstitial Al(8) at z=0.07 is almost the same as the number of defect atoms at the Al(1) site(z=0.15) and twice as many as that of interstitial O(11) in the mirror plane indicates that the defect mechanism is of the Reidinger type. In barium beta-alumina, the Reidinger defect occurs singly; in other words, only one of three Al(1) sites(z=0.15) becomes vacant with creation of an interstitial Al(8) according to the Frenkel defect mechanism and a pair of the interstitial Al(8) ions was bridged by an interstitial oxygen in the mirror plane (Fig.3-8a). These interstitials create a Ba vacancy in the z=0.0 mirror plane. Accordingly, the sum of the number of Ba and interstitial oxygens for one mirror plane of a single unit cell becomes unity in this case. On the other hand, in the case of barium lead beta(II)-alumina, it sums up to about 1.68, which is significantly larger than 1.0. Since Ba or Pb cannot coexist with interstitial Al and oxygen in the same mirror plane of a single unit cell from the viewpoint of ionic radius, it follows that the Reidinger defects should occur in multiple state in a mirror plane at z = 0.0 of a single unit cell. On the assumption that the Reidinger defects occur triply, the occupancy of the atoms in the z=0.0 mirror plane can be explained well. We would like to refer to this type of defect as "the triple Reidinger defects." As shown in Fig.3-8b, the interstitial oxygen O(11) ions are so crowded that electrostatic repulsion may cause the displacement from the ideal mO site(5/6,2/3,0.0) toward the

aBR site(0.0,0.0,0.0). In addition to interstitial oxygens, interstitial Al(8) also shifts a little from the ideal site (5/6,2/3,0.07) to (0.0,0.0,0.07), causing a partial shift of O(3) to O(12). Al(8) makes bonds to two O(12) and O(7) as well as O(11) forming a nondistorted tetrahedron.

Defects are not confined to these atoms but also exhibited in Al(4) and O(5) within the spinel block. The fact that occupancy of Al(4) of 0.74 is almost the same as that of Al(1) suggested to us the occurrence of the simultaneous defect of Al(4) and Al(1). In the case of Al(4) and Al(1) defects, O(5) remains surrounded by twelve oxygens as the nearest neighbors at a distance of about 2.8 A. Thus it is reasonable to assume that O(5) also becomes vacant simultaneously with Al(4) and Al(1). As shown in Table 3-10, however, the occupancy of O(5) is not consistent with this assumption. Probably this discrepancy can be attributed to the large electron density of Ba(3) ion at z=0.220 which, in the average structure, effects the occupancy of O(5) at z=0.200. The combination of the triple Reidinger defects and inside-spinel defects forms a 12-coordinated polyhedral site in the spinel block as shown in Fig.3-9, the site that Ba(Pb) ions occupy. In conclusion, the triple Reidinger defects together with Al(4) and O(5) defects produce a large 12-cornered polyhedral site inside the spinel block, where large cations as Ba and/or Pb are situated. Such an inside-spinel site has not been reported up to now.

The remaining problem is the species of the cation and the ratio of Pb/Ba at each large cation site. As the occupancy is varied at each large cation site in the refinement, the Pb/Ba ratio at each site cannot be determined exactly by the least-squares calculation. We noted that there exist two distinct inside-spinel sites, (2/3,1/3,0.22) and

(2/3,1/3,0.24). The latter site may as well be called "9-coordinated polyhedral site" rather than "distorted" 12-coordinated polyhedral site. Here we supposed that the large cation sites of (2/3,1/3,0.22) and (2/3,1/3,0.24) are attributable to Ba and Pb ions, respectively. This assumption is based on the following reasons: At the site(2/3,1/3,0.24), the distance to the nearest oxygen O(2) is only 2.3 A, which is too short for the large Ba-O distance of about 2.8 - 3.0 A. It would be better to assume that the smaller Pb ion might be situated at this site (2/3,1/3,0.24). The refinement was accomplished on this assumption with the result that total number of Ba and Pb cations per unit cell is 2.27, which is in good agreement with the value of 2.34 deduced from EPMA, density, and lattice parameters. The ratio Pb/Ba becomes about 0.20, which is only a little smaller than the previously reported value of 0.25. So, it may be that Pb ions are concentrated at the site (2/3,1/3,0.24), although a small amount of Pb ions might substitute for Ba ions at the other site.

On the basis of the atomic parameters of the average structure and defect mechanism discussed above, we can propose a structure model for barium lead beta(II)-alumina after the method used for elucidation of the structure of barium beta-alumina and rare-earth hexaaluminates. Because simultaneous occupation of the Ba ion, and interstitial Al and O ions is not possible in the same mirror plane of a single unit cell, we can assume at least two types of unit cells in barium lead beta(II)-alumina as shown in Figs.3-10a and b. In one kind of unit cell, one Ba ion is situated near the BR site at z = 0.0, so the composition is "$Ba_2Al_{22}O_{34}$" with charge of +2. This cell contains no defects and shows an ideal formula of beta-alumina($MAl_{11}O_{17}$, where M=large cation). In contrast, the defect

of a Ba ion at z=0.0, the triple Reidinger defects and defects of Al(4) and O(5) take place in the other kind of unit cell, the composition of which becomes "$(BaPb)_3Al_{20}O_{35}$" with the charge of -4. As there is no evidence for other types of cells, we supposed that these perfect and defect cells constitute barium lead beta(II)-alumina. These cells are not electrostatically neutral, so the ratio for perfect cell to defect cell would be 2 to 1. The comparison of the occupancy deduced from the structure model and the refined parameters are given in Table 3-13. These data are in good agreement except for O(5) probably for the reason already described in this section. The resulting chemical formula "$(BaPb)_{2.33}Al_{21.33}O_{34.33}$" based on the model is very near to the formula "$(Ba_{0.8}Pb_{0.2})_{2.34}Al_{21.00}O_{33.84}$" obtained by using EPMA, lattice parameters, and density data. This structure model can be directly applied to pure barium beta(II)-alumina. Furthermore, it seems that this peculiar structure is not confined to barium beta(II)-alumina. Zandvergen et al. (1984) reported the compound "$1.31BaO{\cdot}6Ga_2O_3$", and presented its structure image, which resembled that obtained for barium beta(II)-alumina by using high-resolution electron microscope(Bando, 1984). Probably barium beta(II)-alumina and "$1.31BaO{\cdot}6Ga_2O_3$" are isostructural compounds.

The structure model described above is readily applicable to explain the intergrowth phenomenon reported by several works (Morgan & Shaw, 1983; Yamamoto & O'Keeffe, 1984), and the presence of "APB"(Iyi et al.,1983; Zandbergen et al.,1984) and the superstructure. The $a\sqrt{3}$ x $a\sqrt{3}$ superstructure is very characteristic of beta(II)-alumina compounds, and has been observed by these researchers. This superstructure can be attributed to these three cells (two perfect cells and one defect cell), which form a large unit cell as shown in Fig.3-11. In the figure the

defect cells are so arranged as not to be adjacent to each other. The diffuse reflections along c^*-axis observed previously can also be explained by assuming that there are almost no correlations between the defect Ba-O layers in arrangement of the mirror planes containing the interstitial oxygen ions.

The problem of the intergrowth can be also clearly solved. The intergrowth between barium beta-alumina and barium beta(II)-alumina was observed in the sintered specimens (Morgan & Shaw, 1983; Yamamoto & O'Keeffe, 1984). It could be also observed in the crystal boules grown by using the intermediate composition as the starting materials. In the previous section, barium beta-alumina was revealed to be composed of a fully occupied half cell "$BaAl_{11}O_{17}$" and a defect half cell "$\square Al_{11}O_{17}$." The former is also a component of barium beta(II)-alumina. The presence of the cell, common to these two compounds, would be the reason for the intergrowth between barium beta-alumina and barium beta(II)-alumina, formed probably under the inhomogeneous growth conditions. In Fig.3-12, the intergrowth between them is depicted. The solid solution range reported by Stevels(1978) is, in reality, due to the intergrowth phenomenon of barium beta- and beta(II)-aluminas. He accomplished the solid state reaction at low temperature, which would favor the intergrowth.

Another problem concerns "APB" of barium beta(II)-alumina. It was mentioned that the boundary shown in Fig.3-4 was "APB" (anti-phase boundary) with a displacement vector of 1/2 c. Indeed, when only two kinds of BaO layers are taken into consideration, this nomenclature may not be wrong, but spinel blocks do not fit with those which have migrated by 1/2 c. It would be reasonable to think that the coherency of the spinel block is preserved across the "APB." Accordingly, it would be

better to consider the boundary to be a twin boundary instead of APB. Twins are related by glide reflection in (100) plane. Between twins, the c-axis is held in common, and the a-, and b- axes are placed in parallel but opposite directions. From the viewpoint of the origin, it may be a growth twin, and, from the viewpoint of the axial relations, it would be called a "coaxial twin" (Takano, 1973). As long as the size of twin domain is large, the intensities of X-ray reflections would not be influenced by twinning. The schematic representation of twin model is given in Fig.3-13.

3-6 The Crystal Structure of Mg-doped Barium Hexaaluminate

At present, two compounds, $BaMgAl_{10}O_{17}$ and $BaMg_3Al_{12}O_{21}$, are known as Mg-doped barium hexaaluminate compounds(Stevel, 1976; Kimura, 1983). As can be seen from the formula, $BaMgAl_{10}O_{17}$ is supposed to have a beta-alumina structure (Stevel, 1976), but the structure analysis has not been made. In this section, the crystal structure of $BaMgAl_{10}O_{17}$ is described.

3-6-1 Experimental and Refinement

The single crystal of "$BaMgAl_{10}O_{17}$" was grown by the FZ method using a xenon arc lamp as the heat source (Kimura, 1983). The growth rate was 1 mm/hr and nitrogen was used as the growth atmosphere. The grown boule was in large part "$BaMgAl_{10}O_{17}$", but a small amount of $BaMg_3Al_{14}O_{25}$ coexisted in the center of the boule. Part of "$BaMgAl_{10}O_{17}$" was analyzed by EPMA, which showed a small amount of Ba-deficiency from the ideal composition $BaMgAl_{10}O_{17}$. The chemical formula was determined to be $Ba_{0.955}Mg_{0.962}Al_{10.056}O_{17.0}$. In this calculation the number of oxygen per unit formla was assigned to 17.0. Ba-deficiency of "Ba·Mg beta-alumina" was already noted in the phase study of Kimura(1983). This compound is referred to as $Ba_{0.955}$·Mg beta-alumina.

The structure of $Ba_{0.955}$·Mg beta-alumina was refined in a similar way to barium beta-alumina. The specimen was ground to a sphere with radius of 70μ , and the collected non-zero unique intensity data amounted to 677. Absorption corrections were also applied in this case, as the linear absorption coefficient was 42.7 cm^{-1}. The structure of $Ba_{0.955}$·Mg beta-alumina was refined without any troubles. The refinement was carried out with the positional parameters of barium beta-alumina(not including

interstitials) used as the starting parameters. (R = 0.122). The refinement using a general temperature factor gave R=0.045 when the occupancy of Ba was varied. Further isotropic refinement reduced the R-factor to 0.035. The final anisotropic refinement converged to yield R=0.031 (wR=0.035, w=1.0). The difference Fourier synthesis at the last stage showed featureless depressions and peaks within the limit of +1.1 to -1.2 e/A^3 with an exception of the slightly large peak of 2.9 e/A^3 at (1/3,2/3,0.23).

Crystallographic data are shown in Table 3-14. Refined parameters are given in Table 3-15, and the bond length and angles are presented in Tables 3-16 and 17, respectively.

3-6-2 Results

The refinement showed $Ba_{0.955}$·Mg beta-alumina to be a typical beta-alumina, having Ba at the BR site and without any interstitial ions. From the bond lengths, Mg is supposed to be situated at the Al(2) tetrahedral site within the spinel block, as was found in other Mg-doped beta-alumina compounds (Collin et al., 1980). The $Ba_{0.955}$·Mg beta-alumina used for refinement had slightly less Ba-content than the ideal formula $BaMgAl_{10}O_{17}$. Table 3-14 contains the composition of both Mg-doped compounds calculated from the occupancy obtained in the refinements. From EPMA data (Table 4-2), we obtained a formula, $Ba_{0.955}Mg_{0.962}Al_{10.056}O_{17.0}$. In these calculations the number of oxygen per unit formula was assigned to 17.0. The formulae derived from X-ray data and from EPMA data agreed very well with each other.

The positional and thermal parameters

Position		Number per unit cell	x	z	$\beta 11 \times 10^4$	$\beta 22 \times 10^4$	$\beta 33 \times 10^5$	$\beta 23 \times 10^5$
Pb	2d	2	2/3	1/4	112(2)	$\beta 11$	75(2)	0
Al(1)	12k	12	0.8317(4)	0.1080(1)	33(5)	30(7)	21(3)	6(21)
Al(2)	4f	4	1/3	0.02809(18)	30(8)	$\beta 11$	13(5)	0
Al(3)	4f	4	1/3	0.19013(18)	34(8)	$\beta 11$	21(5)	0
Al(4)	2a	2	0	0	21(13)	$\beta 11$	30(9)	0
Al(5)	2b	2	0	0.2406(5)	31(17)	$\beta 11$	96(31)	0
O(1)	12k	12	0.1545(7)	0.0519(2)	45(12)	34(22)	15(5)	-7(30)
O(2)	12k	12	0.5016(7)	0.1471(2)	41(13)	57(19)	12(6)	11(34)
O(3)	4f	4	2/3	0.0541(4)	19(16)	$\beta 11$	34(12)	0
O(4)	4e	4	0	0.1479(4)	14(18)	$\beta 11$	36(14)	0
O(5)	6h	6	0.1823(11)	1/4	50(21)	98(41)	42(10)	0

The thermal parameters are of the form : $\exp[-(h^2\beta 11 + k^2\beta 22 + l^2\beta 33 + 2hk\beta 12 + 2hl\beta 13 + 2kl\beta 23)]$. $\beta 12 = 1/2\,\beta 22$; $\beta 13 = 1/2\,\beta 23$.

Table 3-1. The positional and thermal parameters of Pb hexaaluminate.

INTERATOMIC DISTANCES

	Number of bonds	Distance (A)
	Octahedral coordination	
Al(1) - O(1)	2	1.992(7)
- O(2)	2	1.811(7)
- O(3)	1	1.987(6)
- O(4)	1	1.847(6)
Al(3) - O(2)	3	1.880(7)
- O(5)	3	1.966(8)
Al(4) - O(1)	6	1.879(6)
	Tetrahedral coordination	
Al(2) - O(1)	3	1.804(7)
- O(3)	1	1.812(10)
	Polyhedron 5-coordinated	
Al(5) - O(4)	1	2.044(14)
- O(4)'	1	2.458(14)
- O(5)	3	1.771(11)
	Polyhedron 12-coordinated	
Pb - O(2)	6	2.772(5)
- O(5)	6	2.790(9)

Table 3-2. Interatomic distances of Pb hexaaluminate.

BOND ANGLES

	Bond angles (°)
Octahedral coordination	
O(1) - Al(1) - O(1)'	80.80(37)
- O(2)	89.75(29)
- O(3)	88.98(26)
- O(4)	84.71(24)
O(2) - Al(1) - O(3)	86.12(21)
- O(4)	99.20(25)
O(2) - Al(3) - O(2)'	96.79(25)
- O(5)	91.07(33)
O(5) - Al(3) - O(5)'	79.87(34)
O(1) - Al(4) - O(1)'	86.79(24)
- O(1)"	93.21(24)
Tetrahedral coordination	
O(1) - Al(2) - O(1)'	111.90(17)
- O(3)	106.92(19)
Polyhedron 5-coordinated	
O(5) - Al(5) - O(4)	96.72(36)
- O(4)'	83.28(36)
- O(5)'	118.65(14)

Table 3-3. Bond angles of Pb hexaaluminate.

CRYSTALLOGRAPHIC DATA

Formula	$Ba_{2.34}Al_{21.0}O_{33.84}$
Symmetry	hexagonal
Space group	$P\bar{6}m2$
a =	5.601 A
c =	22.91 A
V =	622.42 A^3
Z =	1

Table 3-4. Crystallographic data of Ba-phase II.

CRYSTALLOGRAPHIC DATA

Formula	$Ba_{0.75}Al_{11.0}O_{17.25}$
Symmetry	hexagonal
Space group	$P6_3/mmc$
a =	5.588(2) A
c =	22.769(9) A
V =	615.7(4) A^3
Z =	2
$D_{obs.}$ =	3.657 gcm^{-3}

Table 3-5. Crystallographic data of Ba beta-alumina.

	Position	Number per unit cell	x	z	$\beta 11 \times 10^5$	$\beta 22 \times 10^5$	$\beta 33 \times 10^6$	$\beta 23 \times 10^6$	B
Ba	6(h)	1.485(6)	0.6717(6)	1/4	1144(19)	2514(150)	197(4)	0	
Al(1)	12(k)	10.86(4)	0.83256(8)	0.10462(2)	576(15)	461(19)	212(6)	-259(35)	
Al(2)	4(f)	4	1/3	0.02356(4)	381(17)	β11	164(9)	0	
Al(3)	4(f)	4	1/3	0.17537(4)	907(22)	β11	146(10)	0	
Al(4)	2(a)	2	0	0	502(26)	β11	166(14)	0	
Al(5)[b]	12(k)	0.93(3)	0.8426(8)	0.1769(3)	136(141)	110(202)	146(66)	-12(311)	
O(1)	12(k)	12	0.1580(1)	0.04953(5)	822(27)	395(35)	245(10)	80(66)	
O(2)	12(k)	12	0.5039(2)	0.14721(5)	534(23)	670(37)	422(13)	-281(73)	
O(3)	4(f)	4	2/3	0.05574(8)	652(36)	β11	175(19)	0	
O(4)	4(e)	4	0	0.14110(8)	468(32)	β11	211(21)	0	
O(5)	2(c)	0.38(9)	1/3	1/4					0.4(4)
O(6)	6(h)	1.63(10)	0.290(2)	1/4	2601(348)	2451(754)	104(54)	0	
O(7)[b]	6(h)	0.55(4)	0.881(3)	1/4					0.9(6)

[a] The thermal parameters are of the form : $\exp[-(h^2\beta 11 + k^2\beta 22 + l^2\beta 33 + 2hk\beta 12 + 2hl\beta 13 + 2kl\beta 23)]$.
$\beta 12 = 1/2\ \beta 22$; $\beta 13 = 1/2\ \beta 23$.

[b] Interstitials.

Table 3-6. The positional and thermal parameters of Ba beta-alumina.

	Number of bonds	distance (Å)
Octahedral coordination		
Al(1) - O(1)	2	2.015(2)
- O(2)	2	1.863(2)
- O(3)	1	1.954(2)
- O(4)	1	1.821(2)
Al(4) - O(1)	6	1.900(2)
Tetrahedral coordination		
Al(2) - O(1)	3	1.797(2)
- O(3)	1	1.806(3)
Al(3) - O(2)	3	1.771(2)
- O(5)	1	1.699(2)
Al(5) - O(2)	2	1.777(7)
- O(4)	1	1.728(8)
- O(7)	1	1.705(9)
Polyhedron 9-coodinated		
Ba - O(2)	4	2.808(4)
- O(2)'	2	2.849(4)
- O(5)	2	3.202(5)
- O(5)'	1	3.275(6)

Table 3-7. Interatomic distances of Ba beta-alumina.

	Bond angles (°)
Octahedral coordination	
O(1) - Al(1) - O(1)'	82.18(9)
O(1) - Al(1) - O(2)	91.68(9)
O(1) - Al(1) - O(3)	89.67(7)
O(1) - Al(1) - O(4)	84.63(7)
O(2) - Al(1) - O(2)'	94.14(13)
O(2) - Al(1) - O(3)	86.31(9)
O(2) - Al(1) - O(4)	98.81(7)
O(1) - Al(4) - O(1)'	88.40(9)
O(1) - Al(4) - O(1)"	91.60(9)
Tetrahedral coordination	
O(1) - Al(2) - O(1)'	109.77(10)
O(1) - Al(2) - O(3)	109.16(10)
O(2) - Al(3) - O(2)'	107.64(11)
O(2) - Al(3) - O(5)	111.25(10)
O(2) - Al(3) - O(6)	103.9(7)
O(2) - Al(3) - O(6)'	125.1(6)
O(2) - Al(5) - O(2)'	100.3(4)
O(2) - Al(5) - O(4)	105.9(4)
O(2) - Al(5) - O(7)	118.9(12)
O(4) - Al(5) - O(7)	105.6(10)

Table 3-8. Bond angles of Ba beta-alumina.

CRYSTALLOGRAPHIC DATA [a]

Formula	$(Ba_{0.80}Pb_{0.20})_{2.34}Al_{21.0}O_{33.84}$
Symmetry	hexagonal
Space group	$P\bar{6}m2$
a =	5.6003(5)Å
c =	22.922(2)Å
V =	622.57(9)Å^3
Z =	1
$D_{obs.}$ =	3.88 gcm^{-3}

[a] For subcell structure.

Table 3-9. Crystallographic data of BaPb beta(II)-alumina.

THE POSITIONAL[a] AND THERMAL PARAMETERS

Atom	Position	Number per unit cell	x	z	B[b]
Ba(1)	3j	0.685(10)	0.6770(12)	0	0.73(7)
Ba(2)	3k	1.002(10)	0.3202(6)	1/2	0.51(5)
Ba(3)	2i	0.211(19)	2/3	0.2202(6)	0.35(21)
Pb	2i	0.375(9)	2/3	0.2422(2)	0.42(6)
Al(1)	6n	3.96(7)	0.8351(8)	0.1515(2)	0.35(7)
Al(2)	6n	6	0.1660(6)	0.3573(1)	0.34(3)
Al(3)	2h	2	1/3	0.2302(3)	0.44(8)
Al(4)	2i	1.48(5)	2/3	0.2767(3)	0.54(15)
Al(5)	6n	1.99(6)	0.3084(9)	0.0741(3)	0.20(16)
Al(6)	2i	2	2/3	0.4249(2)	0.26(7)
Al(7)	2g	2	0	0.2532(3)	0.18(6)
Al(8)[c]	6n	1.90(8)	0.8565(10)	0.0694(3)	0.19(16)
O(1)	6n	6	0.1607(12)	0.2062(3)	0.86(10)
O(2)	6n	6	0.8460(10)	0.3048(2)	0.50(9)
O(3)	6n	4.76(18)	0.5053(16)	0.1080(4)	0.84(18)
O(4)	6n	6	0.4942(11)	0.3996(3)	0.53(10)
O(5)	2i	1.86(18)	2/3	0.2004(10)	0.64(26)
O(6)	2h	2	1/3	0.3102(5)	0.46(16)
O(7)	2g	2	0	0.1131(5)	0.29(17)
O(8)	2g	2	0	0.3962(5)	0.33(16)
O(9)	3j	1.18(10)	0.261(4)	0	2.3(8)
O(10)	3k	1	0.686(4)	1/2	0.40(42)
O(11)[c]	3j	0.99(10)	0.916(4)	0	1.1(6)
O(12)	6n	1.67(18)	0.494(3)	0.0827(9)	0.23(37)

[a] $y = 2x$.

[b] Isotropic temperature factor ($Å^2$).

[c] Interstitials.

Table 3-10. The positional and thermal parameters of BaPb beta(II)-alumina.

	Number of bonds	Distance(Å)
	Octahedral coordination	
Al(1) - O(1)	2	2.017(11)
- O(3)	2	1.886(14)
- O(5)	1	1.982(15)
- O(7)	1	1.826(9)
Al(2) - O(2)	2	1.966(9)
- O(4)	2	1.865(10)
- O(6)	1	1.949(8)
- O(8)	1	1.841(8)
Al(7) - O(1)	3	1.895(11)
- O(2)	3	1.905(9)
	Tetrahedral coordination	
Al(3) - O(1)	3	1.763(12)
- O(6)	1	1.833(13)
Al(4) - O(2)	3	1.854(10)
- O(5)	1	1.748(24)
Al(5) - O(3)	2	1.744(18)
- O(9)	1	1.759(12)
- O(12)	1	1.810(28)
Al(6) - O(4)	3	1.771(10)
- O(10)	1	1.731(6)
Al(8) - O(7)	1	1.715(11)
- O(11)	1	1.694(15)
- O(12)	2	1.790(24)
(- O(3)	2	1.93(2))
	Polyhedron 9-coordinated	
Ba(1) - O(3)	6	2.931(13) (averaged)
- O(9)	3	2.95(4) (averaged)
Ba(2) - O(4)	6	2.783(9) (averaged)
- O(10)	3	3.14(4) (averaged)
	Inside-spinel site	
Ba(3) - O(1)	6	2.819(10)
- O(2)	3	2.604(13)
- O(12)	3	3.570(26)
(- O(3)	3	3.011(16))
Pb - O(1)	6	2.920(10)
- O(2)	3	2.255(9)
(- O(3)	3	3.450(12))

Table 3-11. Interatomic distances of BaPb beta(II)-alumina.

	Bond angles (°)
Octahedral coordination	
O(1) - Al(1) - O(1)'	84.04(62)
- O(3)	91.78(58)
- O(5)	89.05(54)
- O(7)	86.76(56)
O(3) - Al(1) - O(3)'	91.92(88)
- O(5)	85.82(70)
- O(7)	98.08(55)
O(2) - Al(2) - O(2)'	82.31(52)
- O(4)	92.29(44)
- O(6)	91.54(33)
- O(8)	85.03(39)
O(4) - Al(2) - O(4)'	92.84(62)
- O(6)	84.91(40)
- O(8)	98.21(40)
O(1) - Al(7) - O(1)'	90.88(44)
- O(2)	91.73(36)
O(2) - Al(7) - O(2)'	85.54(39)
Tetrahedral coordination	
O(1) - Al(3) - O(1)'	110.72(31)
- O(6)	108.19(32)
O(2) - Al(4) - O(2)'	108.63(27)
- O(5)	110.30(26)
O(3) - Al(5) - O(3)'	111.87(62)
- O(9)	110.0(15)
- O(12)	106.8(9)
O(9) - Al(5) - O(12)	111.2(14)
O(4) - Al(6) - O(4)'	109.80(27)
- O(10)	105.9(11)
O(7) - Al(8) - O(11)	105.7(14)
- O(12)	110.8(10)
O(11)- Al(8) - O(12)	110.6(13)
O(12)- Al(8) - O(12)'	108.2(17)
(O(3) - Al(8) - O(11)	128.1(9))

Table 3-12. Bond angles of BaPb beta(II)-alumina.

	The number of atoms per unit cell	
Atom	Result of refinement	Model
Ba(1)	0.685(10)	0.667
Ba(2)	1.002(10)	1.000
Ba(3)	0.211(19)	0.20
Pb	0.375(9)	0.467
Al(1)	3.96(7)	4.00
Al(4)	1.48(5)	1.33
Al(5)	1.99(6)	2.00
Al(8)	1.90(8)	2.00
O(3)	4.76(18)	4.00
O(5)	1.86(18)	1.33
O(9)	1.18(10)	1.00
O(11)	0.99(10)	1.00
O(12)	1.67(18)	2.00

Table 3-13. Comparison of the site occupancy between the model and the refined parameters of BaPb beta(II)-alumina.

Formula	$Ba_{0.956}Mg_{0.912}Al_{10.088}O_{17.0}$
Symmetry	hexagonal
Space group	$P6_3/mmc$
a =	5.6275(7) Å
c =	22.658(7) Å
V =	621.42(21) $Å^3$
Z =	2
$D_{calc.}$ =	3.728 gcm^{-3}

Table 3-14. Crystallographic data of Ba·Mg beta-alumina.

The positional and thermal[a] parameters of $Ba_{0.956}$·Mg β-alumina

Position		Number per unit cell	x	z	$\beta 11 \times 10^4$	$\beta 22 \times 10^4$	$\beta 33 \times 10^5$	$\beta 23 \times 10^5$
Ba	2d	1.912(9)	0.6778(11)	1/4	80(9)	89(19)	26(1)	0
Al(1)	12k	12	0.8343(1)	0.10544(4)	32(2)	33(3)	24(1)	-3(6)
Al(2)	4f	4	1/3	0.02400(7)	50(4)	β 11	25(2)	0
Al(3)	4f	4	1/3	0.17416(7)	33(3)	β 11	18(2)	0
Al(4)	2a	2	0	0	29(5)	β11	18(3)	0
O(1)	12k	12	0.1534(3)	0.05152(9)	55(5)	67(9)	27(2)	-31(12)
O(2)	12k	12	0.5042(3)	0.14799(9)	43(5)	41(6)	30(3)	7(13)
O(3)	4f	4	2/3	0.05901(17)	39(7)	β 11	45(5)	0
O(4)	4e	4	0	0.14437(16)	42(7)	β 11	27(4)	0
O(5)	2c	2	1/3	1/4	198(19)	β11	28(7)	0

[a] The thermal parameters are of the form : $\exp[-(h^2\beta 11 + k^2\beta 22 + l^2\beta 33 + 2hk\beta 12 + 2hl\beta 13 + 2kl\beta 23)]$. $\beta 12 = 1/2\ \beta 22$; $\beta 13 = 1/2\ \beta 23$.

Table 3-15. The positional and thermal parameters of Ba·Mg beta-alumina.

	Number of bonds	Distance (Å)
Octahedral coordination		
Al(1) - O(1)	2	1.980(3)
- O(2)	2	1.876(3)
- O(3)	1	1.943(3)
- O(4)	1	1.841(2)
Al(4) - O(1)	6	1.897(3)
Tetrahedral coordination		
Al(2) - O(1)	3	1.862(3)
- O(3)	1	1.881(4)
Al(3) - O(2)	3	1.768(3)
- O(5)	1	1.718(2)
Polyhedron 9-coordinated		
Ba - O(2)	4	2.773(6)
- O(2)'	2	2.865(7)
- O(5)	2	3.196(9)
- O(5)'	1	3.358(11)

Table 3-16. Interatomic distances of Ba·Mg beta-alumina.

	Bond angles (°)
	$Ba_{0.956}$·Mg-β
Octahedral coordination	
O(1) - Al(1) - O(1)'	81.63(15)
- O(2)	92.06(12)
- O(3)	91.98(11)
- O(4)	84.89(13)
O(2) - Al(1) - O(2)'	93.96(17)
- O(3)	84.32(13)
- O(4)	98.48(12)
O(1) - Al(4) - O(1)'	86.08(10)
- O(1)"	93.92(10)
Tetrahedral coordination	
O(1) - Al(2) - O(1)'	109.38(8)
- O(3)	109.57(8)
O(2) - Al(3) - O(2)'	109.34(9)
- O(5)	109.60(8)

Table 3-17. Bond angles of Ba·Mg beta-alumina.

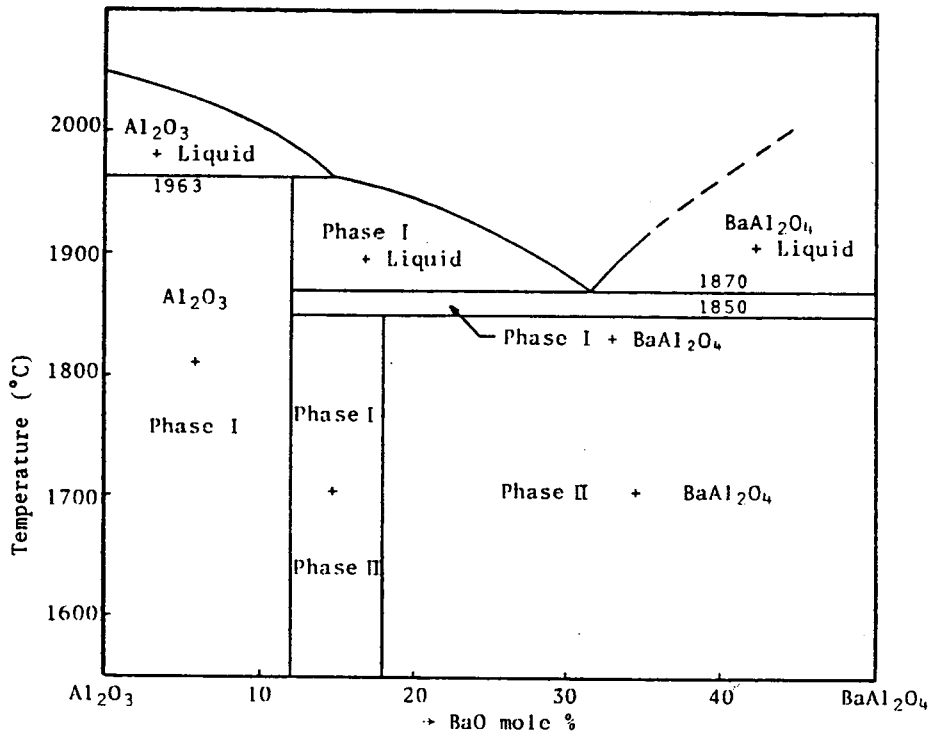

Fig.3-1. Phase diagram of the system Al_2O_3-$BaAl_2O_3$.

(Kimura et al., 1982).

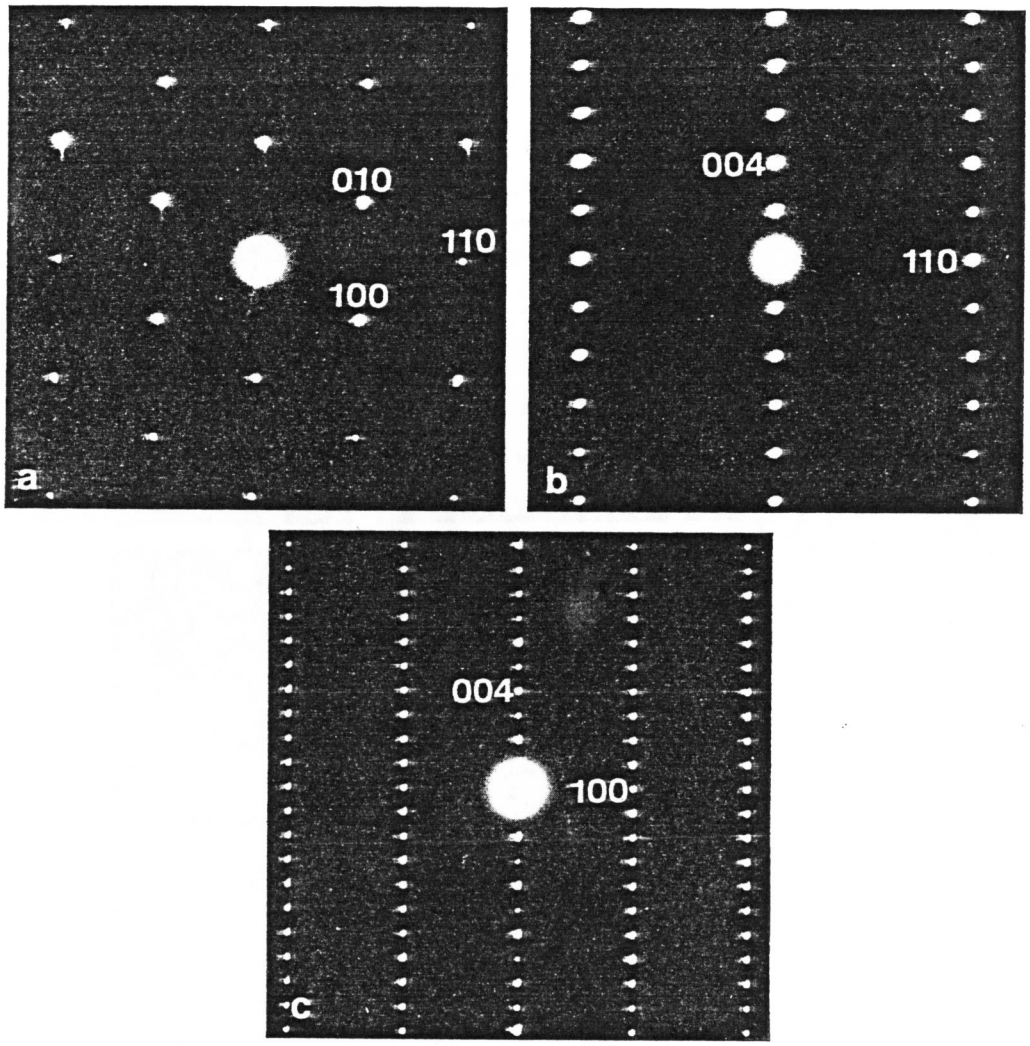

Fig.3-2. Electron diffraction patterns from Ba-phase I crystal fragments. The incident beam is normal to the (a) (001), (b) (100), and (c) (110) planes.

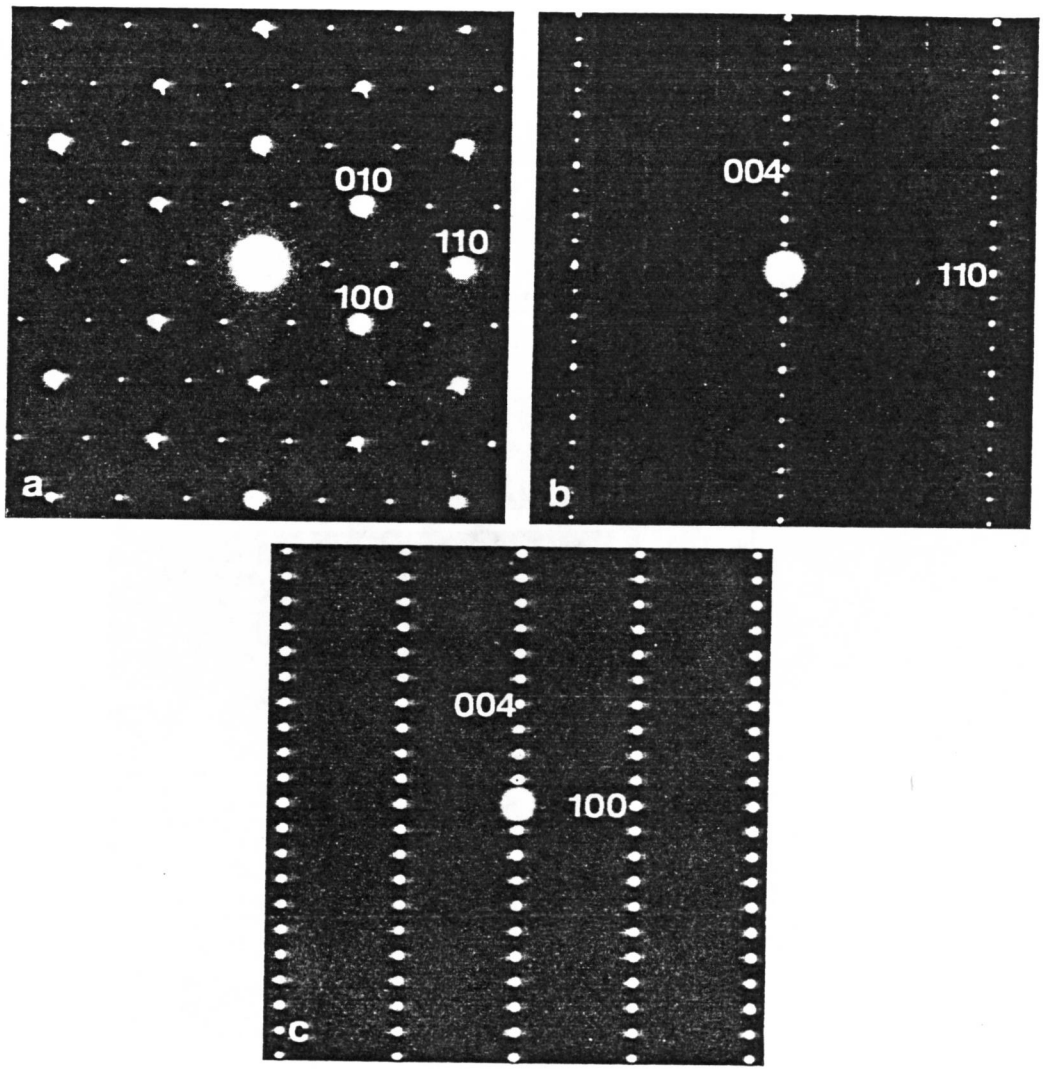

Fig.3-3. Electron diffraction patterns from Ba-phase II crystal fragments. The incident beam is normal to the (a) (001), (b) (100), and (c) (110) planes. The indices are based on the beta-alumina-type subcell.

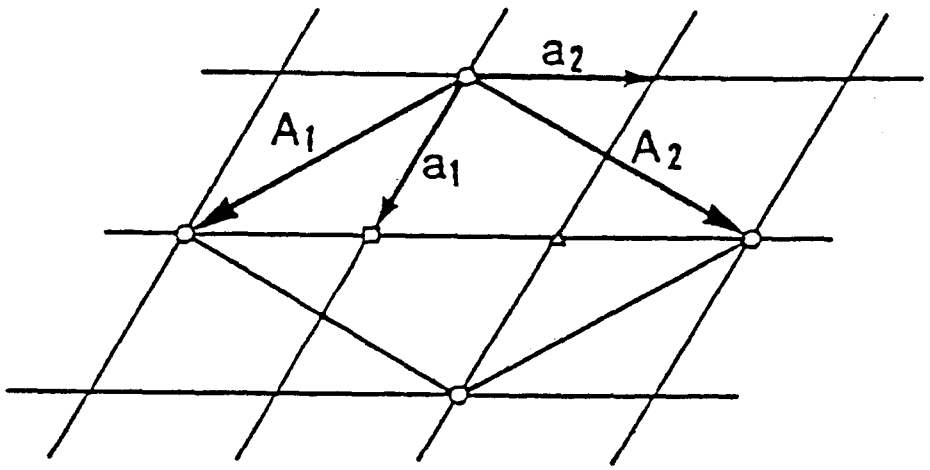

Fig.3-4. Lattice relation between subcell and superstructure cell (supercell) of Ba-phase II projected on the c plane. The a_1 and a_2 are lattice vectors of subcell, and A_1 and A_2 are those of supercell.

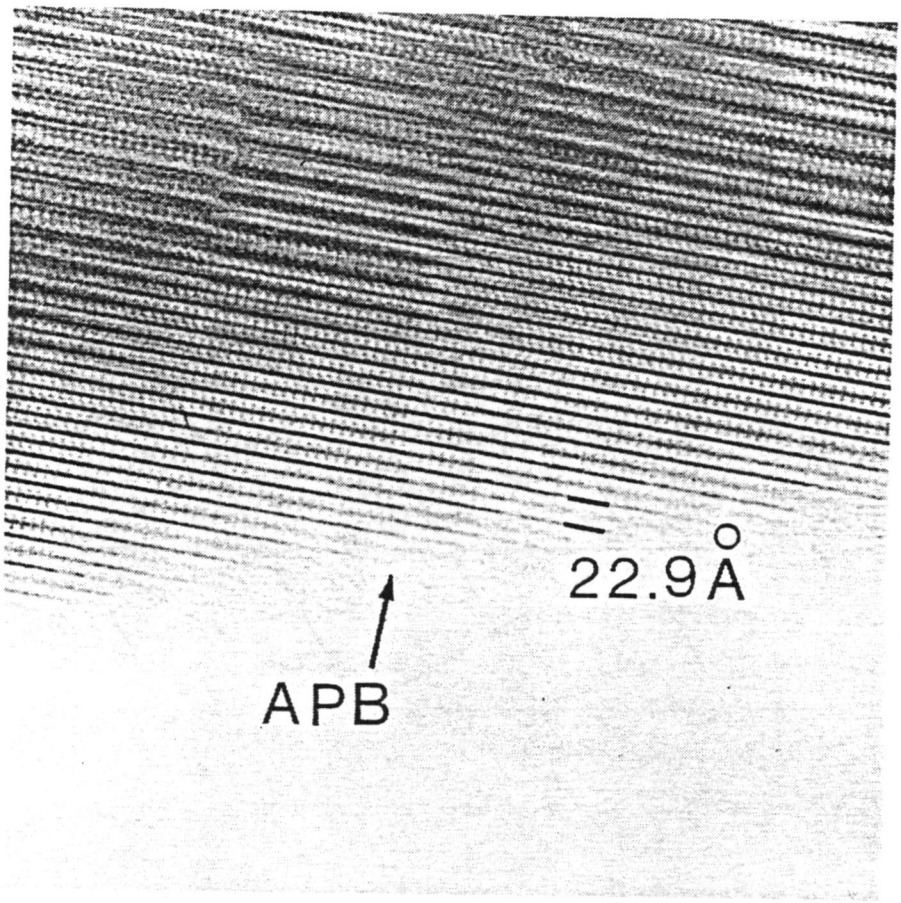

Fig.3-5. Electron micrograph of Ba-phase II projected along [100] direction, revealing the existence of an "anti-phase boundary(APB)". In reality, it is twin boundary as discussed in section 3-5.

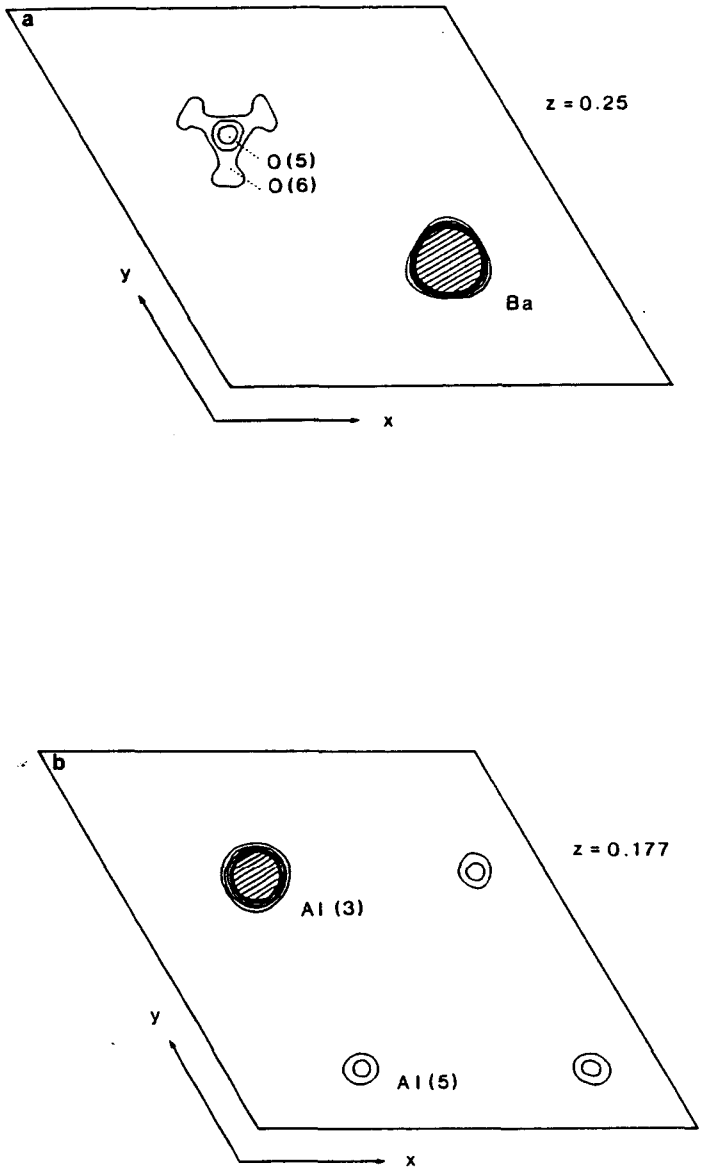

Fig.3-6. Electron density of Ba beta-alumina at the sections of (a) z = 0.25 and (b) z = 0.177.

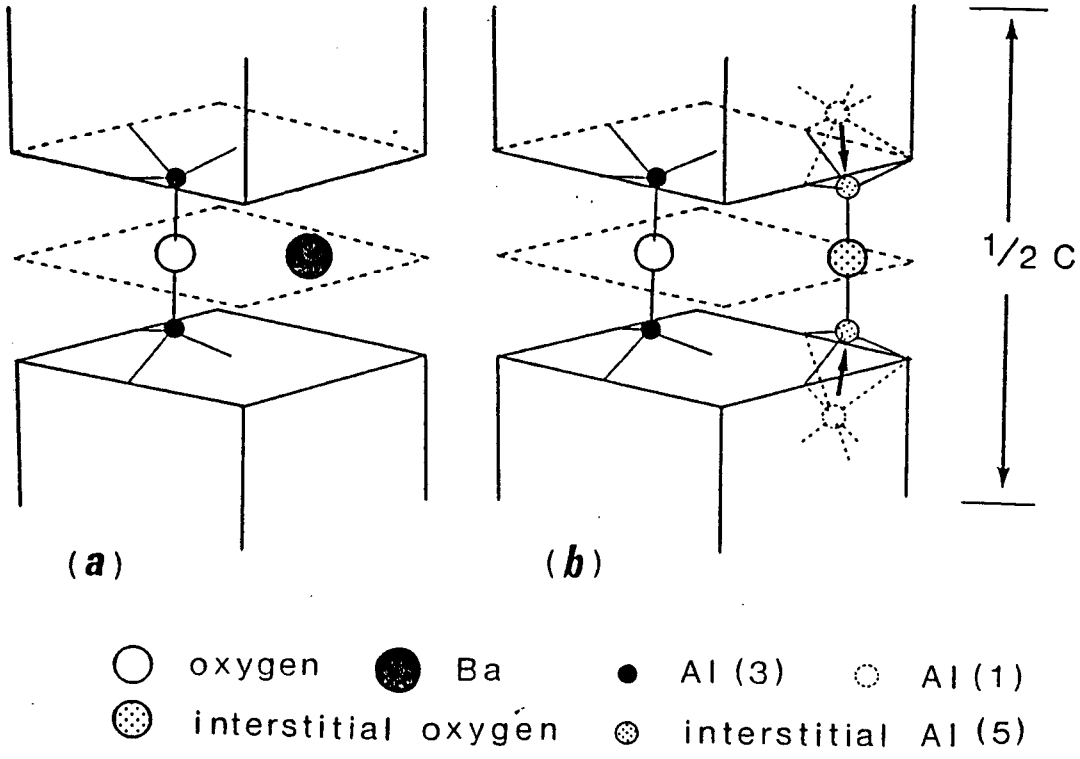

Fig.3-7. Two kinds of half unit cell assumed to constitute barium beta-alumina. (a) Half unit cell containing a Ba and an oxygen ions in the mirror plane. (b) Half unit cell containing interstitial Al and oxygen ions with the defect of Ba ion. The arrow indicates the shift of Al ions due to Frenkel defect mechanism.

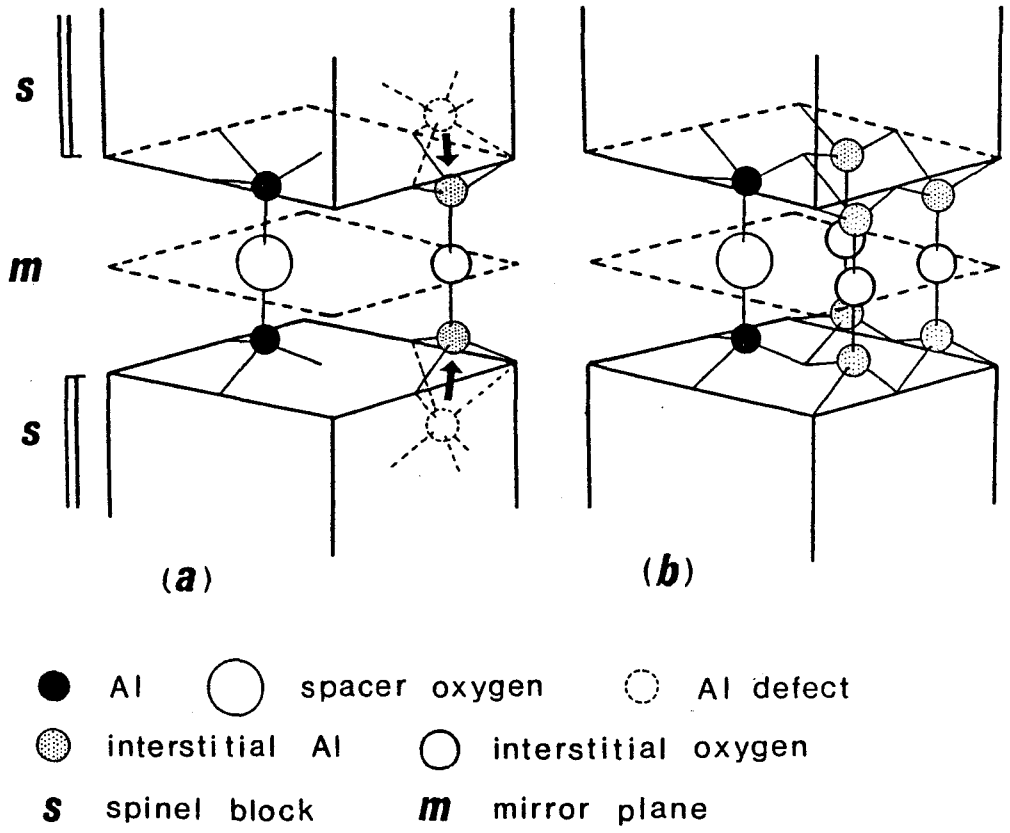

Fig.3-8. (a) The Reidinger defect. The bold arrows indicate the shift of Al ions after the Frenkel defect mechanism. (b) "Triple Reidinger defects". In this case, the Reidinger defects take place triply in a mirror plane of a single unit cell. For simplification, Al vacancies are not shown in the figure(b).

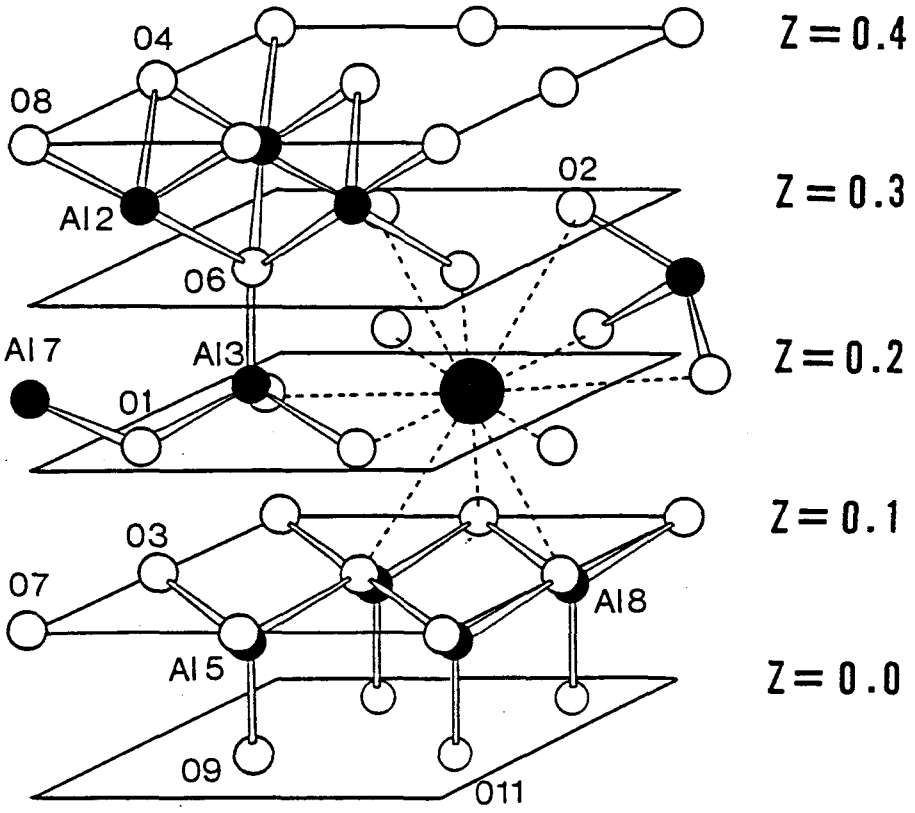

Fig.3-9. A schematic depiction of the "inside-spinel site" which is formed by the triple Reidinger defects followed by the defects of Al(4) and O(5). A large filled circle represents a Ba (or Pb) ion at the inside-spinel site, and small ones are Al ions. Oxygen ions are shown by open circles. O(11) and Al(8) are interstitials.

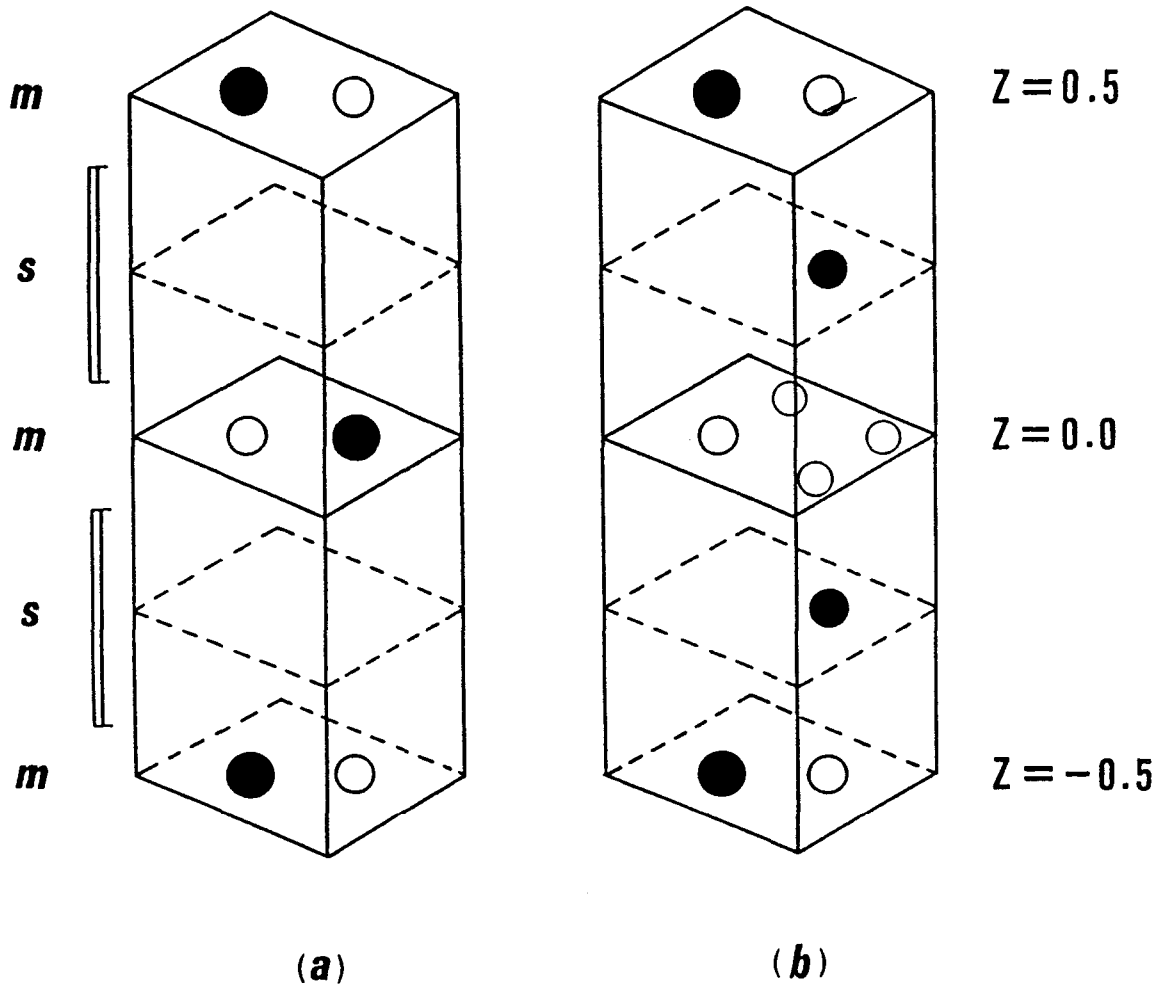

Fig.3-10. Simplified models representing two kinds of unit cells assumed to constitute the structure of barium (lead) beta(II)-alumina. Filled circles indicate large cations Ba (or Pb), and oxygen ions are shown by open circles. "S" and "M" are abbreviations for "spinel block" and "mirror plane", respectively. (a) Unit cell containing a Ba and an oxygen ion in each mirror plane. This cell is free from any defects (i.e. "perfect cell"), and has a formula "$Ba_{2.0}Al_{22.0}O_{34.0}$". (b) Unit cell containing Ba (or Pb) ions at the inside-spinel sites and interstitials due to the triple Reidinger defects. Interstitial ions cause a Ba vacancy at the large cation site(z=0.0). This "defect cell" has a formula "$Ba_{3.0}Al_{20.0}O_{35.0}$".

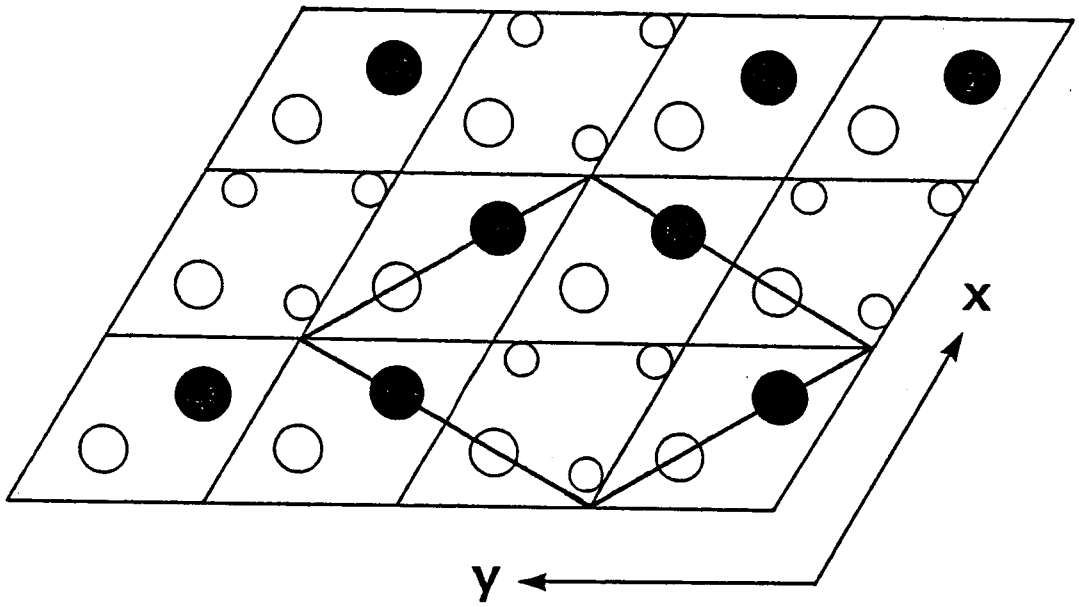

Fig.3-11. Schematic representation of the two-dimensional superstructure cells in the z=0.0 mirror planes. Filled circles indicate Ba ions, large open circles represent spacer oxygens O(9), and small open circles are interstitial O(12) ions. The outlines of the $a\sqrt{3}$ x $a\sqrt{3}$ superstructure are indicated by heavy lines.

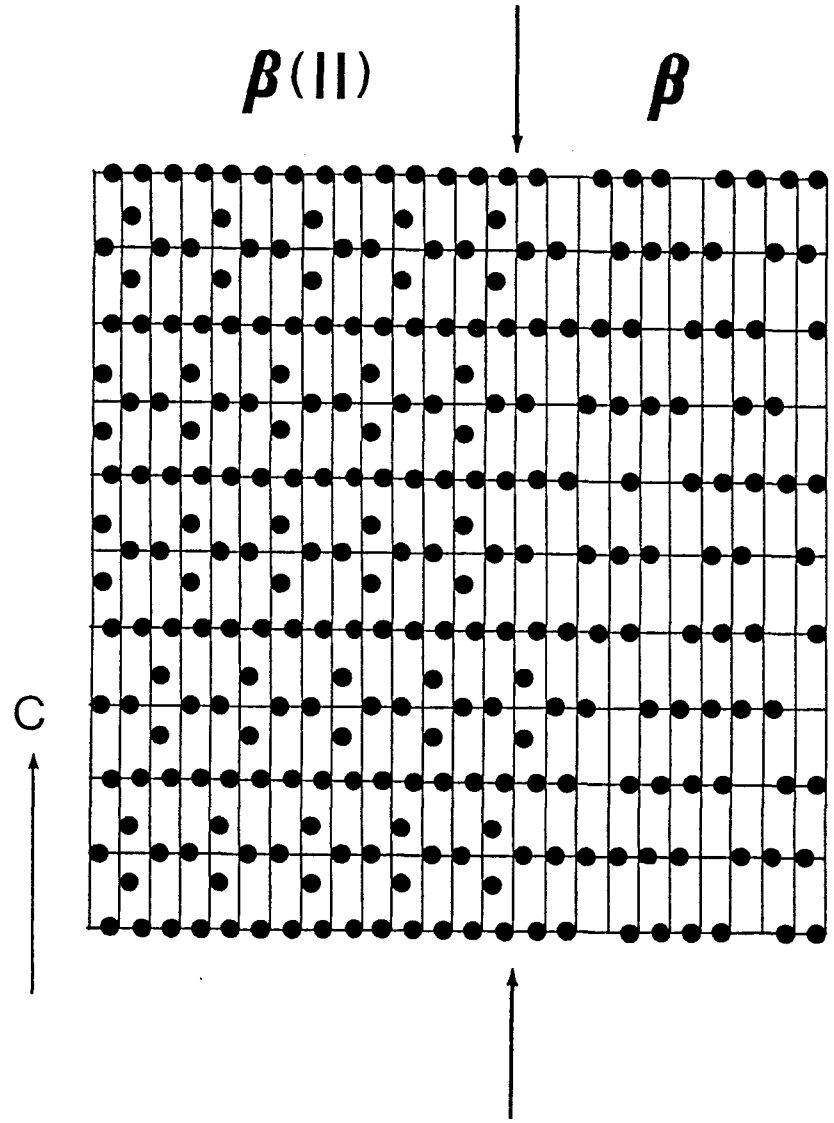

Fig.3-12. (110) plane depicting the intergrowth between barium beta-alumina(β) and barium beta-alumina(β(II)). Black circles represent Ba ions. Other ions are omitted.

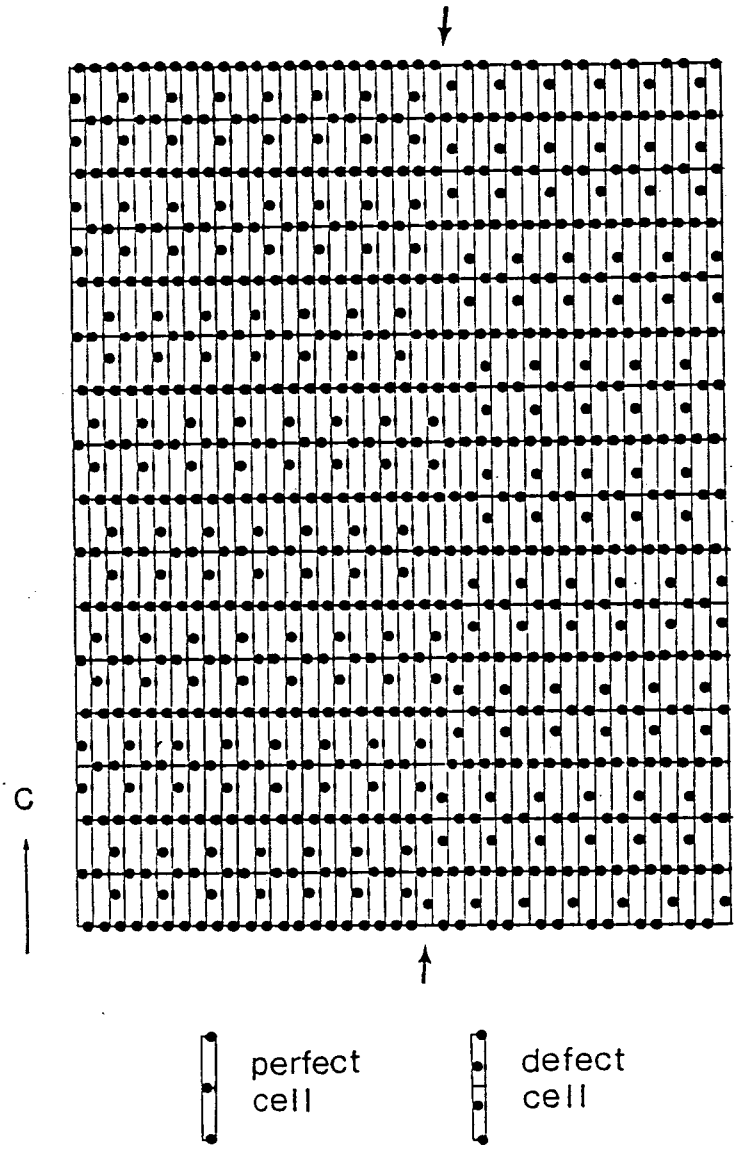

Fig.3-13. The model of twinning in barium beta-alumina. Black circles are Ba ions in the mirror planes and inside spinel blocks. Arrows show the boundary.

4. HEXAALUMINATES CONTAINING MONOVALENT CATIONS

4-1 Introduction

The unit formula of a beta-alumina containing monovalent cations can be expressed as $M_{1+x}Al_{11}O_{17+x/2}$, where M is a mono-valent cation, and beta-alumina compounds usually show non-stoichiometry with the level of $x \approx 0.3$. Up to now, many structural investigations on beta-alumina compounds have been published (e.g., Peters et al.,1971; Roth, 1972), and it was revealed that charge compensation was accomplished by the interstitial oxygen in the mirror plane(Reidinger,1979; Roth et al., 1977). The specimens were almost always obtained by the ion-exchange of sodium beta-alumina, which has the composition with $x \approx 0.3$. Accordingly, their compositions were determined by the composition of sodium beta-alumina used as the starting material for ion-exchange. For investigation of the cation distribution or configuration in the mirror plane, it is necessary to prepare beta-aluminas containing more or less cations than the usual composition $x \approx 0.3$. For example, beta-aluminas of the poorest cation content with x=0.0, in other words "ideal" stoiciometric beta-alumina compounds, $MAl_{11}O_{17}$(M ; mono-valent cations), were prepared by the elegant synthetic route via. $(H_3O)Al_{11}O_{17}$ (Boilot et al., 1980) or $DAl_{11}O_{17}$ (Newsam & Tofield, 1981a), and subjected to structural analysis using X-ray single crystal diffraction or powder neutron diffraction.

Since systematic ion exchange experiments on beta-alumina compounds were first reported by Yao and Kummer(1967), the exchange reactions of Na^+ in beta-alumina with other monovalent cations have been widely applied to prepare some beta-aluminas which can not be obtained directly. These facts show that ion exchange reaction is very common to

beta-alumina compounds. In Chapter 3, barium hexaaluminate phase I was revealed to have a beta-alumina structure and the nonstoichiometry was attributed to the same interstitial oxygen mechanism as was found in M^{1+} beta-alumina. If monovalent ion exchanges Ba^{2+} in barium hexaaluminate phase I (Ba beta-alumina), the twice as many cations as Ba^{2+} would enter according to the reaction:

$$Ba_{0.75}Al_{11.0}O_{17.25} + 1.5\ M^{+} = M_{1.5}Al_{11.0}O_{17.25} + 0.75\ Ba^{2+}$$

(where M^{+} : monovalent cation) (4.1)

Similarly, in the case of $Ba_{0.955}$ Mg beta-alumina, the reaction would be:

$$Ba_{0.955}Mg_{0.962}Al_{10.056}O_{17.0} + 1.91\ M^{+} =$$

$$M_{1.91}Mg_{0.962}Al_{10.056}O_{17.0} + 0.955\ Ba^{2+} \qquad (4.2)$$

By this way, highly nonstoichiometric beta-alumina compounds would be prepared.

The ion exchange reaction of "$BaO{\cdot}6Al_2O_3$" was previously reported by Toropov and Stukalova(1939, 1940); however, the reaction equation as well as the formula and structure of the starting material "$BaO{\cdot}6Al_2O_3$" was not made clear at that time.

In order to obtain the highly nonstoichiometric beta-aluminas, ion-exchange experiments on Ba beta-alumina and $BaMgAl_{10}O_{17}$(Ba·Mg beta-alumina) was conducted. Section 4-2 deals with the results of ion-exchange and the optimum exchange conditions(Iyi et al.,1985a). The crystal structure of K^{+}-exchanged Ba beta-alumina is described in Section 4-3(Iyi et al. 1986a), and that of K^{+}-exchanged $Ba_{0.955}{\cdot}Mg$ beta-alumina appeares in Section 4-4(Iyi et al. 1986b).

4-2 Ion Exchange Reaction of Barium Beta-Alumina

4-2-1 Experimantal

Single crystals of Ba beta-alumina and $Ba_{0.955}$·Mg beta-alumina grown by the FZ method were used as the starting materials. Unless otherwise described, they were cut into about 0.4x0.4x0.4 mm cubes, which were treated with a large excess of the molten salt (more than 300 times in weight) in a Pt crucible under air. The resultant crystals were examined by means of EPMA to check the extent of replacement. The powder X-ray diffraction data were obtained by a Phillips diffractometer and the lattice parameters were calculated by the least-squares method. To ascertain the retention of $P6_3/mmc$ space group symmetry during the ion-exchange, the obtained specimens were examined by the precession photographs taken by using MoKα radiation. Density was measured according to the method of Archimedes.

4-2-2 Results and Discussion

K^+ ion. Ba beta-alumina: Ba beta-alumina exchanged successfully with molten K_2CO_3 at 980 ℃ for 20hr, giving transparent potassium beta-alumina crystals with the formula $K_{1.5}Al_{11.0}O_{17.25}$($K_{1.5}$ beta-alumina) as can be expected from the reaction equation(4.1). They were free from cracks but very brittle. The remaining BaO was revealed to be only of the order of 0.1 mol% by EPMA. The crystal has hexagonal symmetry with the lattice parameters a=5.599 A, c=22.73 A, and X-ray powder diffraction data are shown in Table 4-1. The density of 3.39 g/cm^3 is well in accordance with the formula. The precession photographs showed the systematic absence of l=2n+1 for hhl reflections, where n is an integer. There were also observed superstructure diffuse reflections (Fig.4-1), but the average structure agreed with the $P6_3/mmc$ space group which beta-alumina compounds usually take. When a specimen 1.5 mm in length perpendicular to the c-

axis was used, the BaO content was unchanged near the center of the crystal under the same exchange condition. Treament at the lower temperature of 600°C with molten KOH for 20hr lead to only partial replacement in the periphery.

$Ba_{0.955}$ Mg beta-alumina: K^+ ion successfully replaced Ba^{2+} ion in $Ba_{0.955}$ Mg beta-alumina when K_2CO_3 flux was applied for 20 hr at 980°C. The crystals lost transparency owing to tiny cracks. The compositions of the starting and resultant crystals, which were determined by EPMA, are given in Table 4-2. These data clearly show the equimolar interchange between Ba and K_2, so the reaction equation could be written as equation (4.2).

The starting material $Ba_{0.955}$ Mg beta-alumina have a typical beta-alumina structure with a symmetry of $P6_3/mmc$. The ion-exchanged product was also proved to have the same space group symmetry by the precession camera. There appeared no reflections due to superstructure. The lattice parameters a=5.641A and c=22.64A were obtained by using 2θ-data of 20 reflections collected on the four-circle diffractometer.

<u>Na^+ ion</u>. Ba beta-alumina: Complete exchange of Ba^{2+} in Ba beta-alumina for Na^+ was attained in the molten Na_2CO_3 at 980°C for 20hr, yielding crystals with some tiny cracks. No remaining Ba^{2+} was detected by EPMA but Na content tended to vary because of the migration of Na^+ ion during the analysis. Wet chemical analysis revealed the equimolar exchange between Ba and Na_2, so the obtained compound can be denoted as $Na_{1.5}Al_{11.0}O_{17.25}$($Na_{1.5}$ beta-alumina). It possesses hexagonal symmetry with lattice parameters a=5.591A and c=22.62A. X-Ray powder diffraction

data are given in Table 4-3. The retention of the space group symmetry $P6_3/mmc$ was confirmed by the precession photographs. Density was $3.29 g/cm^3$. Exchange reactions were also undertaken on the specimen of 1.2mm in length perpendicular to the c-axis, yielding a completely exchanged crystal. This fact suggests the faster exchange rate as compared with the case of $K_{1.5}$ beta-alumina.

Treatment of Ba beta-alumina with excess molten NaCl-$NaNO_3$(3:7 mole ratio) for 72hr at 650 C resulted in only partially exchanged crystals in the periphery.

Exchange between Na^+ and K^+:

When $K_{1.5}$ beta-alumina was used as the starting material, Na^+ ion replaced completely K^+ in $K_{1.5}$ beta-alumina after the treatment with NaCl-$NaNO_3$(3:7 molar ratio) for 22hr at 600°C. Complete ion-exchange can also be done in excess $NaNO_3$ for 15 hr at a low temperature of 350°C. The obtained crystals remained transparent and free from cracks.

On the other hand, the specimens of $Na_{1.5}$ beta-alumina were treated in excess KNO_3 at 380°C for 15 hr with the result of incomplete exchange. In the same conditions, $Na_{1.24}$ beta-alumina (grown by the flux method by Bannai(1982)) showed complete ion-exchange with K. For $Na_{1.5}$ beta-alumina, thorough ion-exchange took place when it was subjected to molten K_2CO_3 at 980°C for 15 hr; the composition of the products was confirmed to be $K_{1.5}Al_{11.0}O_{17.25}$ by EPMA. The yielded crystals were clear and free from cracks.

Thus, complete replacement of Ba^{2+} by monovalent cations was shown to take place according to the reaction equation(4.1) and (4.2) in

every cases. Furthermore, the retention of space group symmetry was proved for all ion-exchanged products; this means no alteration of the host lattice of the original beta-alumina. Other beta-alumina compounds could be obtained by further ion exchange of $K_{1.5}$ beta-alumina or $Na_{1.5}$ beta-alumina, so this method was proved to be a new route for preparation of highly cation excess M^{1+} beta-aluminas.

4-3 Crystal Structure of Highly Nonstoichiometric Non-doped Potassium Beta-Alumina

As yet, several reports were published on the excess-cation containing beta-alumina compounds beyond $x \approx 0.3$. Mg-doped beta-aluminas with excess cation have been extensively investigated by Collin et al.(1980). However, in these compunds, there operates another type of charge compensation mechanism, in which Mg^{2+} compensates the excess cation in the mirror plane. Indeed non-doped beta-alumina compounds with excess cation have been prepared and reported (Bourke et al., 1980), but enough characterizations for discussing the structure are lacking. England et al.(1982), for the first time, prepared Ag beta-alumina and Na beta-alumina with $x \approx 0.45$ composition, and refined the occupancy and positional parameters by using powder neutron diffraction data. For determination of cation distribution, it would be preferable to analyse by the single crystal X-ray diffraction method.

On the basis of simple ion-ion interaction analysis, Newsam(1982) assumed the existence of a triply occupied mirror plane and predicted the upper limit of excess cation to be x=0.571 per unit formula in the case of

interstitial oxygen compensating the charge of excess cations. The obtained compound $M_{1.50}Al_{11.0}O_{17.25}$ ($M_{1.50}$ beta-alumina) is near to the upper limit composition.

4-3-1 Experimental

A 0.4x0.4x0.4 mm^3 cube of barium beta-alumina single crystal, which was grown by the FZ method, was ground into a tiny sphere by the Bond method. This spherical specimen was directly buried in a great excess of K_2CO_3 (10 gm.) contained in a Pt crucible. The crucible was placed in a Muffle furnace at the temperature of 980°C and held for 20 hr in air atmosphere. The radius of the specimens was 99 μm, and the absorption factor (μR) for this specimen was 0.162. After examination by the precession method to ascertain the crystallinity and the space group symmetry, the intensity data were collected on the computer-controlled four-circle diffractometer using graphite-monochromatized MoKα radiation. A set of three check reflections (107),(220) and (00,10) was measured every 50 reflections. The independent non-zero reflections with total number of 558 were collected under 2θ=120 . The final set of Fo's were obtained by applying the Lorenz-polarization and absorption corrections. Values of neutral atom scattering factors were taken from the I.T.(Vol. IV). The lattice parameters were obtained from a least-squares procedure applied to 2θ-values of 20 reflections measured on the four-circle diffractometer. Crystallographic data are shown in Table 4-4.

4-3-2 Refinement

The precession photographs revealed diffuse spots of a sperstructure as shown in Fig.4-1, so the average crystal structure was investi-

gated only using Bragg reflections. The space group was determined to be $P6_3/mmc$ from the systematic absence of $\underline{l} = 2n + 1$ for $\underline{hhl}$ reflections, where n is an integer. As the fundamental structure was assumed to be a beta-alumina structure, Fourier and difference Fourier syntheses were made by using the positional parameters Al(1) to Al(4) and O(1) to O(5) of potassium beta-alumina with x=0.3 per unit formula ($K_{1.30}$ beta-alumina)(Collin et al., 1977). Potassium was placed at the BR site, and the occupancy was assigned to unity for all atoms. The R-factor was 0.278 at this stage. The difference Fourier sections show the deficiency of K at the BR site and Al(1) at z=0.10. On the other hand, additional electron density was indicated at the mO site in the mirror plane. In the next refinement, K at the BR site was assigned to K(1) and K was added to the mO site as K(2). With varing the occupancy of K ions and Al(1), the refinement was accomplished on the positional parameters to give an R-value of 0.145. Difference Fourier synthesis at this stage indicated the off-centering of K(1) from the ideal BR site, and O(5) from the 2c site (1/3,2/3,1/4). Further addition of K at the mO site nearer to the aBR site than K(2) position was indicated, which was referred to as K(3) in the successive refinement. After shifting K(1) and O(5) to the 6h sites, the refinement with a general temperature factor gave 0.116 as an R-value. At this stage, secondary extinction effects were observed, so secondary extinction corrections were introduced in the successive refinements. By this treatment an R-value dropped to 0.080 immediately. Further refinements was accomplished by adding interstitial Al(5) at Z=0.17 according to the indications of the difference Fourier maps, yielding an R-value of 0.068. Subsequent isotropic refinement reduced the R-factor to 0.053. At this time interstitial O(6) was included in the refinement because the

scattering power of 0.5 oxygen per unit cell estimated from the chemical formula could not be neglected as compared with that of potassium atom. The residual electron density just inside K(2) was attributed to interstitial oxygen. Final anisotropic refinement gave R=0.029 and wR= 0.035 with w=1.0. The g-value for the secondary extinction was $2.76(9) \times 10^4$. Final difference electron maps showed featureless peaks and depressions of electron density not exceeding the range of +0.6 to -0.8 e/A^3. The final positional parameters are given in Table 4-5. The data of bond lengths and angles are shown in Tables 4-6 and 4-7, respectively. Fig.4-2 shows the electron density at the section of z = 0.25.

4-3-3 Discussion

If Al defect and interstitial oxygen are retained through the ion-exchange reaction, the reaction formula can be written as the equation (4.1). The result of refinement showed the total number of K ion to be 1.47(4) per unit formula, which is well in accordance with the chemical formula derived by the data of EPMA, cell parameters and density in the previous section. So the ion-exchange reaction was supposed to take place according to the reaction equation(4.1) without alteration of the host lattice.

From the crystallographic point of view, the change of the number of cations in the mirror plane in beta-alumina presents two interesting problems. One is the problem of cation distribution among cation sites in the mirror plane. The other is the effect of excess cations on the positional parameters of the other atoms of the host lattice. To reveal these problems, a comparison was made with ordinary cation-excess potassium beta-alumina($K_{1.30}Al_{11.0}O_{17.15}$; $K_{1.30}$ beta-alumina) reported

by Collin et al.(1977). Some of positional and occupational parameters to be discussed are given in Table 4-8 for $K_{1.30}$ beta-alumina and $K_{1.50}$ beta-alumina.

To explain the cation distribution among various sites in these two potassium beta-aluminas, at first, K(3) site at x=0.97 was assumed to be caused by the shift from the mO site due to cation-cation interaction. Dernier and Remeika (1976) also reported the crystal structure of $K_{1.3}$ beta-alumina independently. Their results differ from those of Collin et al.(1977) in the respect of no occupation of K(3) site near the aBR site. However, the number of potassium ion besides K at the BR site becomes similar with each other when considering K(3) to be shifted from the mO site. The still remaining discrepancy may be attributed to the different amount of potassium ion between them, and to the inappropriate refinement of Dernier and Remeika (1976) in which interstitial Al was not taken into account. The shift of the mO site might stem from the preparation conditions, and K ion besides the K at the BR site may as well be regarded as "K-ion at the mO site."

In the second place, we tried to explore the simplest model in which the smallest number of cell types constitute potassium beta-alumina. In the case of divalent beta-alumina $Ba_{0.75}Al_{11.0}O_{17.25}$, $(BaAl_{11}O_{17})^{+1}$ and $(OAl_{11}O_{17})^{-3}$ were considered to be the cells constituting barium beta-alumina. As there were only two types of cells oppositely charged, the composition of barium beta-alumina was fixed for attaining charge neutrality. In fact, there has not been found no solid solution either to Al_2O_3-rich side or BaO-rich side along $BaO-Al_2O_3$ tie-line. To explain the existence of solid solution as in the present case, a neutral cell is needed besides the oppositely charged cells. A non-defective cell

($KAl_{11}O_{17}$) corresponds to the basic neutral cell, in which K is situated at the BR site. The K ion at the mO site with x=0.88 could not coexist with K at the BR site in the same single mirror plane due to short distance of 2.4A between them, and also K ions at the mO sites with x=0.97 (near to aBR site) would not be found in the same single mirror plane with K at the BR site. Besides neutral cells ($KAl_{11}O_{17}$), the other cells assumed to constitute potassium beta-alumina were triply occupied cells (or "triplet cells") $(K_3Al_{11}O_{17})^{+2}$ and $(K_2O \cdot Al_{11}O_{17})^{-1}$ (Fig.4-3). The former has three K ions at the mO sites, i.e. K-K-K triplet cluster, in a single mirror plane. The latter has two K ions and one interstitial oxygen at the mO sites, forming K-K-Oi triplet cluster where Oi stands for interstitial oxygen. For attaining charge neutrality, $(K_3Al_{11}O_{17})^{+2}$ and $(K_2O \cdot Al_{11}O_{17})^{-1}$ cells should be 1 to 2 in number. Thus potassium beta-alumina could be expressed as $(KAl_{11}O_{17})_{1-z}$ $((K_3Al_{11}O_{17}) \cdot 2(K_2O\ Al_{11}O_{17}))_z$.

These triplet cells were already thought to constitute potassium beta-gallate structure by Anderson et al.(1981). Furthermore, the concept of triply occupied mirror plane was used to predict the upper limit of cation content by Newsam(1982). The number of the mO site cation would be 7x/4 and cation at the BR site would be 1-3x/4, when taking x as the excess cation number per unit formula. The calculated occupation number is shown in Table 4-9. For comparison, the occupancy calculated by the model of Wang et al.(1975) is also shown. According to them, the occupation number at the mO site and the BR site would be 2x and 1-x, respectively. (Their model is equivalent to considering M-M doublet cell $(M_2Al_{11}O_{17})^{+1}$ and M-M-Oi triplet cell $(M_2O \cdot Al_{11}O_{17})^{-1}$ besides the neutral cell ($MAl_{11}O_{17}$), where M is monovalent cation.) In both cases of potassium beta-alumina, the triplet model fits well with the real

occupation as can be seen from Table 4-9. When considering doublet cells like ($K_2Al_{11}O_{17}$) in which a K-K doublet cluster is situated at the mO sites, the number of the BR occupation decreases only to agree with that of Wang et al.(1975)'s model finally. If the cation near the aBR site is regarded as the aBR-cation, the number of the BR occupation increases.

The conclusions above were based on the average structure obtained by using the sharp Bragg reflections. As described in the previous section, there were found somewhat broader superstructure reflections besides Bragg reflections. Here it is necessary to clarify the causes of superstructure by using above discussed structure model. The precession photographs (Fig.4-1) revealed the superstructure to be essentially of $a\sqrt{3}$ x $a\sqrt{3}$ x c type with some diffuseness indicating short coherent range. We assumed that two singlet cells and one triplet cell constitute $a\sqrt{3}$ x $a\sqrt{3}$ superstructure as shown in Fig.4-4. Here, the triplet cell part is randomly occupied by K-K-K triplet or K-K-Oi triplet cells, in total 1 to 2 ratio. This two-dimentional $a\sqrt{3}$ x $a\sqrt{3}$ arrangement would give a composition with x-level of 0.444, which is slightly less than the present composition of x=0.5. Accordingly some singlet cells , in the ratio of about 1 to 20 singlet cells, might be converted into K-K-K triplet cells with causing the partial discontinuity of $a\sqrt{3}$ x $a\sqrt{3}$ fundamental superstructure long-range ordering. The observed slightly broad diffuseness can be interpreted by this partial disordering.

4-4 Crystal Structure and Cation Distribution of Highly Nonstoichiometric Magnesium Doped Potassium Beta-Alumina

Besides non-doped beta-alumina, Mg-doped beta-alumina constitutes one of the important series of beta-aluminas. The charge compensation has been supposed to be due to Mg^{2+} substituted for Al^{3+} in the spinel block in contrast to that of non-doped beta-alumina. Collin et al.(1980) have studied on Mg-doped beta-alumina and prepared $M_{1+y}Mg_yAl_{11-y}O_{17}$ with y=0.62 by the method of cooling the melt of a given composition. By this direct reaction, beta"-alumina formation was reported (Boilot et al., 1981) when starting with the composition beyond y=0.667. The ion exchanged product which we have prepared showed large excess cation content, greater than y=0.667, while maintaining the fundamental structure of a beta-alumina type. Newsam (1982) has predicted the upper limit of the cation content in Mg-doped beta-alumina to be y=0.667, if there occurs no occupation of the aBR sites. It is, therefore, of great interest to determine how many excess cations can be accommodated in the mirror plane of the Mg-doped beta-alumina host lattice.

4-4-1 Experimental

The single crystal of the starting material $Ba_{0.955}$·Mg beta-alumina was grown by the FZ method as described in the previous section 3-6. The crystalline part of $Ba_{0.955}$ · Mg beta-alumina was cut into cubes with dimension approximately 0.4x0.4x0.4 mm^3 and was used as the starting material for ion exchange. Several specimens were placed in a Pt crucible and a great excess of K_2CO_3 powder (about 10g) was added. The crucible was placed in a Muffle furnace and heated at 980°C for 20 hr in an air atmosphere. The resulting crystal was further cut into a 200x200x100 μ^3 cube and directly examined by EPMA. The composition was almost the same

as the previously described one, showing that the mole fraction of the remaining Ba was 0.0118 relative to the K content. The specimen was checked for crystallinity and space group by the precession method. The space group was determined to be $P6_3/mmc$; we found no superstructure spots or diffuse scattering. For intensity data collection, the crystal was mounted on an automatic four-circle diffractometer with monochromatized MoKα radiation. Reflections below $2\theta = 120°$ were collected by checking with a set of reflections, (107) and (00,10), measured every 50 reflections. After Lorenz polarization and absorption corrections, we obtained 775 non-zero independent intensities. The linear absorption coefficient (μ) was calculated as 17.7 cm^{-1} and the intensity data were further subjected to an absorption correction, producing a final set of Fo's. The neutral atom scattering factors were taken from the I.T. (Vol.IV). The lattice parameters were refined by using data collected on the four circle diffractometer with MoK radiation. Table 4-10 contains crystallographic data of $K_{1.875}$·Mg beta-alumina.

4-4-2 Refinement

The fundamental structure of $K_{1.875}$·Mg beta-alumina was supposed to be the beta-alumina type, Fourier and difference Fourier syntheses were, at first, carried out using the positional parameters of Al(1) to Al(4) and O(1) to O(5) of potassium beta-alumina refined by Collin et al.(1977). K was placed as K(1) at the ideal BR site with full occupancy. The Fourier synthesis of this model with an R-value = 0.270 indicated a slight deficiency at K(1), and additional electron density at the mO site. After addition of K(2) at the mO site, further refinement was made varing the occupancy of K(1), giving an R-factor of 0.136. At this stage, there was

residual electron density around the BR site. So K(1) was split into the 6h site near the BR site. After addition of K(3) at the aBR site(0,0,1/4) as indicated by the difference Fourier maps, R-value was reduced to 0.105 using a general temperature factor. Successive refinement using individual isotropic temperature factors further reduced the R-value to 0.077. Still there remained electron density probably due to K ions at the mO (x = 0.82) just inside the K(2) position; thus, we added K as K(4). The final isotropic refinement yielded R=0.065. As next anisotropic refinement indicated a tendency of K(1) at the 6h site to shift back to the BR site, further refinements were accomplished with K(1) being situated at the BR site. In this manner, an anisotropic refinement was successfully conducted, yielding an R-value of 0.034 (wR = 0.045 : w=1.0). As pointed out earlier, EPMA revealed that Ba still remained in the molar ratio of 0.0118 relative to K, so Ba was included in the successive anisotropic refinement by assuming Ba to be situated at the same site having the same temperature factor(in the form $B_{eq.}$) as in barium beta-alumina($Ba_{0.75}Al_{11.0}O_{17.25}$). In the refinement the Ba occupancy was calculated by the total potassium occupation multiplied by the factor 0.0118, while the positional parameters and temperature factor of Ba were held fixed. With this treatment, only the K(1) occupation changed, without affecting the other parameters beyond the esd's. The R-value also remained unchanged. As a check, difference Fourier sections were taken, which showed a slight depression of -1.7 e/A^3 at (0,0,0.21), with a noise level not exceeding the range of -1.0 to +0.8 e/A^3.

The positional parameters of $K_{1.875}$·Mg beta-alumina are given in Table 4-11. Interatomic distances and angles are shown in Tables 4-12

and 4-13. Fig.4-5 shows the Fourier section at z = 0.25 of $K_{1.875}$·Mg beta-alumina.

4-4-3 Discussion

As pointed out in the previous section, Mg-doped barium beta-alumina used as the starting material had slightly less Ba-content than the ideal formula $BaMgAl_{10}O_{17}$, so the resulting Mg-doped potassium beta-alumina also exhibited a somewhat smaller K-content than expected for the ideal reaction formula:

$$BaMgAl_{10}O_{17} + 2K^{+} = K_2MgAl_{10}O_{17} + Ba^{2+}$$

Table 4-10 specifies the composition of both Mg-doped compounds calculated from the occupancy obtained in the refinements. From EPMA data, the formulae, $Ba_{0.955}Mg_{0.962}Al_{10.056}O_{17.0}$ and $K_{1.872}Ba_{0.022}Mg_{0.921}Al_{10.08}O_{17.0}$, were obtained for the starting material and product, respectively. In these calculations the number of oxygen per unit formula was assigned to 17.0. The formulae derived from X-ray data and from EPMA data agreed very well with each other and the result clearly shows that the reaction proceeded with equimolar exchange as in the case of $K_{1.50}$ beta-alumina.

The cation distribution of $K_{1.875}$·Mg beta-alumina is a very interesting problem, as there are more cation than the upper limit of y=0.667 in $K_{1+y}Mg_yAl_{11-y}O_{17}$ which Newsam(1982) predicted on the basis of the "triply occupied mirror plane" concept. Furthermore, Collin et al. (1980) studied the cation distribution of Mg-doped potassium beta-alumina up to y=0.62 . With the standard preparative method they were unable to extend the synthesis of beta-alumina compounds beyond y=0.667; instead, beta"-alumina having rhombohedral symmetry was obtained. The present

compound $K_{1.875}$·Mg beta-alumina is one of the compounds of the series $K_{1+y}Mg_yAl_{11-y}O_{17}$, with y=0.875 far beyond 0.667, which retains the fundamental beta-alumina structure. In $K_{1.667}$·Mg beta-alumina, it was assumed that K-K-K triply occupied cells (triplet cells ; K ions are situated at the three mO sites) and K singly occupied cells (K ion is situated at the BR site) make up the structure in the ratio of 1 to 2 (Boilot et al., 1981). For y=0.667, the occupation numbers per unit formula were calculated to be 0.667 and 1.00 for the BR and mO sites, respectively. The composition y=0.667 was considered to be the upper limit of K-content in Mg-doped potassium beta-alumina because there was no room for accommodating the K-K-K triplet cells without coming in contact with other triplet cells as a nearest neighbor. The distance between K at the mO site of one cell and the nearest K at the mO of the neighboring cell was considered by Newsam (1982) to be too short. In the present compound, there are more cations than in the compound with y=0.667, so the excess cation might occupy the aBR site. However, there are no aBR sites which are far enough apart to avoid K-K interaction: all aBR sites are too close to the occupied mO sites, at a distance of only about 1.75 A, even at the composition of y=0.667. Accordingly it is appropriate to consider that triplet cells would change into cells of an aBR - BR arrangement for accommodating excess cations, as shown in Fig.4-8(b). According to this model, the occupancy at the mO site would decrease and that at the BR site would increase in proportion to the increment of cation content beyond y=0.667. However, the results of refinement of $K_{1.875}$·Mg beta-alumina clearly show that this model is not correct. Surprisingly the BR and mO occupancies changed little compared with that of $K_{1.62}$·Mg beta-alumina, as shown in Table 4-14, and also showed nearly the same values as the

expected occupancies for $K_{1.667}$·Mg beta-alumina. The fact indicates that there are triplet cells in contact with other triplet cells. The difference in cation arrangement between $K_{1.62}$·Mg beta-alumina and $K_{1.875}$·Mg beta-alumina may be reflected in the positional parameters of mO sites. As shown in Table 4-14, there are two mO sites in $K_{1.875}$·Mg beta-alumina. One of the mO sites, x = 0.82, is inside the usual mO site; some K ions are displaced toward the BR site, which cannot be observed in $K_{1.62}$·Mg beta-alumina. This mO position, which K(4) occupies, seems to play an important role. The distances between various sites in the same and adjacent cells are given in Fig.4-6. The mO site at x=0.82 (K(4) position) could coexist with the mO site at x=0.82 of the next cell because the separation of 3.03 A is not too short as a K-K distance. The K(4) position may be interpreted as the shift of K(2) to avoid a very short separation to the nearest mO site. K(4) at x=0.82 itself cannot coexist with the symmetrical equivalent K(4) in the same single mirror plane, owing to the short distance of 2.61 A between them. So it is reasonable, considering the radius of the K ion, to assume the existence of a K(4)-K(2)-K(2) triplet in contact with another K(4)-K(2)-K(2) triplet via K(4) cations. Furthermore, from this K-K-K triplet arrangement in a mirror plane, triple triplet-cells cluster as shown in Fig.4-7 may be supposed to be produced, because a chain-like connection of the K-K-K triplet can not exist in so far as the triplet is in a K(4)-K(2)-K(2) arrangement. The triple triplet-cell clusters thus formed, referred to as TTC-clusters below, enable some aBR sites to accommodate the extra K ions as shown in Fig.4-8(a). As TTC-cluster formation occurs beyond the y=0.667 composition, the occupation numbers at the mO and BR sites remain unchanged in spite of the cation content increment beyond y=0.667. Table

4-15 presents the occupancy as obtained from the refinement process and that calculated from the TTC-cluster model for comparison; there is good agreement between them. The maximum K-content by this TTC-cluster mechanism would be y=0.889. Unexpectedly, the present compound $K_{1.875}$·Mg beta-alumina is very close to this upperlimit of y=0.889. Fig.4-9 schematically shows the supposed K ion arrangement in the mirror plane for the composition y=0.889 close to the composition of the present compound. In the figure, TTC-clusters are so arranged as to avoid the contact with each other, and no superstructure domains are formed. Beyond the y=0.889 composition, TTC-clusters would change into BR - aBR arrangement of cations. This could be confirmed by preparing a specimen obtained by the ion exchange of $BaMgAl_{10}O_{17}$ having no Ba-defects. In the Mg-doped potassium beta-alumina system, it seems that the K ion resists the formation of the BR - aBR configuration, judging from the formation of the TTC-cluster.

4-5 Cation Distribution in the Mirror Plane

As shown in the previous sections, monovalent cation distribution in the mirror plane can be explained by the "triplet model" for potassium beta-alumina. Cation distribution of other beta-aluminas can also be interpreted by this model. Sodium beta-alumina has a similar cation configuration with that of potassium beta-alumina. Peters et al.(1971) reported the site occupation number of Na at the BR site and the mO site to be 0.75(4) and 0.52(5) per unit formula for $Na_{1.29}$ beta-alumina. From the triplet model, the site occupations would be 0.78 and 0.51, respec-

tively. Furthermore, site occupation numbers per unit formula in $Ag_{1.25}$ beta-alumina(Boilot et al., 1980) were assigned to be 0.815 and 0.435 for the "BR site" (BRD(1)+BRD(2)) and the "aBR site"(aBR(3)), respectively. If the "aBR site" with x=0.976 is considered as only caused by the shift from the mO site, the triplet model can be also applied and the number would be 0.813 and 0.438, respectively. In this way, the triplet model has a wide applicability to explanation of the cation site occupancy in the mirror plane of beta-alumina compounds.

At present, ionic conduction theory of beta-alumina is based on the doublet configuration model proposed by Wang et al.(1975), which was later refined by Wolf(1979) who took interstitial oxygen ions into consideration. Ingram & Moynihan(1982) discussed the mix-alkaline effect in these lines. McWhan et al.(1978) also presented doublet configuration model by measuring the intensities of diffuse X-ray scattering reflections. These results are contradictory to the triplet configuration model deduced from the site occupancy obtained by X-ray structure analysis. To reveal the causes of this discrepancy, preliminary potential energy for each configuration was calculated.

4-5-1 Force Model

In calculation of the potential energy, the following terms are taken into consideration:

(1) Long range Coulomb energy, $z_i e \cdot z_j e / r_{ij}$.

Here, $z_i e$ and $z_j e$ are the electric charge of each ions, and r_{ij} is the distance between them. The summation of this term was according to the Ewald method(Kittel, 1956). The computer algorism of the method was according to Catti(1978) and quick convergence conditions were

calculated by using the method of Williams(1971). The program was checked with the results of the energy calculation of $SrCl_2$ and TiO_2(Yuen et al.,1974; Busing, 1970)

(2) Repulsion energy, $f(p_i+p_j)\exp[(R_i+R_j-r_{ij})/(p_i+p_j)]$.

This formulation is taken from Gilbert(1968), and as yet, used by Yuen et al.(1974, 1978) and Busing (1970), where f: factor for fitting R to the ionic radii(Yuen et al., 1974), R: ionic radius(A), and p_i,p_j: hardness parameters(A).

(3) van der Waals energy, C_iC_j/r_{ij}.

Electronic polarizabilities C_i, C_j are taken from Yuen et al.(1974), and, partly, calculated as $\sqrt{(3/4)I_i\alpha_i^2}$ where α_i is the ionic polarizability and I_i is the ionization energy(Busing, 1970).

Repulsion energy and van der Waals terms were also checked by comparing the calculation results with those of Busing(1970) and Yuen et al.(1974, 1978). In reality, the repulsion and van der Waals terms compensate with each other, so change in the total energy is dominated by the Coulomb energy term and little affected by these short range potential energy terms. The values used for the calculation are listed in Table 4-16. The positional parameters are taken from Collin et al.(1977) and species of the cation(in the mirror plane) is limited to potassium(K). Energy change for ions displaced from the ideal position was calculated after the method of Dienes(1948).

4-5-2 Calculation Results and Discussion

Energy calculation was made on the following subjects:

(1) The energy change when a cation in a single mirror plane is displaced

along BR-aBR line in the case of the stoichiometric beta-alumina structure.

(2) The energy change in the triplet and doublet cation configurations at various coordinates, and the difference of the energy between these two configurations at their minimum energy levels.

(3) Estimation of the interaction energies between doublets and between triplets, in order to assume the total energy difference for both configurations.

The change in the potential energy was calculated as a function of the cation position along the BR-aBR line. This calculation was already accomplished by Wang et al.(1975). It can be calculated by the formula $F(x,2x,1/4) - z_i z_j e^2/r_{ij}$, where $F(x,2x,1/4)$ is site energy of the coordinates (x,2x,1/4), and the second term represents the interaction between the migrated ion and vacancy produced at the BR site. The result is shown in Fig.4-10, which is almost the same as those obtained by Wang et al.(1975). The energy difference between the BR and aBR sites amounts to approximately 3.0 eV.

To calculate the equiliblium position of the doublet and triplet configuration of the cations in the mirror plane, a doublet or triplet cell was produced at a single mirror plane by adding extra ions, where only one cell was altered with other cells being unchanged. In the next step, a cation was placed at the 6h site near the BR site and moved along BR-aBR line with simmultaneous migration of the other cations of the same mirror plane to symmetrically equivalent position. To make the amount of excess cations equal for each case, two cells are considered in the case of the doublet configuration. Here, no interaction between them was taken into account. The interstitial oxygens and Frenkel defects are not con-

sidered in these calculations. The energy change in both configurations are plotted in Fig.4-11. For the triplet case, the energy minimum is observed at about x = 0.95; for the doublet case, the minimum is at about x = 0.88. The energy difference between these two configurations is shown to be about 1.5 eV in their equiliblium positions. This corresponds to the situation with extremely low amount of excess cations in the mirror plane. The potential energy for two mirror planes with the BR-aBR configuration is also calculated with the result of slightly higher(0.3 eV) value than the most stable doublet energy level. In this case , the interaction between BR-aBR cells was not considered, too. These results indicate that the cells in the doublet configuration with x-coordinate = 0.88 would be formed in the case very small amount of excess monovalent cations are introduced in a stoichiometric beta-alumina.

Indeed, for a slightly nonstoichiometric beta-alumina, doublet cells would be formed, but the interaction between the doublet or triplet cells cannot be ignored as the number of excess cations increases. For a given excess cation number, the cells with excess cations in the doublet configuration are twice as many as those in the triplet configuration. So in the next step, preliminary estimation of interaction between doublet and triplet cells was made as shown in Fig.4-12. For doublet cells, the interaction energy would be approximately e^2/r, and, for triplet cells, it would be $4e^2/r$, where r is the distance between the BR sites of the cells. In this calculation, cation-vacancy interactions were also taken into consideration(Dienes, 1948). Here two-dimensional small domains containing the same excess cations was considered for simplicity. The domain is supposed to be surrounded by a stoichiometric beta-alumina matrix. The total energy change of triplet or doublet cells inside the domain would be

directly related to the relative stability of these configurations. (Fig.4-13). In this way, the difference of interaction energy can be estimated. For 9 x 9 domain, the energy difference between the doublet and triplet configuration is almost 2.3 eV. This is equivalent to the excess cation amount of x=0.11 per unit formula. As the energy difference between two configurations without interactions is 1.5 eV per one triplet cell (or per two doublet cells), the interaction energy gain for two triplet cells should be larger than 2 x 1.5 = 3.0 (eV) for attaining the triplet configuration in this case. For 4 x 4 domain, the difference of energy amounts to almost 3.4 eV. In this case, triplet configuration would be preferred. This is equivalent to excess cation x=0.25 per unit formula. The complex interaction in the real cation arrangement was oversimplified in these calculations, and more precise calculation should be needed. Nevertheless, the tendency toward the triplet configuration of beta-alumina containing a large excess cations was implied.

In conclusion, the configuration of cations in the mirror plane changes from doublet to triplet configuration according to increase of the number of excess cations. For certification of this conclusion, further structure investigations of beta-aluminas with various cation content are required.

h	k	l	$d_{obs.}$	$d_{calc.}$	I/I_o
0	0	2	11.382	11.369	85
0	0	4	5.689	5.685	43
0	1	2	4.462	4.461	16
0	1	3	4.083	4.085	4
0	1	6	2.987	2.986	5
0	0	8	2.843	2.842	18
1	1	0	2.800	2.800	26
0	1	7	2.700	2.699	100
1	1	4	2.511	2.512	42
0	1	8	2.453	2.452	6
0	2	1	2.411	2.411	23
0	2	2	2.371	2.371	17
0	0	10	2.275	2.274	14
1	1	6	2.252	2.252	16
0	2	4	2.231	2.230	12
0	2	5	2.140	2.140	20
0	1	10	2.060	2.059	3
0	2	6	2.043	2.042	31
0	2	7	1.943	1.943	16
0	2	8	1.846	1.845	8
1	2	2	1.812	1.810	3
1	1	10	1.768	1.765	3
0	2	9	1.749	1.749	3
0	2	10	1.658	1.659	3
0	1	13	1.645	1.645	2
0	0	14	1.624	1.624	3
1	2	7	1.596	1.596	17
0	2	11	1.573	1.573	16
1	1	12	1.569	1.569	16
0	3	4	1.554	1.555	5
0	1	14	1.540	1.540	3

Table 4-1. X-ray powder data for K^+-exchanged Ba beta-alumina. ($K_{1.5}Al_{11.0}O_{17.25}$).

Material	Composition (mol%)*			
	BaO	K_2O	MgO	Al_2O_3
Ba·Mg β-Al_2O_3	13.75	-	13.85	72.40
After K^+-Exchange	0.32	13.53	13.31	72.84

* by EPMA

Table 4-2. Composition of Ba Mg beta-alumina before and after K^+ exchange.

h	k	l	$d_{obs.}$	$d_{calc.}$	I/I_o
0	0	2	11.255	11.312	100
0	0	4	5.632	5.656	51
0	1	1	4.751	4.735	1
0	1	2	4.464	4.451	4
0	1	3	4.081	4.075	4
0	0	6	3.755	3.771	1
0	1	6	2.970	2.975	1
0	0	8	2.814	2.828	4
1	1	0	2.802	2.796	7
0	1	7	2.682	2.688	18
1	1	4	2.509	2.506	11
0	1	8	2.435	2.442	3
0	2	1	2.413	2.407	9
0	2	2	2.373	2.367	3
0	0	10	2.250	2.262	6
1	1	6	2.246	2.246	7
0	2	4	2.227	2.226	3
0	2	5	2.136	2.135	6
0	2	6	2.038	2.037	9
0	2	7	1.937	1.938	5
0	2	8	1.838	1.839	2
1	2	7	1.592	1.593	5
1	1	12	1.563	1.563	3
0	3	4	1.553	1.552	1

Table 4-3. X-ray powder data for Na^+-exchanged Ba beta-alumina. ($Na_{1.5}Al_{11.0}O_{17.25}$).

Formula	$K_{1.50}Al_{11.0}O_{17.25}$
Symmetry	hexagonal
Space group	$P6_3/mmc$
a =	5.598(1)Å
c =	22.732(5)Å
V =	616.9(2)Å^3
Z =	2
$D_{obs.}$ =	3.39 gcm^{-3}
$D_{calc.}$ =	3.399 gcm^{-3}

Table 4-4. Crystallographic data of $K_{1.5}$ beta-alumina.

The positional and thermal[a] parameters.

Position		Number per unit cell	x	z	$\beta 11 \times 10^5$	$\beta 22 \times 10^5$	$\beta 33 \times 10^6$	$\beta 23 \times 10^6$	B
K(1)	6h	1.23(2)	0.6786(30)	1/4	2083(192)	5705(1125)	384(39)	0	
K(2)	6h	1.45(5)	0.8830(12)	1/4	2364(206)	6073(652)	284(49)	0	
K(3)	6h	0.26(4)	0.9672(49)	1/4	3734(1703)	1949(1907)	723(320)	0	
Al(1)	12k	10.70(6)	0.8318(1)	0.10426(3)	484(23)	358(29)	165(9)	-96(54)	
Al(2)	4f	4	1/3	0.02430(5)	401(26)	β_{11}	148(16)	0	
Al(3)	4f	4	1/3	0.17454(6)	954(33)	β_{11}	145(15)	0	
Al(4)	2a	2	0	0	452(40)	β_{11}	227(24)	0	
Al(5)[b]	12k	0.89(4)	0.8377(14)	0.1748(4)					0.485[c]
O(1)	12k	12	0.1575(2)	0.04953(7)	817(45)	456(58)	227(18)	-40(101)	
O(2)	12k	12	0.5033(3)	0.14626(8)	592(39)	659(59)	477(21)	-401(123)	
O(3)	4f	4	2/3	0.05503(13)	709(63)	β_{11}	205(33)	0	
O(4)	4e	4	0	0.14138(13)	471(56)	β_{11}	243(38)	0	
O(5)	6h	2	0.318(10)	1/4	3060(770)	5905(3536)	121(64)	0	
O(6)[b]	6h	0.5	0.799(5)	1/4					0.485[c]

[a] The thermal parameters are of the form : $\exp[-(h^2\beta 11 + k^2\beta 22 + l^2\beta 33 + 2hk\beta 12 + 2hl\beta 13 + 2kl\beta 23)]$. $\beta 12 = 1/2\ \beta 22$; $\beta 13 = 1/2\ \beta 23$.

[b] Interstitials.

[c] Fixed.

Table 4-5. The positional and thermal parameters of $K_{1.5}$ beta-alumina.

	Number of bonds	Distance (Å)
	Octahedral coordination	
Al(1) - O(1)	2	2.012(2)
- O(2)	2	1.857(2)
- O(3)	1	1.953(2)
- O(4)	1	1.836(2)
Al(4) - O(1)	6	1.897(2)
	Tetrahedral coordination	
Al(2) - O(1)	3	1.799(2)
- O(3)	1	1.803(3)
Al(3) - O(2)	3	1.769(3)
- O(5)	1	1.722(9)
Al(5) - O(2)	2	1.747(10)
- O(4)	1	1.747(13)
- O(6)	1	1.750(14)
	Polyhedron 9-coordinated	
K(1) - O(2)	4	2.811(13)
- O(2)'	2	2.907(17)
- O(5)	3	3.24(9) (averaged)
	Polyhedron 8-coordinated	
K(2) - O(2)	4	3.024(7)
- O(4)	2	2.717(6)
- O(5)	2	2.87(8)
	Polyhedron 9-coordinated	
K(3) - O(2)	4	3.456(30)
- O(4)	2	2.490(7)
- O(5)	2	3.09(8) (averaged)
- O(5)'	1	3.40(11)

Table 4-6. Interatomic distances of $K_{1.5}$ beta-alumina.

	Bond angles (°)
Octahedral coordination	
O(1) - Al(1) - O(1)'	82.18(11)
- O(2)	91.16(10)
- O(3)	89.95(8)
- O(4)	84.34(9)
O(2) - Al(1) - O(2)'	95.25(17)
- O(3)	86.41(11)
- O(4)	98.67(8)
O(1) - Al(4) - O(1)'	88.38(8)
- O(1)"	91.62(8)
Tetrahedral coordination	
O(1) - Al(2) - O(1)'	110.33(6)
- O(3)	108.59(6)
O(2) - Al(3) - O(2)'	107.57(8)
- O(5)	108.8(26)
O(2) - Al(5) - O(2)'	103.45(65)
- O(4)	106.56(44)
- O(6)	104.85(85)
O(4) - Al(5) - O(6)	128.2(17)

Table 4-7. Bond angles of $K_{1.5}$ beta-alumina.

Occupancy and positional parameters of potassium β-aluminas

		$K_{1.30}$-β[a]	$K_{1.50}$-β
K(1)	x	0.6887(3)	0.6786(30)
	occup.[b]	1.56(1)	1.23(2)
K(2)	x	0.8824(9)	0.8830(12)
	occup.[b]	0.75(1)	1.45(5)
K(3)	x	0.9707(22)	0.9672(49)
	occup.[b]	0.28(1)	0.26(4)
O(2)	x	0.5027(2)	0.5033(3)
	z	0.1454(1)	0.14626(8)
O(4)	x	0.0	0.0
	z	0.1411(2)	0.1414(1)
		lattice parameters	
	a	5.602 Å	5.598(1) Å
	c	22.734 Å	22.732(5) Å

[a] Collin et al.(1977).

[b] Number of atoms per unit cell.

Table 4-8. Occupancy and positional parameters of potassium beta-aluminas.

Comparison of the occupation number[a] with the models.

	$K_{1.30}-\beta$		$K_{1.50}-\beta$	
	BR'	mO'	BR'	mO'
Wang's model	0.700	0.600	0.500	1.000
Triplet model	0.775	0.525	0.625	0.875
The result of refinement	0.78	0.52	0.62	0.86

[a] The number of atoms per unit formula

Table 4-9. Comparison of the occupation number in potassium beta-aluminas with the models.

Formula	$K_{1.875}Ba_{0.022}Mg_{0.919}Al_{10.081}O_{17.0}$
Symmetry	hexagonal
Space group	$P6_3/mmc$
a =	5.6408(5) Å
c =	22.645(3) Å
V =	623.98(9) $Å^3$
Z =	2
$D_{calc.}$ =	3.420 gcm^{-3}

Table 4-10. Crystallographic data of $K_{1.875}$·Mg beta-alumina.

The positional and thermal[a] parameters of $K_{1.875}$·Mg β-alumina

Position		Number per unit cell	x	z	$\beta_{11}\times10^4$	$\beta_{22}\times10^4$	$\beta_{33}\times10^5$	$\beta_{23}\times10^5$	$B_{eq.}$[b]
K(1)	2d	1.34(3)	2/3	1/4	333(15)	β11	35(4)	0	2.4(2)
K(2)	6h	1.32(22)	0.9112(39)	1/4	276(56)	726(205)	38(8)	0	3.0(12)
K(3)	2b	0.39(8)	0	1/4	685(148)	β11	33(18)	0	4.6(19)
K(4)	6h	0.70(19)	0.821(12)	1/4	372(148)	1212(565)	29(12)	0	4.3(33)
Ba	6h	0.044[c]	0.6717[d]	1/4					1.14[e]
Al(1)	12k	12	0.8330(1)	0.10521(3)	30(2)	31(2)	21(1)	-4(5)	0.34(16)
Al(2)	4f	4	1/3	0.02481(6)	42(3)	β11	23(2)	0	0.42(3)
Al(3)	4f	4	1/3	0.17345(6)	40(3)	β11	13(2)	0	0.34(4)
Al(4)	2a	2	0	0	32(4)	β11	19(3)	0	0.33(4)
O(1)	12k	12	0.1533(2)	0.05150(7)	58(4)	73(7)	27(2)	-51(10)	0.59(6)
O(2)	12k	12	0.5035(3)	0.14714(7)	39(3)	42(5)	28(2)	16(11)	0.45(12)
O(3)	4f	4	2/3	0.05815(16)	37(5)	β11	38(4)	0	0.50(5)
O(4)	4e	4	0	0.14389(15)	42(6)	β11	32(4)	0	0.49(6)
O(5)	2c	2	1/3	1/4	137(13)	β11	12(5)	0	0.95(27)

a The thermal parameters are of the form : $\exp[-(h^2\beta_{11} + k^2\beta_{22} + l^2\beta_{33} + 2hk\beta_{12} + 2hl\beta_{13} + 2kl\beta_{23})$. $\beta_{12} = 1/2\,\beta_{22}$; $\beta_{13} = 1/2\,\beta_{23}$.

b $B_{eq.} = 4/3 \sum_i \sum_j B_{ij} a_i a_j$.

c Constrained n(K(1)+K(2)+K(3)+K(4)) x 0.0118 = n(Ba) , n; occupation number.

d Fixed.

e Fixed isotropic temperature factor.

Table 4-11. The positional and thermal parameters of $K_{1.875}$·Mg beta-alumina.

	Number of bonds	Distance (Å)
Octahedral coordination		
Al(1) - O(1)	2	1.985(2)
- O(2)	2	1.869(2)
- O(3)	1	1.943(2)
- O(4)	1	1.851(2)
Al(4) - O(1)	6	1.898(2)
Tetrahedral coordination		
Al(2) - O(1)	3	1.860(2)
- O(3)	1	1.879(4)
Al(3) - O(2)	3	1.766(3)
- O(5)	1	1.733(2)
Polyhedron 9-coordinated		
K(1) - O(2)	6	2.822(2)
- O(5)	3	3.2568(3)
Polyhedron 8-coordinated		
K(2) - O(2)	4	3.14(2)
- O(4)	2	2.555(14)
- O(5)	2	2.921(30)
Polyhedron 9-coordinated		
K(3) - O(2)	4	3.658(2)
- O(4)	2	2.403(4)
- O(5)	3	3.2567(3)
Polyhedron 8-coordinated		
K(4) - O(2)	4	2.80(5)
- O(4)	2	2.97(7)
- O(5)	2	2.82(9)

Table 4-12. Interatomic distances of $K_{1.875}$·Mg beta-alumina.

	Bond angles (°) $K_{1.875}$·Mg-β
Octahedral coordination	
O(1) - Al(1) - O(1)'	81.59(12)
- O(2)	91.48(10)
- O(3)	92.06(10)
- O(4)	84.14(10)
O(2) - Al(1) - O(2)'	95.22(14)
- O(3)	84.72(11)
- O(4)	98.64(10)
O(1) - Al(4) - O(1)'	86.20(8)
- O(1)"	93.80(8)
Tetrahedral coordination	
O(1) - Al(2) - O(1)'	109.98(6)
- O(3)	108.96(6)
O(2) - Al(3) - O(2)'	109.23(7)
- O(5)	109.71(7)

Table 4-13. Bond angles of $K_{1.875}$·Mg beta-alumina.

Occupancy and positional parameters
of Mg-doped potassium β-aluminas

		Site	$K_{1.62}$·Mg-β [a]	$K_{1.875}$·Mg-β
K(1)	x	BR	0.6716(10)	0.6667
	occup.[b]		1.37(1)	1.34(3)
K(2)	x	mO	0.8844(6)	0.9112(39)
	occup.[b]		1.88(1)	1.32(22)
K(3)	x	aBR	—	1.000
	occup.[b]		—	0.39(8)
K(4)	x	mO	—	0.821(12)
	occup.[b]		—	0.70(19)
		lattice parameters		
	a		5.608(2) Å	5.6408(5) Å
	c		22.56(1) Å	22.645(3) Å

[a] Collin et al.(1980).
[b] Number of atoms per unit cell.

Table 4-14. Occupancy and positional parameters of Mg-doped potassium beta-aluminas.

Comparison of the occupancy[a] with the model

Site	Result of Refinement	TTC-Cluster Model
BR	0.67	0.667
mO(1)[b]	0.35	0.313
mO(2)	0.66	0.687
aBR	0.195	0.208
Total	1.875	1.875

[a] Number per unit formula.

[b] Inner mO site.

Table 4-15. Comparison of the occupation number in $K_{1.875}$·Mg beta-alumina with the "TTC" model.

Ion	Charge	C	R	p
K	+1.0	31.2[a]	1.24[b]	0.106[b]
Al	+3.0	2.6	0.50	0.050
O	-2.0	52.8[c]	1.41[c]	0.211[c]

a. Derived from $C=\sqrt{(3/4)I_i\alpha_i^3}$ (I_i : ionization energy, α_i : ionic polarizability).

b. Gilbert(1968).

c. Yuen et al.(1978).

Table 4-16. Values of the parameters used in the energy calculation.

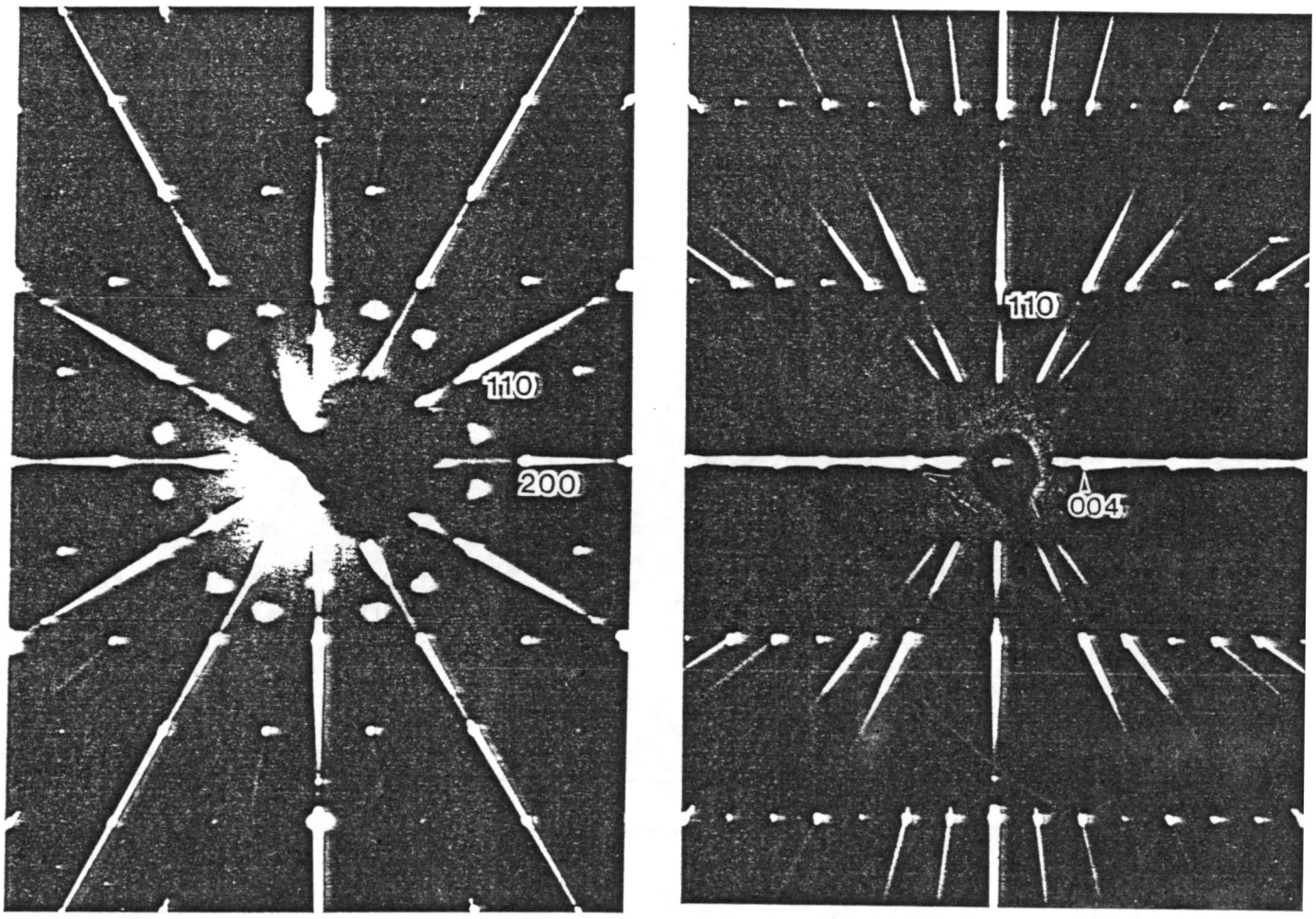

Fig.4-1. X-Ray diffraction patterns taken by the precession method using MoK radiation with Zr-filter. The incident X-ray beam is normal to (a) (001), and (b) (100) planes. Diffuse superstructure reflections were shown by the long exposure. The hkl indices are based on the Bragg reflections.

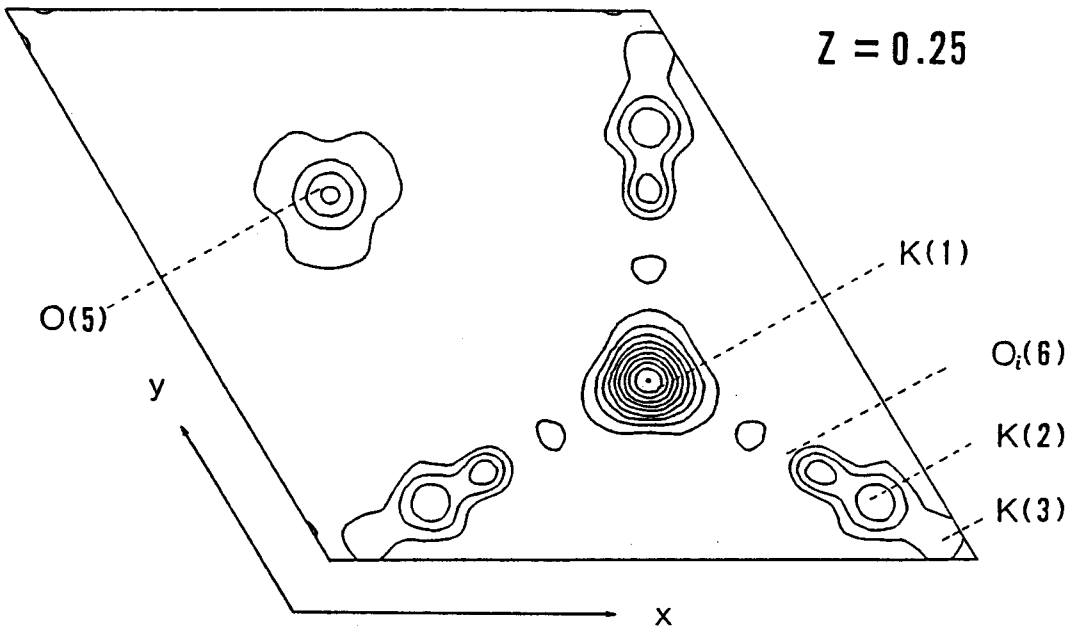

Fig.4-2. Fourier section showing the electron density in the mirror plane at z = 1/4. Contour lines are drawn with the interval of 5 eA^{-3} starting at 5 eA^{-3}.

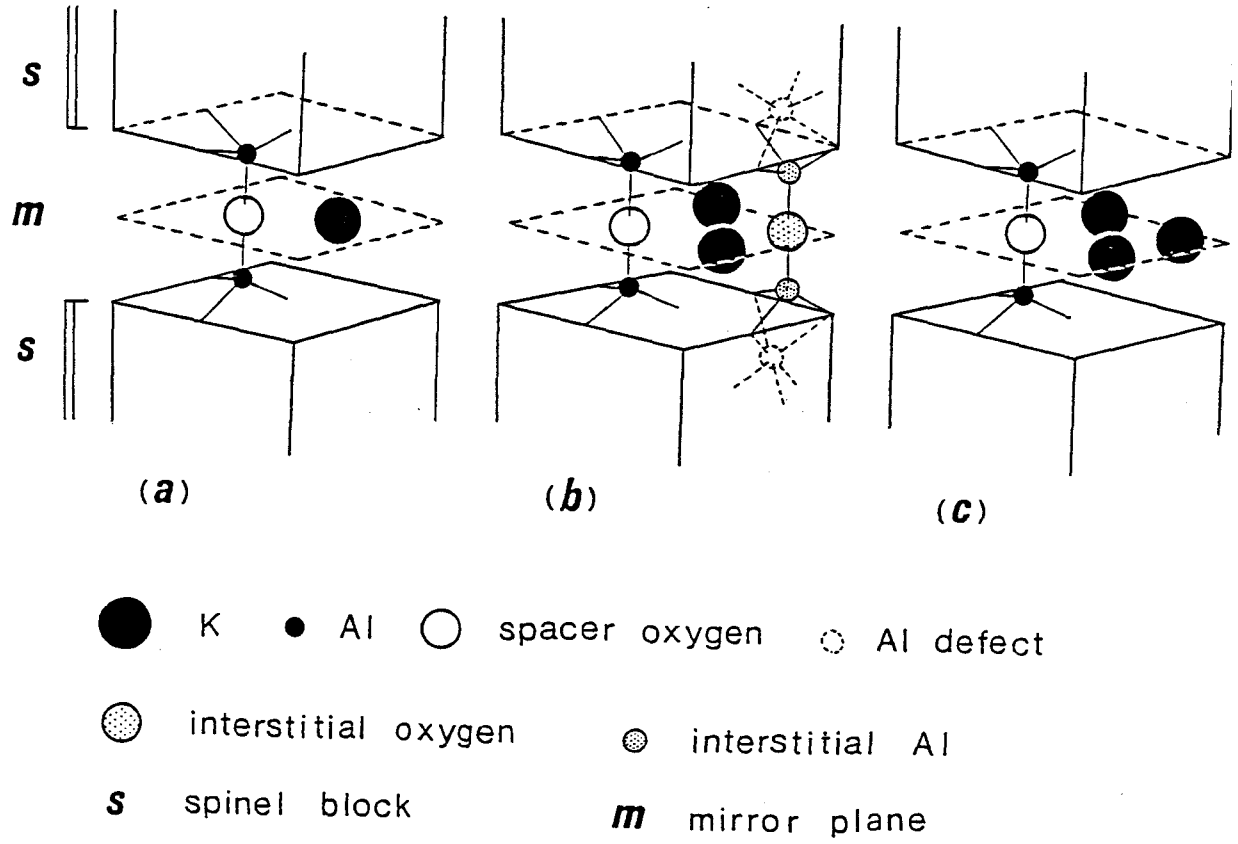

Fig.4-3. Schematic depiction of three types of cells assumed to constitute $K_{1.50}$ beta-alumina structure. (a) singlet cell ($KAl_{11}O_{17}$), (b) K-K-Oi triplet cell $(K_2O \cdot Al_{11}O_{17})^{-1}$, and (c) K-K-K triplet cell $(K_3Al_{11}O_{17})^{+2}$. (b) and (c) should be in the ratio of 2 to 1 for attaining charge neutrality.

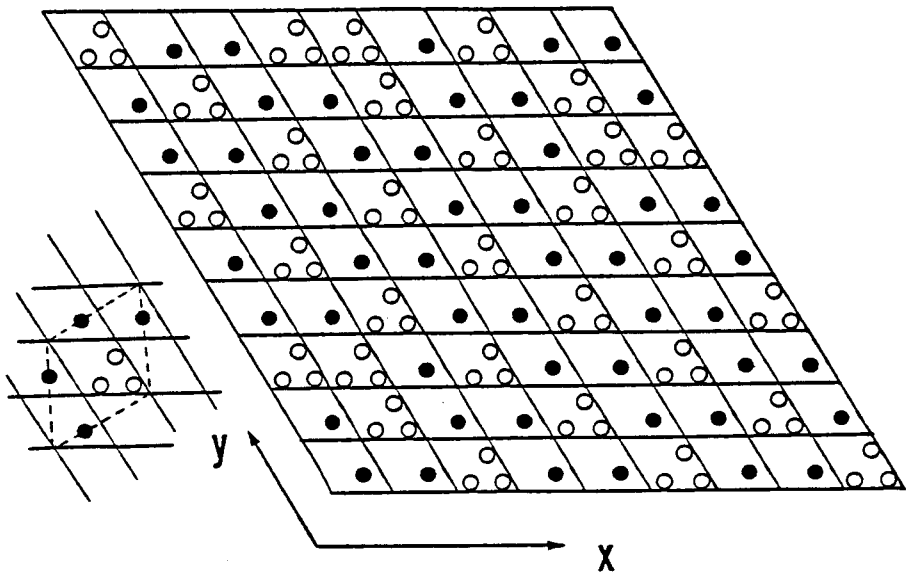

Fig.4-4. Representation of the z = 1/4 sections of two dimensional $a\sqrt{3}$ x $a\sqrt{3}$ superstructure arrangement in $K_{1.50}$ beta-alumina. An $a\sqrt{3}$ x $a\sqrt{3}$ superstructure cell is indicated by the dotted line. Filled circles represent K ions at the BR sites and the open circles are K or interstitial oxygens forming triplet cluster. Spacer oxygens are omitted. In this region, three singlet cells are changed into triplet cells, causing the discontinuity of the arrangement. The triplet clusters should be K-K-K and K-K-Oi in the ratio of 1 to 2 as a whole.

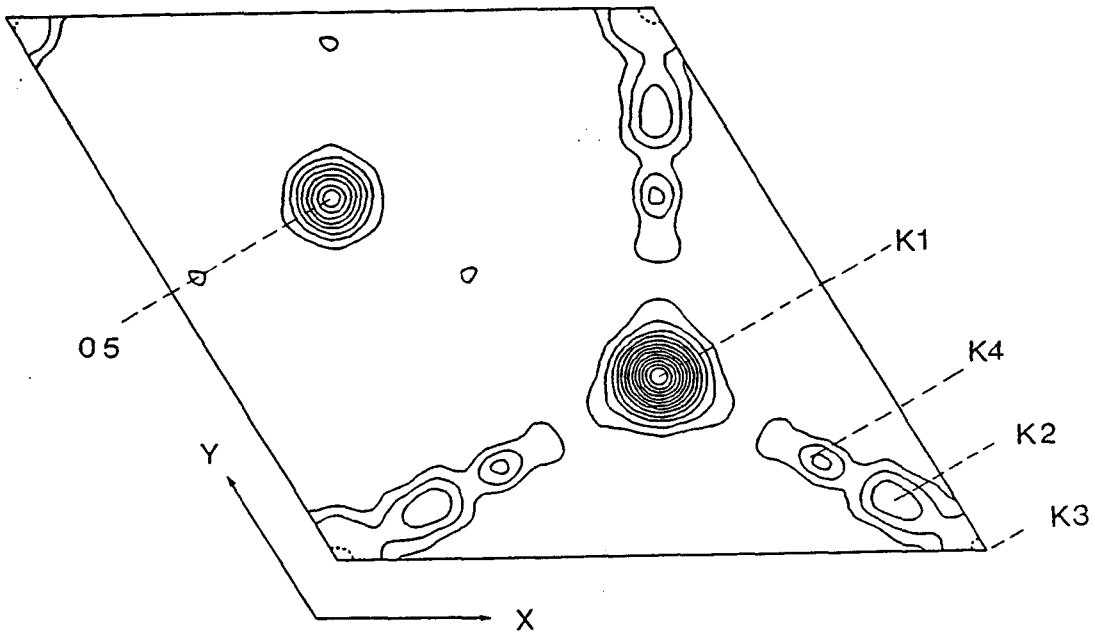

Fig.4-5. The electron density map for z=0.25 section. Contour lines are drawn at the interval of 5 e/A^3 at the minimun value of 5 e/A^3.

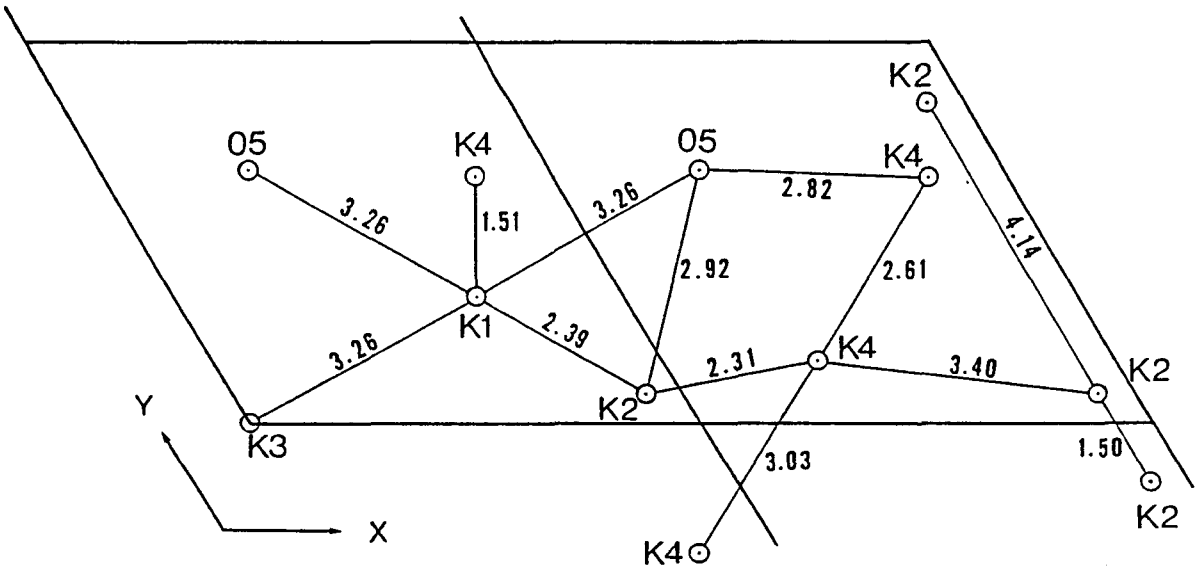

Fig.4-6. The distances between the sites in the z=0.25 mirror planes. They are in angstrom (A) unit.

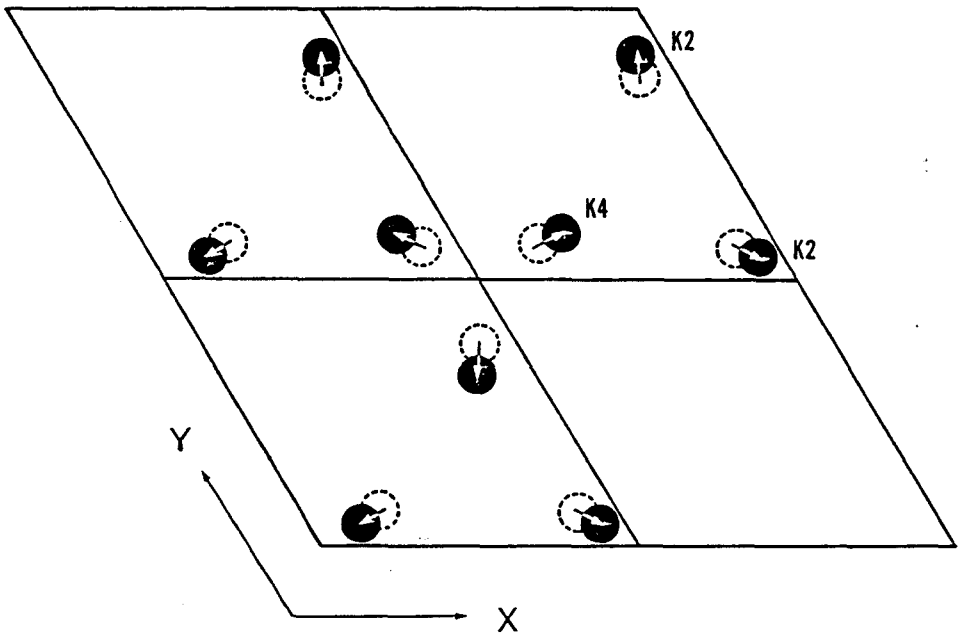

Fig.4-7. Schematic representation of the triple triplet-cell cluster in the mirror planes, showing the shift of K ions in order to avoid the cation-cation interaction. In a single mirror plane, K(2)-K(2)-K(4) triplet is formed. Dotted circles indicate K ion at the mO position of $K_{1.62}$·Mg beta-alumina.

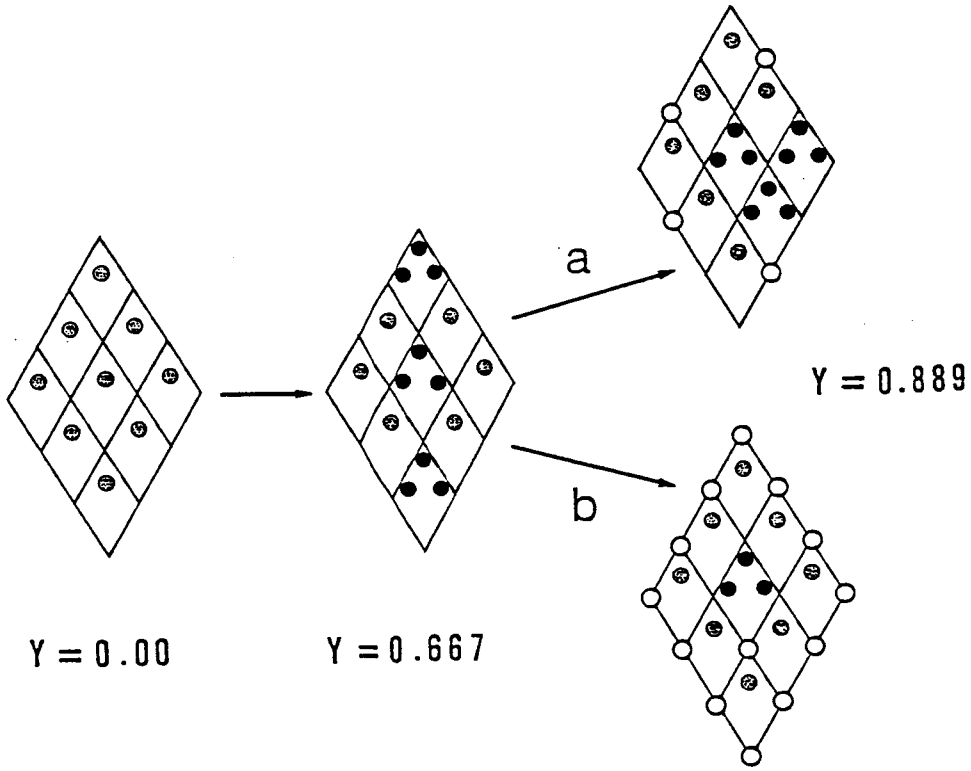

Fig.4-8. The change of cation configuration in the mirror planes of Mg-doped potassium beta-alumina as y = excess cation per unit formula increases. Besides course (a) , there is an alternative course (b), but the the results of the refinement agree with the course (a). Closed circles stand for mO cations, shaded ones are BR cations, and open circles are aBR cations.

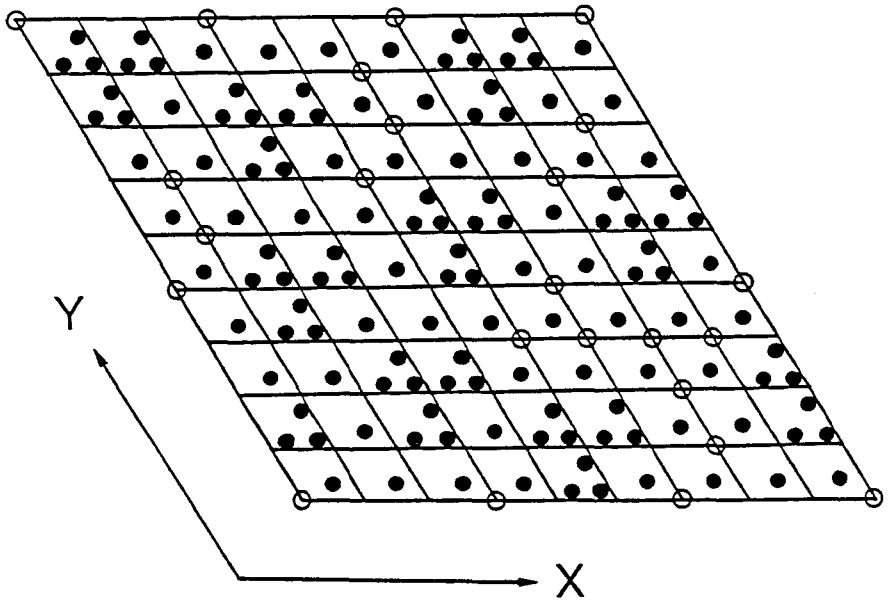

Fig.4-9. Potassium ion distribution in the z=0.25 mirror planes of Mg-doped potassium beta-alumina giving y=0.889 composition, which is a little larger value than that of the present compound, $K_{1.875}$·Mg beta-alumina. Closed circles indicate BR and mO positions, while open circles show aBR positions.

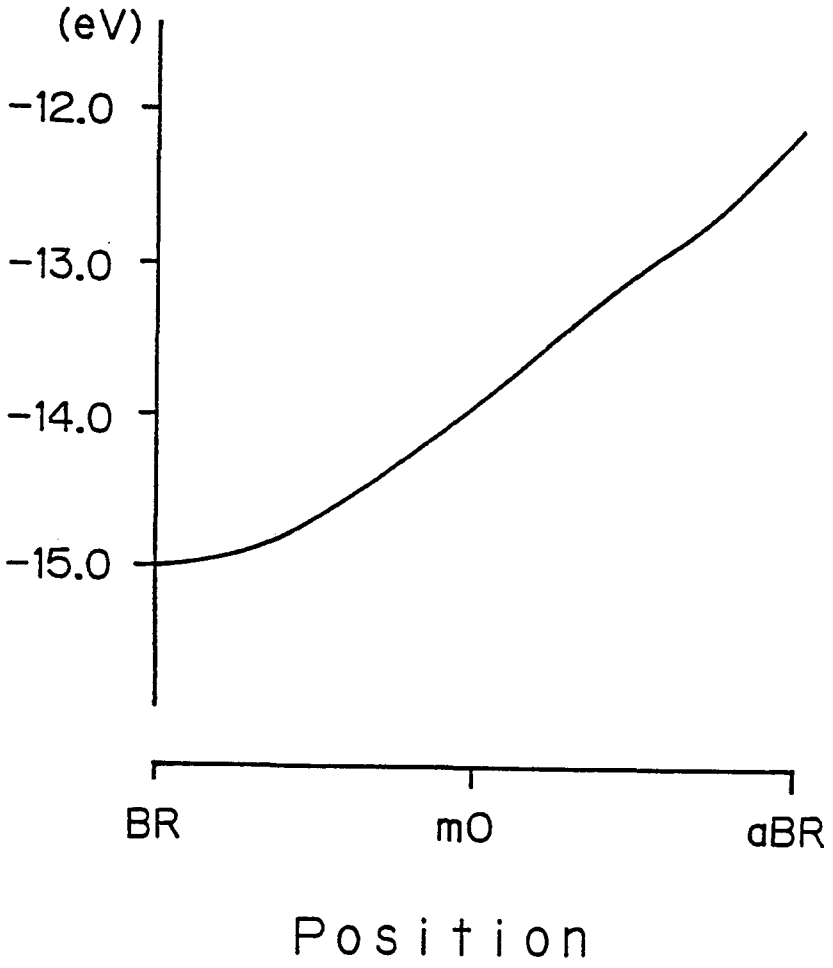

Fig.4-10. Change in potential energy as a function of the cation position along the BR-aBR line.

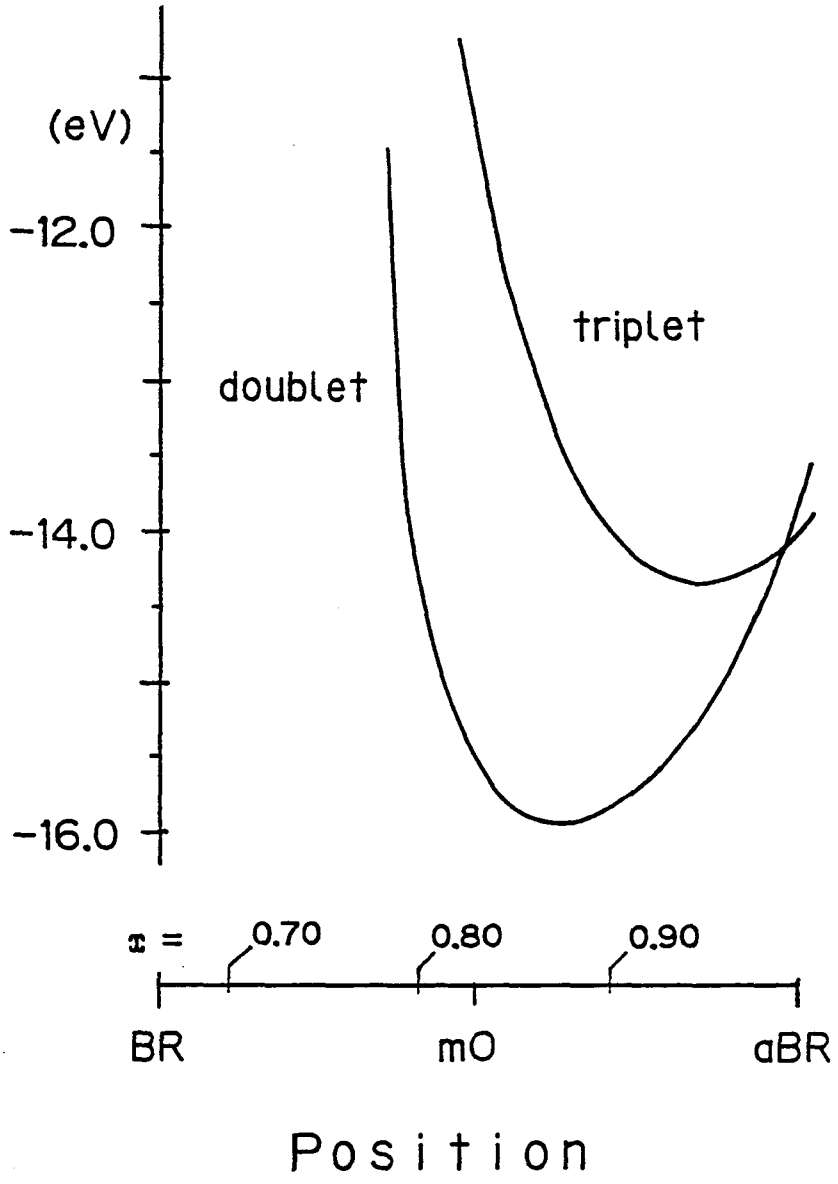

Fig.4-11. Potential energy curves for symmetrically correlated motion in the doublet and triplet configurations.

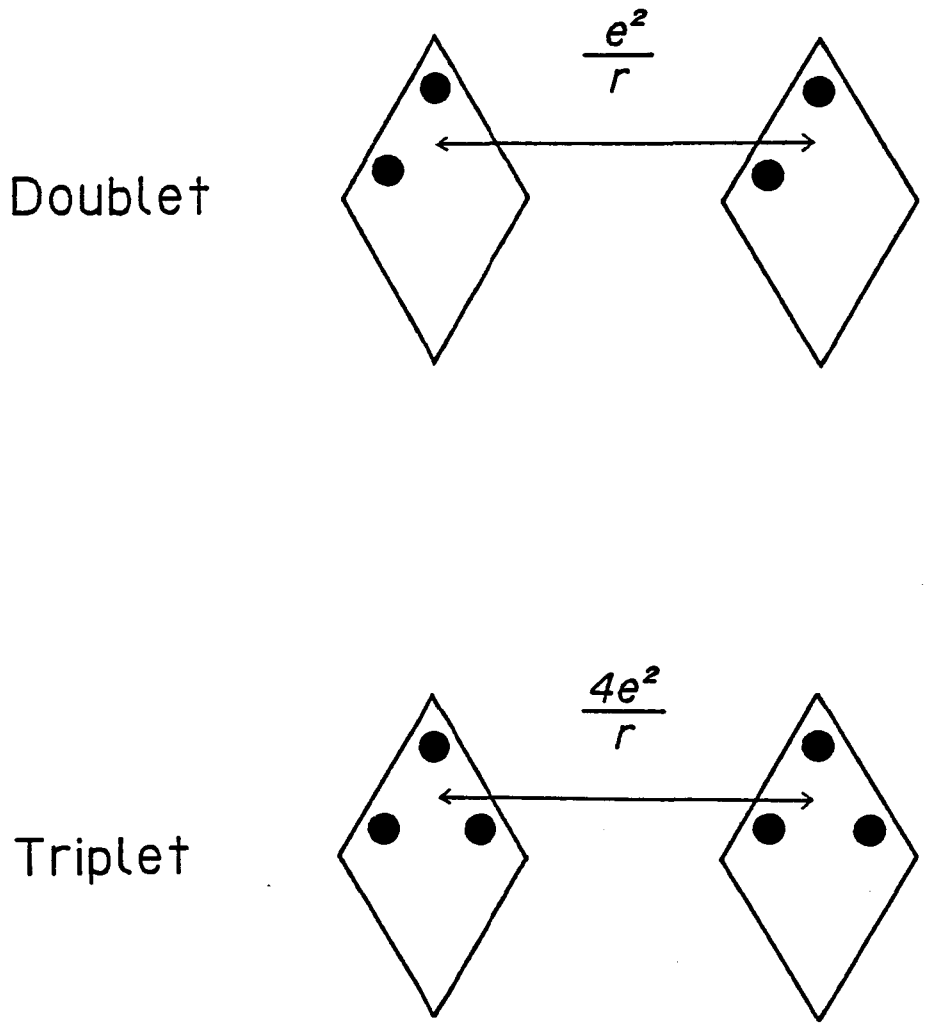

Fig.4-12. Interaction between doublet cells and between triplet cells.

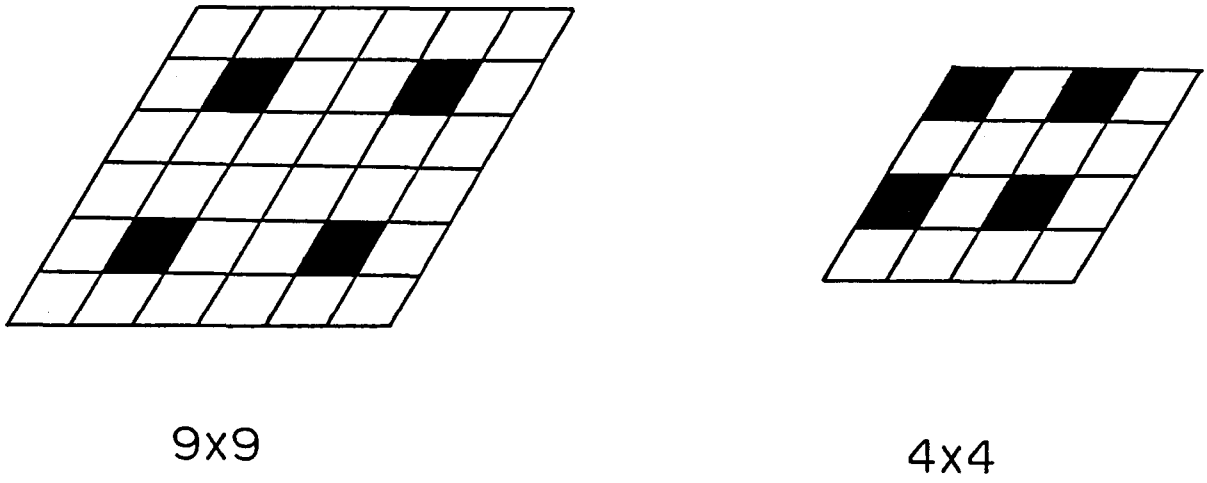

Fig.4-13. Schematic depiction of 9x9 and 4x4 small domains which are formed in the stoichiometric beta-alumina matrix. Shaded cells represent the cells with doublet configuration. In triplet configuration, the number of cells with excess cations reduce to half.

5. CRYSTAL CHEMISTRY OF HEXAALUMINATES

It is clear that the valence, ionic radius, and number of the cations in the mirror plane have an important effect on the structure of hexaaluminates. These influences may be classified into three categories:

(1) The effect of ionic radius and charge on the structure type.

(2) The effect of ionic radius on the mirror plane dimension.

(3) The effect of the number of the cation on the dimension of the mirror plane.

These are explained in the following sections. The Al defects in the spinel block due to the Frenkel defect also have influence on the size of the spinel block, which is to be dealt with in the final section.

5-1 Effect of Ionic Radus and Charge on Structure Type

The structure type of the hexaaluminates are shown in relation to the ionic radii and charge of the cation in the mirror plane in Fig.5-1. The data were partly from Stevels & Schrama-de Pauw(1976), Verstegen & Stevels(1974), Dyson and Johnson(1973) and other references cited in the previous chapters. These hexaaluminates are confined to non-doped ones; namely Al ions in their spinel blocks are not substituted for other ions, and to the compounds directly synthesized from the component oxides. The hexaaluminates obtained only by the ion exchange reaction are omitted in the discussion because they are not considered to be stable. The values of the ionic radius were taken from Shannon & Prewitt (1969) for the 8-coordination.

Ionic Radii and Structure Type

In the series of the hexaaluminates containing divalent cations in the mirror plane, the relation between ionic radii and structure type is typically shown. Small divalent cations such as Mg can not form a compound with the structure related to beta-alumina or magnetoplumbite. And hexa-alumintes containing cations with ionic radii in the range 1.1 A to 1.33 A(ionic radius of the 8-coordination) would form a magnetoplumbite type structure. In the case of the ionic radii larger than 1.33 A, a beta-alumina structure would be preferred. The change in the two M-O lengths (M: cation at the BR site; O: oxygen surrounding M) of the magnetoplumbite type compounds due to ionic radius are very interesting and provide a key to understand the upper limit of ionic radius 1.33 A for the magnetoplumbite structure. In the magnetoplumbite structure, a large cation is coordinated by 12 oxygen ions: six O(2) ions at the 12k sites and six O(5) ions at the 6h sites. Bond lengths M-O(2) and M-O(5) are plotted vs. the ionic radius in Fig.5-2. M-O(5) length shows little increase, which indicates the rigid octahedral connection. On the other hand, M-O(2) increases steeply according to the enlargement of the cation size. The difference between M-O(2) and M-O(5) becomes smaller as the cation radius increases; finally the lengths come to agree when the lines are extrapolated. As M-O(5) length would not change due to the repulsion of O(5) ions, the point where M-O(2) and M-O(5) is equal can be supposed to be the upperlimit of the magnetoplumbite structure. This corresponds to the ionic radius of 1.33 A(8-coordination). This means that the hexaaluminates containing the cations with ionic radii above 1.33A would not take a magnetoplumbite structure due to severe steric hindrance. The cations with ionic radii below 1.33A can take either beta-alumina or magnetoplumbite structure as the case may be. In this case other factors such as

ionic charge and extent of defect to be expected for the supposed structure type should be taken into consideration. The chemical formulae of beta-alumina and magnetoplumbite differ a little, so the amount of defect supposed to be created in each structure type if a certain cation is incorporated would be different in each case. If the ionic raius conditions are met, cations might be accommodated in the less defective structure. In the case of the hexaaluminates containing mono-valent cations, magnetoplumbite structure is not conceivable without creating a huge amount of defects. This preference for less defective structure is also an important factor in considering the structure type of hexaaluminates in addition to the valence to be discussed below.

Charge and Structure Type

Pauling (1967) postulated that formal valence of the anion is close to the bond strength received from the adjacent cations in the stable compounds. By using this criterion, the charge of the cation in the mirror plane required for the ideal stoichiometric beta-alumina and magnetoplumbite structure can be presumed. In this case, valence of a bridging oxygen was assigned to -2.0. For beta-alumina, ideal cationic charge is estimated to be 1.5. This implies the cationic charge in the mirror plane is insufficient for the stoichiometric composition $MAl_{11}O_{17}$ (West, 1979). This rough estimation is supported by the potential energy calculation for the sites in the ideal stoichiometric beta-alumina structure. The site energy of the bridging oxygen is lower than those of oxygens at the other sites. It may be one of the reasons for excess cations to be accommodated in the mirror plane. Furthermore, for the beta-alumina structure, a divalent cation in one mirror plane exhibits a

little excess in positive charge, so it would contain more oxygen ions or it would contain defects of divalent cations in the mirror plane. Such trend favors the Ba beta-alumina formation.

On the other hand, the ideal cationic charge for a magnetoplumbite structure is assumed to be 2.4. For divalent hexaaluminates, slightly more cationic charges are needed, but there are no more space to accommodate further cations. Thus, fully occupied typical magnetoplumbite structure is formed. For the case of hexaaluminates containing trivalent cations, the cationic charge is so large that the reduction of the amount of cations in the mirror plane is needed. This trend suffices the condition that Ln hexaaluminates forms. For monovalent cations, magnetoplumbite structure is not adequate because cationic charge is extremely small and bridging oxygen would be underbonded.

In conclusion, as the cation charge in the mirror plane increases, the magnetoplumbite structure becomes favorable. And, as the cation size increases, the beta-alumina structure would be more stable.

5-2 Effect of Ionic Radius on Mirror Plane Size

It is known that the c-value of the lattice parameters becomes larger as the radius of the monovalent cation in the mirror plane increases(Kummer, 1972). Newsam & Tofield(1981b) also described the tendency of the c-value to decrease according to the increase of the cation population in the mirror plane. However, this trend was not general, as they themselves pointed out. For example, $K_{1.3}$ and $K_{1.5}$ beta-aluminas are shown to have almost the same c-axis parameter of 22.73A. More general parameters than the c-value is proposed to describe the microstructural effects of cation population and radii.

Concepts of "Mirror Plane Thickness" and "Spinel Block Thickness"

Large cations in the mirror plane are coordinated by 6 oxygens at the 12k sites just above and below the mirror plane in addition to 3 oxygens in the mirror plane (in the case of beta-aluminas) or 6 oxygens in the mirror plane (in the case of magnetoplumbites). The change of number and radius of the cation may affect the coordinates of oxygens. Generally, cation-oxygen distance is smaller for M-O(12k) than for M-O(in the mirror plane), so these oxygen ions at the 12k sites would be directly influenced by the change of cation species or population. Since the positional parameter change of oxygen at the 12k site was observed in the z-parameter in the case of K beta-aluminas, the present author(Iyi et al., 1986a) defined the distance between O(2) at the 12k sites just above and below the mirror plane(z=0.25) as the "thickness of the mirror plane"(M_{12k}) as shown in Fig.5-3. In a similar way, the "thickness of the spinel block"(S_{12k}) was defined. This is measured across the spinel block. These hold the equation; $c/2 = M_{12k} + S_{12k}$. When oxygen ions at the 4e sites are taken as a standard, M_{4e} and S_{4e} may be defined similarly. But these are not sensitive to the cation species or population but to types of structure because an Al ion is introduced between oxygens at the 4e sites in the magnetoplumbite structure, so discussions are confined to M_{12k} and S_{12k} in the present thesis.

Relationship between Mirror Plane Thickness and Ionic Radius

As the cation radius become larger, the distance M_{12k} would be larger. This relationship is shown in Fig.5-4, which clearly indicates the linear relation with, however, the lower limit of 4.6A. Below 4.6A limit, it is the region of the magnetoplumbite structure. This lowest

limit may be determined by the distance of Al-O-Al which bridges the spinel blocks. The M_{12k} distance would be ideally 4.67A if tetrahedral Al-O distance is assumed to be 1.752A(Bauer, 1981). The maximum deformation may correspond to the limit of 4.6A thickness. The dependence of M_{12k} thickness on the ionic radius was also observed in the magnetoplumbite structure, in spite that it appeares to have more rigid structure than beta-alumina. As the ionic radius increases, the value M_{12k} becomes larger. In a similar manner to beta-alumina, octahedral Al-O-Al face-sharing connection directly related to the M_{12k} value, which can be ideally calculated as 4.41A if the average octahedral Al-O distance is assumed to be 1.909A. These values do not necessarily reflect the real distance, but, in reality, increase of M_{12k} up to 4.6A would deform Al(VI)-O-Al(VI) connection with three oxygens at the 6h sites coming closer to each other.

5-3 Effect of Cation Population on Mirror Plane Thickness

The values of M_{12k} for $K_{1.30}$ beta-alumina and $K_{1.50}$ beta-alumina are 4.756A and 4.716A, respectively. Here, the contraction of the "thickness of the mirror plane" by 0.040A can be observed. (The values M_{4e} are 4.952A and 4.938A for $K_{1.30}$ beta-alumina and $K_{1.50}$ beta-alumina, respectively. The difference of 0.014 A is little when compared with the difference of M_{12k}. The excess cation might effect the distance M_{12k} more than that of M_{4e}.) Well investigated Ag beta-alumina compounds shows the same tendency for M_{12k}(Fig.5-5a). At the temperature of 4 K, stoichiometric $AgAl_{11}O_{17}$(Newsam & Tofield, 1981) has 4.68A of M_{12k}; on the other hand, cation excess $Ag_{1.45}$ beta-alumina(England et al.,1982) has smaller value 4.60A of M_{12k}. This relation is also true for $Ag_{1.0}$ beta-alumina(Boilot et al.,1980) and $Ag_{1.33}$ beta-alumina(Roth,1972) at room tempera-

ture.

In non-doped beta-alumina compounds, the content of cations is directly related to the amount of interstitial oxygen in the mirror plane due to the Reidinger defect. The contraction of the mirror plane thickness M_{12k} may be attributed to Al_i-O_i-Al_i (i; interstitial) connection, pulling the spinel blocks as Newsam & Tofield(1981b) considered. However this may not be correct. In Fig.5-6, the M_{12k} values of Mg-doped K beta-aluminas are also plotted vs. the cation population per unit cell. Of course, there are no interstitial oxygens or Al ions in the mirror plane in these Mg-doped beta-aluminas. Nevertheless, the trend of M_{12k} contraction can be seen from Fig.5-6. On the basis of these facts, it is concluded that cation population itself affects the M_{12k} distance.

Another example showing this effect is barium hexaaluminates. Ba beta(II)-alumina was revealed to have perfect and defect layers in the previous chapter. The perfect layer contains 1.0 Ba ion in a single mirror plane, and M_{12k} can be calculated in a similar way for the perfect layer. The M_{12k} values of Ba beta-alumina, Ba·Mg beta-alumina and the perfect layer of Ba beta(II)-alumina are plotted vs. Ba-content in the Fig.5-7. The result agrees well with the above assumption.

The cause of the M_{12k} increase can be attributed to the change in the local electronic charge in the hexaaluminate structure. As the number of the cation increases in the mirror plane, positive charge concentrates in this layer; on the other hand, spinel block becomes more negative in charge relatively. Accordingly, spinel blocks are pulled closer to each other by the attraction of the mirror plane as the excess number of cation increases.

Thus, it seems that the mirror plane thickness M_{12k} shows monotonic

decrease as cation population becomes large, although the behavior of M_{12k} contraction near the lowest limit of 4.6A still remains unclear. In magnetoplumbite system of La hexaaluminate, which slightly varies in the La-content according to the divalent cation content in the spinel block, the contraction of M_{12k} was not observed, probably because the mirror plane is too rigid to be influenced by the cation content.

5-4 Frenkel Defects and Spinel Block Thickness

The distance S_{12k} for $K_{1.30}$ beta-alumina is 6.611A and that for $K_{1.50}$ beta-alumina is as large as 6.650A. The contraction of M_{12k} and enlargement of S_{12k} owing to the excess potassium ion in the mirror plane compensate each other to make little difference of the lattice parameter c between $K_{1.30}$ beta-alumina and $K_{1.50}$ beta-alumina. This relation is shown in Fig.5-5a,b. The increase of S_{12k} might be attributed to the concentration of Al defect in the spinel block. This is also the case with Ag beta-alumina as shown in Fig.5-5a,b. Surprisingly, in spite of the c-axis variation according to the species of the monovalent cation, the values of S_{12k} of the non-doped monovalent beta-alumina compounds(e.g., Peters et al.,1971; Roth, 1972; Kodama & Muto, 1976) having the x-level of about 0.3 , namely having the same amount of Al defects within the spinel block, are confined to the range of 6.59 ~ 6.61 A. A slight smaller value of 6.58A in Tl beta-alumina(Collin et al., 1977) is due to smaller amount of the excess cations. The values of S_{12k} are plotted vs. Al(1) vacancy for magnetoplumbites as well as beta-aluminas in Fig.5-8. Save for the S_{12k} of Ca hexaaluminate and $K_{1.5}$ beta-alumina, the relation between the spinel block thickness S_{12k} and Al-vacancy are clearly indicated. This is because the defects of Al in the spinel block, which is equivalent to

putting negative charge there, drives the neighboring negatively charged oxygen ions away causing the expansion of the spinel block. Of course, Al vacancy is not the only factor determining the S_{12k} value. For example, M_{12k} of Ba beta-alumina and $K_{1.5}$ beta-alumina have a slight different S_{12k} value, in spite there are same amount of Al-vacnacy content. As far as non-doped monovalent cation containing beta-alumina compounds are concerned, it can be assumed that the mirror plane thickness M_{12k} reflects the population and the radius of the cation in the mirror plane, and that the spinel block thickness S_{12k} might reflects mainly the defect concentration in the spinel block. However, accurate positional parameters of the beta-aluminas with various cation contents are needed to draw a more precise conclusion.

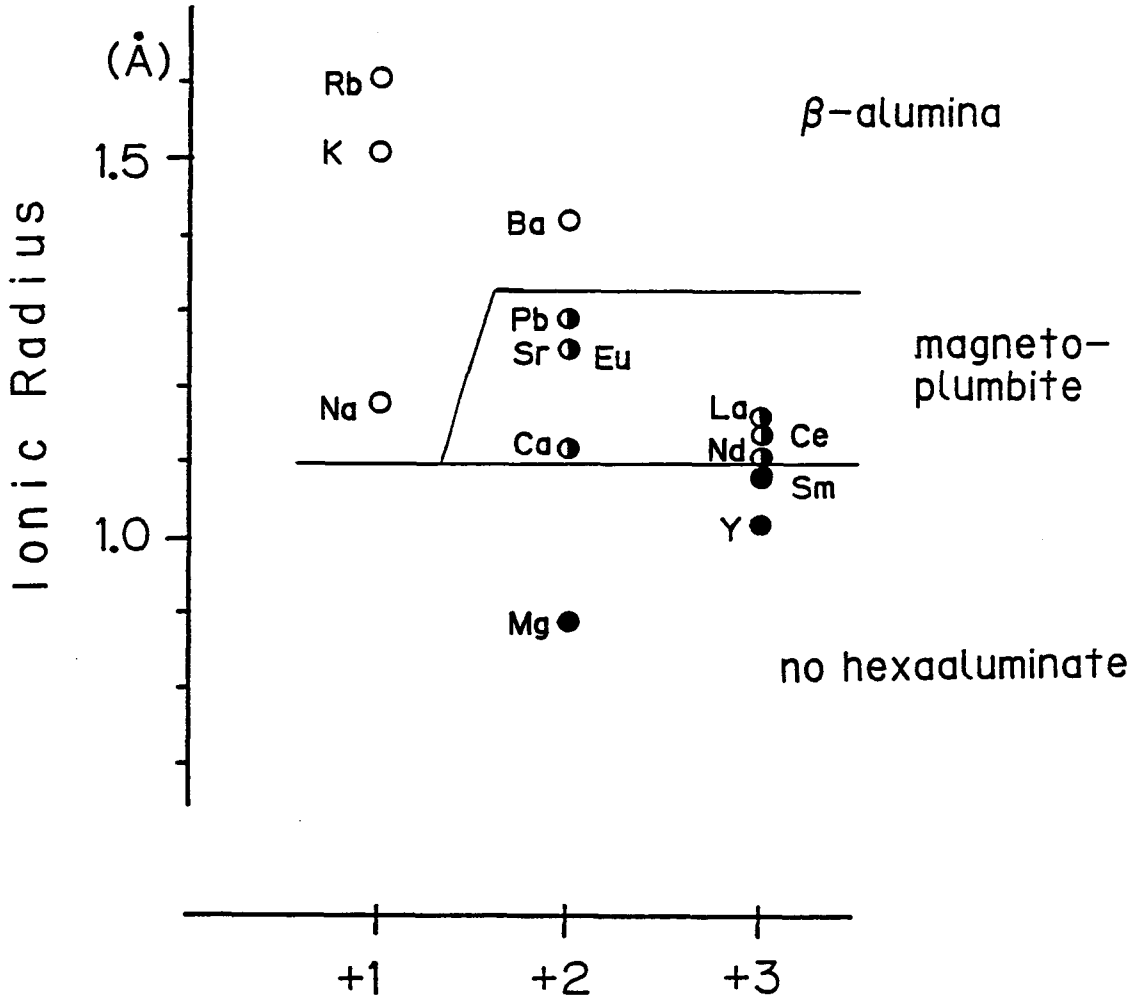

Fig.5-1. Schematic drawing of the range of beta-alumina and magneto-plumbite structure.

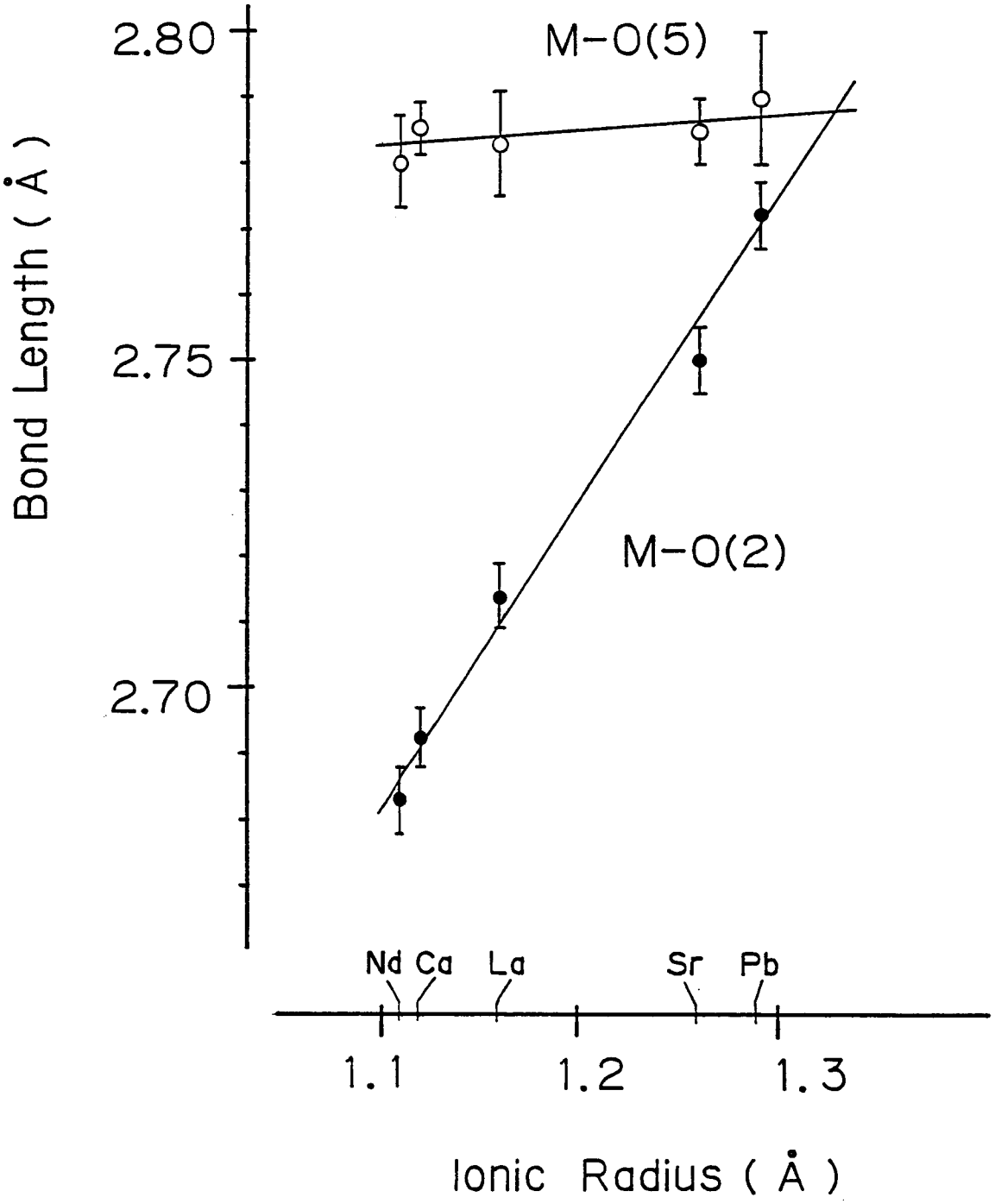

Fig.5-2. Change in two M-O lengths as a function of ioic radii of the large cations(M).

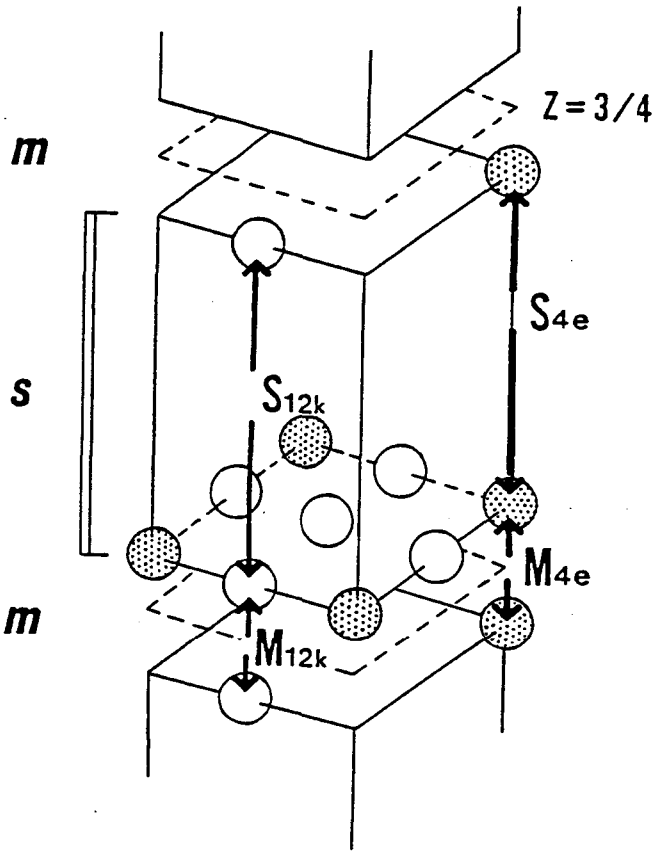

Fig.5-3. The simplified beta-alumina structure showing the thickness of the mirror plane M_{12k}, M_{4e}, and the thickness of the spinel block S_{12k}, S_{4e}. Open circles represent O(2) at the 12k site and shaded circles are O(4) at the 4e site. S and M stand for the spinel block and the mirror plane, respectively.

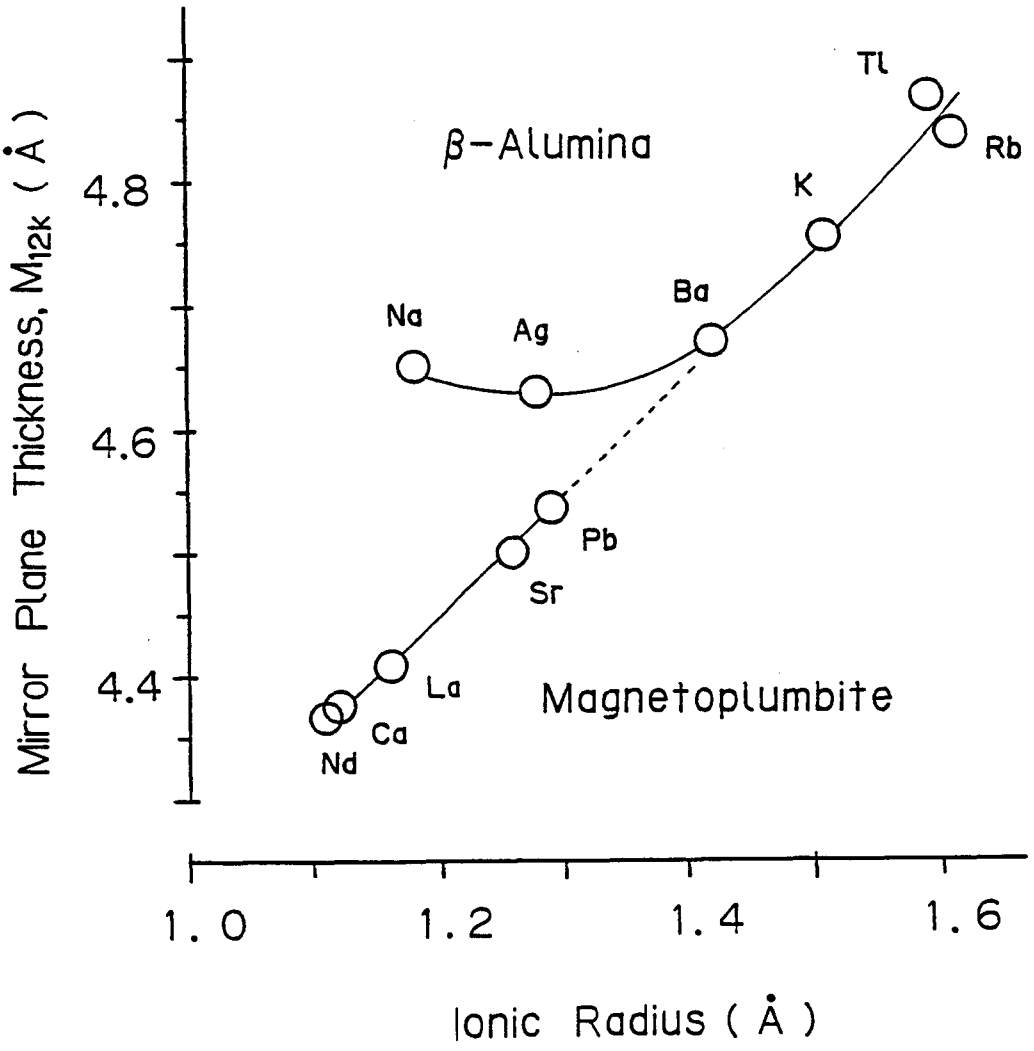

Fig.5-4. Dependence of the mirror plane thickness M_{12k} on the ionic radius.

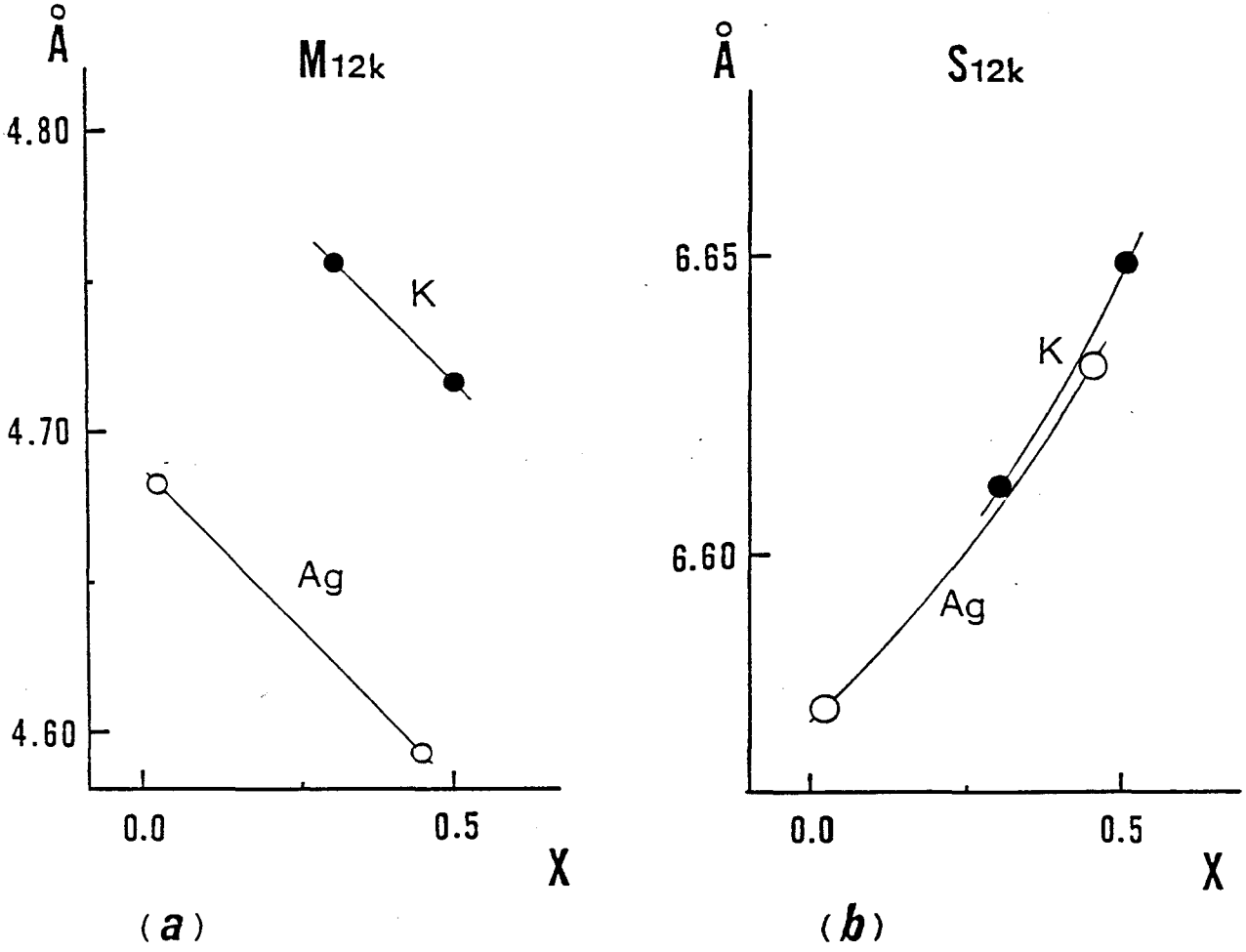

Fig.5-5. Relation between x = excess cation content per unit formula and (a) M_{12k} , (b) S_{12k} in the case of K beta-alumina and Ag beta-alumina compounds.

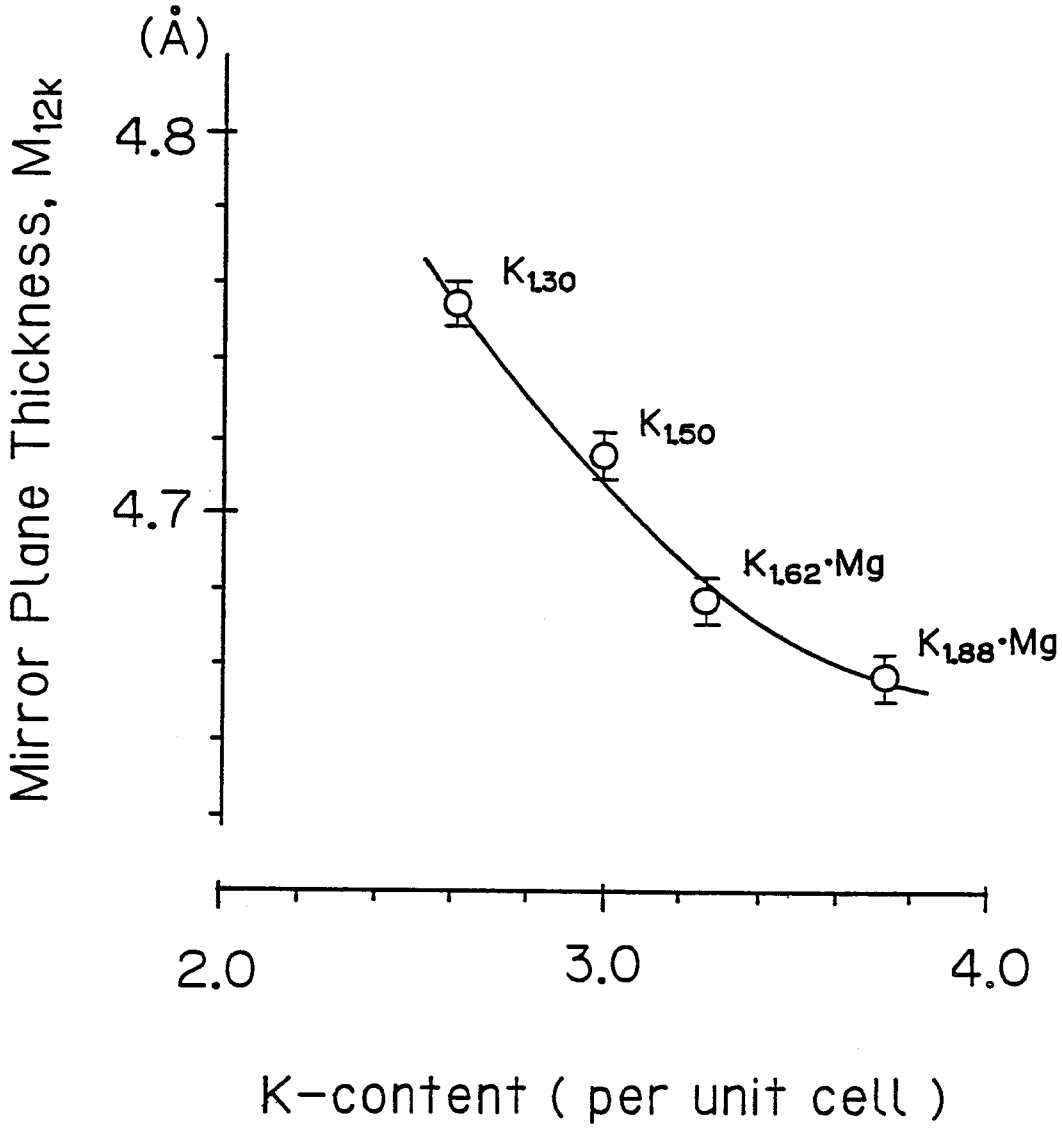

Fig.5-6. Relation between the mirror plane thickness M_{12k} and K-content in non-doped and Mg-doped K beta-aluminas.

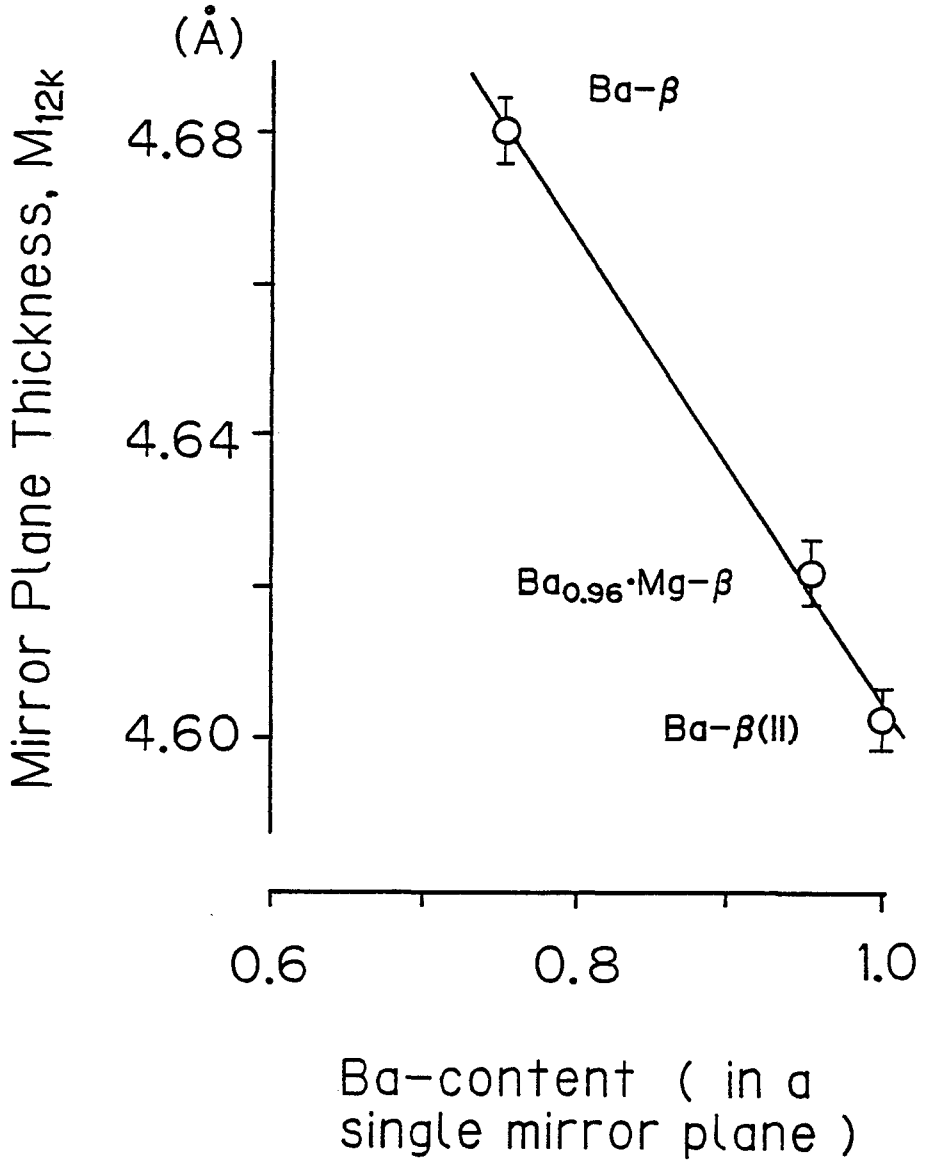

Fig.5-7. Relation between the mirror plane thickness M_{12k} and Ba-content in the Ba beta-alumina related compounds.

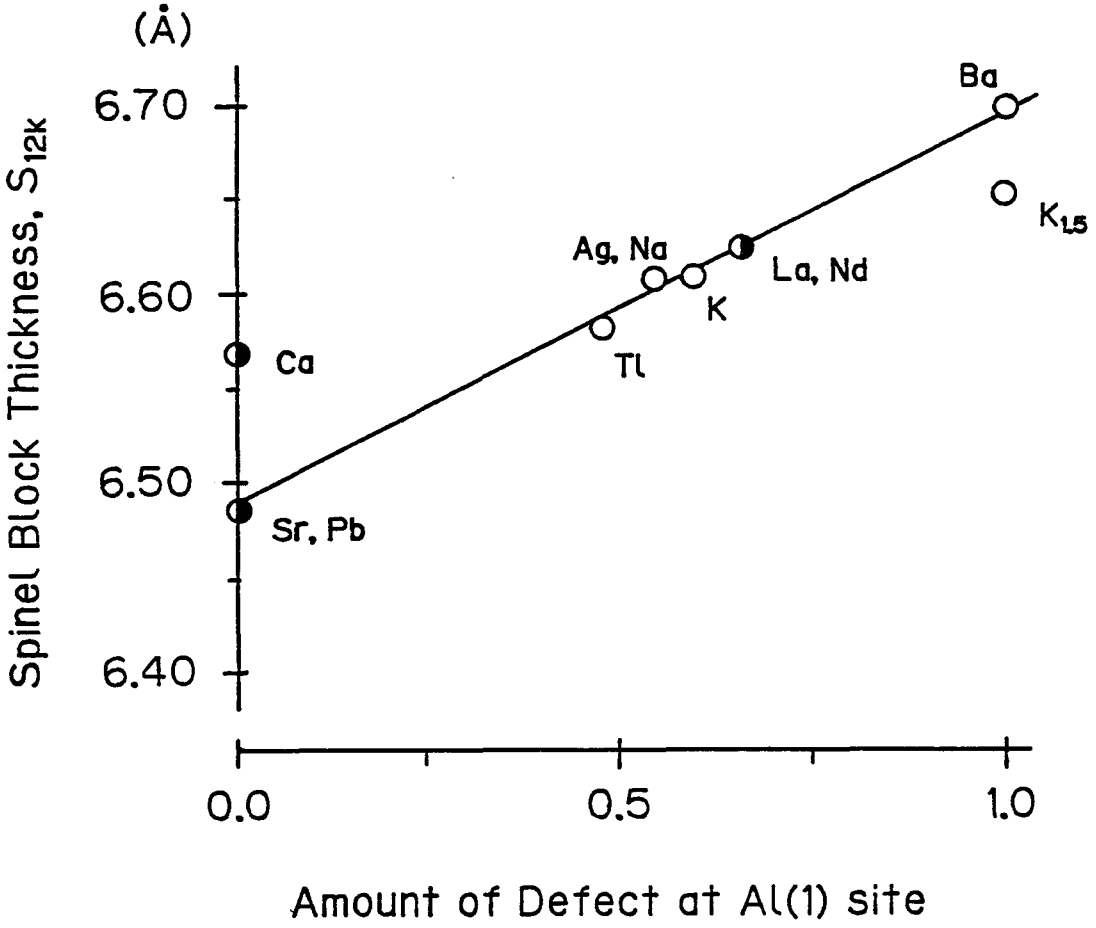

Fig.5-8. Change in the spinel block thickness S_{12k} as a function of the amount of defect in the Al(1) (12k) site. The number of defect is per unit cell.

6. SUMMARY

The crystal structure and defect mechanism of several hexaaluminates containing mono-, di-, trivalent cations in the mirror plane was analysed by using the X-ray single crystal diffraction data in order to clarify the effects of the large cations on the hexaaluminate structure and to explain their nonstoichiometric composition.

(1) The least-squares refinement of lanthanum hexaaluminate ($La_{0.827}Al_{11.9}O_{19.09}$) was accomplished using single crystal X-ray diffraction data. The result of the final anisotropic refinement, corresponding to an R-value of 0.039, revealed the structure of a magnetoplumbite type. In the structure interstitial Al ions were found, which were probably formed by the Frenkel defect mechanism. These interstitial Al ions were supposed to be situated in a pair making a bridge between spinel blocks while causing Al and La defects in the mirror plane(z=0.25). The nonstoichiometry of lanthanum hexaaluminate was attributed to these defects. By combination of perfect cells "$LaAl_{12}O_{19}$" and defect cells "$Al_{11}O_{19}$," the nonstoichiometric composition was explained well.(Section 2-2).

The structure of neodymium hexaaluminate was also revealed to be the same with that of lanthanum hexaaluminate. The final R-value was 0.044.(Section 2-3).

(2) The crystal structure of lead hexaaluminate ($PbAl_{12}O_{19}$) was analysed. It was revealed to have a typical magnetoplumbite structure. (Section 3-2).

The crystallographic relation between barium hexaaluminate phase I and phase II, which had been considered as the single compound "barium hexaaluminate ($BaAl_{12}O_{19}$)," was investigated using principally the

electron diffraction method. Phase I has a formula $Ba_{0.75}Al_{11.0}O_{17.25}$ and it was revealed to have a beta-alumina structure with space group $P6_3/mmc$. On the other hand, phase II ($Ba_{2.34}Al_{21.0}O_{33.84}$) exhibits an $a\sqrt{3}$ x $a\sqrt{3}$ superstructure. (Section 3-3).

The crystal structure of barium hexaaluminate phase I ($Ba_{0.75}Al_{11.0}O_{17.25}$) was determined by single crystal X-ray reflection data. The refinements were carried out by the least-squares method to give a final R-value of 0.023. The structure was revealed to be essentially of a beta-alumina type and the Ba ion was detected only at the 6h site near the BR site. The charge compensation for nonstoichiometry was found to be principally effectuated by the interstitial oxygen due to Frenkel defects of Al ions. The structure was supposed to be made of two types of cells; perfect cells "$BaAl_{11}O_{17}$" and defect cells "$OAl_{11}O_{17}$" in a 3:1 ratio. From structural point of view, phase I was referred to as "barium beta-alumina." (Section 3-4).

A refinement was performed on the average crystal structure of barium lead hexaaluminate phase II ($(Ba_{0.8}Pb_{0.2})_{2.34}Al_{21.0}O_{33.84}$) by using single crystal X-ray diffraction data, giving a final R-value of 0.030 with space group symmetry $P\bar{6}m2$. The structure is essentially of a beta-alumina type, but contains a lot of defects and interstitials. The phase II hexaaluminates were referred to as beta(II)-aluminas. Inside the spinel block were found Ba(Pb) ions at the 12-coordinated polyhedral sites, formed by the complex defects, including triple Reidinger defects, in the same unit cell. Barium lead hexaaluminate phase II was found to consist of two kinds of unit cells with formulae "$(BaPb)_{3.0}Al_{20.0}O_{35.0}$" and "$Ba_{2.0}Al_{22.0}O_{34.0}$" in a 1:2 ratio; these three cells combine to form $a\sqrt{3}$ x $a\sqrt{3}$ superstructure. Intergrowth between barium beta- and beta(II)-

alumina as well as "APB" of Barium beta(II)-alumina were interpreted by their structures. (Section 3-5).

The crystal structure and composition of Mg-doped barium hexaaluminate was also made clear. The final R-factor was 0.031. The structure was beta-alumina type. (Section 3-6).

(3) The ion exchange reactions of divalent Ba ions in barium beta-alumina and Mg-doped barium beta-alumina by monovalent cations were shown to occur in a manner that monovalent cations twice as many as Ba ions enter into the mirror plane. In this way, highly nonstoichiometric beta-aluminas containing monovalent cations were synthesized. (Section 4-2).

Crystal structure and cation distribution of highly nonstoichiometric potassium beta-alumina $K_{1.50}Al_{11.0}O_{17.25}$ have been studied by single crystal X-ray diffraction. The single crystal was obtained by the ion-exchange from barium beta-alumina ($Ba_{0.75}Al_{11.0}O_{17.25}$) and the least-squares refinement was accomplished with a final R-value of 0.029. The occupation of K ion in the mirror plane (z=0.25) was explained by assuming the three types of cells; singlet cell ($KAl_{11}O_{17}$), K-K-K triplet cell ($K_3Al_{11}O_{17}$), and K-K-Oi triplet cell ($K_2O{\cdot}Al_{11}O_{17}$) where Oi stands for interstitial oxygen. This model was shown to be applicable to the ordinary potassium beta-alumina($K_{1.30}Al_{11.0}O_{17.15}$). (Section 4-3).

The crystal structure of Mg-doped potassium beta-alumina $K_{1.875}Ba_{0.022}Mg_{0.919}Al_{10.081}O_{17.0}$($K_{1.875}$·Mg beta-alumina), obtained by ion exchange from $Ba_{0.955}Mg_{0.962}Al_{10.056}O_{17.0}$($Ba_{0.955}$·Mg beta-alumina), has been refined from single crystal X-ray data with a final R-value of 0.034. $K_{1.875}$·Mg beta-Alumina contains an extremely large number of K ions while retaining the fundamental beta-alumina structure and space group symmetry $P6_3/mmc$. The structure was found to be consistent with a

model composed of singly occupied cells containing a K ion at the BR site and triplet cells containing three K ions at the mO sites, as in the case of $K_{1+y}Mg_yAl_{11-y}O_{17}$ with y=0.62. The extra cations were assumed to be accommodated in the aBR sites created by clustering of three triplet cells. The occupancies of K ion sites calculated by this model agree well with those obtained by the refinement. The structure of $Ba_{0.955}$·Mg beta-alumina was also refined, yielding R=0.031. (Section 4-4).

Energy calculation was made to see the energy difference between doublet and triplet configurations. Preliminary estimation of the interaction between doublets and between triplets indicated the tendency of the cation arrangements changing into the triplet configuration as the amount of excess cations increases. (Section 4-5).

(4) It was made clear that the cations in the mirror plane have an important effect on the structure of the hexaalumintes. Four aspects of the structural effects were discussed: (a) The effect of ionic radii and charge on the structure type. (b) The effect of ionic radii on the mirror plane size. (c) The effect of the number of the cations on the mirror plane dimension. (d) The influence of Al defects in the spinel block on the spinel block size.

The cations with ionic radii lower than 1.1 A form neither beta-alumina nor related compounds. The cations with ionic radii larger than 1.33 A can not be accomodated in the magnetoplumbite structure due to steric hindrance. As the cation size increases, the beta-alumina structure is more favorable. For the cations with ionic radii between 1.1 and 1.33A, their valence and the number of defects are the important factors. The magnetoplumbite structure is more favorable as the cation charge increases.

The microstructural effects due to the ionic radii and population of cations in the mirror plane were investigated, using the concepts of "mirror plane thickness" and "spinel block thickness." The mirror plane thickness contracts according as the ionic radius of the cation decreases, and as the population of cation in the mirror plane increases. On the other hand, spinel block thickness increases according as the amount of the Frenkel defects increases.(Chapter 5).

(6) In conclusion, (a) as for the structural aspect, the structure type is determined by the ionic radii and charge of large cation in the mirror plane, and mirror plane size is varied due to the ionic radii and population of the cation, and, (b) as for the compositional aspect, the cause of the nonstoichiometry is essentially attributable to the Frenkel type defects of Al ions adjacent to the mirror plane, and the nonstoichiometric composition can be clearly explained by the structure model in which cells containing defects (defect cells) and cells without any defects (perfect cells) are considered as the components of hexaaluminates.

ACKNOWLEDGMENTS

The present author would like to express his sincere thanks to Professor F. Kanamaru, Osaka University, for his critical discussions and for his encouragement throughout this work. He also wishes to express his appreciation to Professors S. Ikeda, H. Suga, and S. Kawai, Osaka University, for their valuable suggestions.

The present research was conducted at National Institute for Research in Inorganic Materials (NIRIM), and the author owes much to several researchers there. He would like to thank Dr.S. Kimura for his pertinent advices and continuous encouragement. Acknowledgment is also due to Dr.Z. Inoue for his helpful advices in X-ray data collection and crystal structure analysis and for his encouragement. Thanks are also due to Mr.S. Takekawa for preparation of the several single crystals of good quality. He is indebted to Dr.Y. Bando and Mr.Y. Kitami for the several electron microscopic data, to Dr.F. Izumi for his suggestions on computer programming, to Dr.A. Ono for his advices in the EPMA measurements, and to Mrs. M. Kobayashi, Messrs.Y. Yajima, K. Kosuda, and S. Takenouchi for the chemical analysis of the specimens.

The author wishes to thank my colleagues, Drs.I. Shindo, K. Kitamura, T. Sawada, and Messrs. S. Homma, E. Bannai for their continuous encouragement and insights.

REFERENCES

Anderson,M.P., L.M.Foster, and S.J.LaPlaca, Solid State Ionics 5, 211 (1981).

Bando,Y., private communication (1984).

Bartels,G., D.Mateika, and J.M.Robertson, J. Cryst. Growth 47, 414 (1979).

Bauer,W.H., in "Structure and Bonding in Crystals. Vol.II.",(M.O'Keeffe and A.Navrotsky eds.) pp.31-52, Academic Press, New York (1981).

Becker,P.J., and P.Coppens, Acta Crystallogr. Sect.A30, 148 (1974).

van Berkel,F.P.F., H.W.Zandbergen, G.C.Vershoor, and D.J.W.Ijdo, Acta Crystallogr. C40, 1124 (1984).

Boilot,J.P., Ph.Colomban, G.Collin, and R.Comes, J.Phys. Chem. Solids. 41, 47 (1980).

Boilot,J.P., G.Collin, Ph.Colomban, and R.Comes, Solid State Ionics, 5, 157 (1981).

Bourke,M.A.M., A.Hooper, P.T.Moseley, and R.G.Taylor, Solid State Ionics, 1, 367 (1980).

Brown,I.D., in "Structure and Bonding in Crystals. Vol.II.",(M.O'Keeffe and A.Navrotsky eds.) pp.1-30, Academic Press, New York (1981).

Busing,W.R., and H.A.Levy, Acta Crystallogr. 10, 180 (1957).

Busing,W.R., Trans. Am. Crystallogr. Assoc., 6, 57 (1970).

Catti,M., Acta Crystallogr. Sect. A34, 974 (1978).

Collin,G., J.P.Boilot, A.Kahn, J.Thery, and R.Comes, J.Solid State Chem. 21, 283 (1977).

Collin,G., R.Comes, J.P.Boilot, and Ph.Colomban, Solid State Ionics,

1, 59 (1980).

Collin,G., Ph.Colomban, J.P.Boilot, and R.Comes, in "Fast ion transport in solids" (P.Vashista, J.N.Mundy and G.K.Shenoy, Eds.), p.309, North-Holland, Amsterdam (1979).

Comer,J.J., W.J.Croft, M.Kestigian, and J.R.Carter, Mat. Res. Bull. 2, 293 (1967).

Coppens,P., and W.C.Hamilton, Acta Crystallogr. Sect.A26, 71 (1970).

Coutures, J.P., J. Am. Ceram. Soc., 68 105 (1985).

Dernier,P.D., and J.P.Remeika, J.Solid State Chem. 17, 245 (1976).

Dexpert-Ghys,J., M.Faucher, and P.Caro, J. Solid State Chem. 41, 27 (1982).

Dexpert-Ghys,J., M.Faucher, and P.Caro, J. Solid State Chem. 19, 193 (1976).

Dienes,G.J., J. Chem. Phys. 16, 620 (1948).

Dubin,R.R., H.S.Story, R.W.Powers, and W.C.Bailey, Mat. Res. Bull. 14, 185 (1979).

Dyson,D.J., and W.Johnson, Trans. J. Brit. Ceram. Soc. 72, 49 (1973).

England,W.A., A.J.Jacobson, and B.C.Tofield, Solid State Ionics, 6, 21 (1982).

Fritsche,E.T., and L.G.Tensmeyer, J. Amer. Ceram. Soc. 50, 167 (1967).

Gasperin,M., M.C.Saine, A.Kahn, F.Laville, and A.M.Lejus, J. Solid State Chem. 54, 64 (1984).

Gilbert,T.L., J. Chem. Phys. 49, 2640 (1968).

Haberey,F., G.Oehlschlegel, and K.Sahl, Ber. Dt. Keram. Ges. 54, 373 (1977).

Ingram,M.D., and C.T.Moynihan, Solid State Ionics, 6, 303 (1982).

Iyi,N., and I.Shindo, J. Cryst. Growth 46, 569 (1979).

Iyi,N., S.Takekawa, Y.Bando, and S.Kimura, J.Solid State Chem. 47, 34 (1983).

Iyi,N., Z.Inoue, S.Takekawa, and S.Kimura, J.Solid State Chem. 52, 66 (1984a).

Iyi,N., Z.Inoue, S.Takekawa, and S.Kimura, J. Solid State Chem. 54, 70 (1984b).

Iyi,N., Z.Inoue, and S.Kimura, J.Solid State Chem. 54, 123 (1984c).

Iyi,N., S.Takekawa, and S.Kimura, J. Solid State Chem. 59, 250 (1985a).

Iyi,N., Z.Inoue, S.Takekawa, and S.Kimura, J. Solid State Chem. 60, 41 (1985b).

Iyi,N., Z.Inoue, and S.Kimura, J. Solid State Chem. 61, 81 (1986a).

Iyi,N., Z.Inoue, and S.Kimura, J. Solid State Chem. 61, 236 (1986b).

Jantzen, C.M., and R.R.Neurgaonkar, Mat. Res. Bull. 16, 519 (1981).

Kahn,A., A.M.Lejus, M.Madsac, J.Thery, D.Vivien, and J.C.Bernier, J.Appl. Phys. 52, 6864 (1981).

Kato,K., and H.Saalfeld, N. Jb. Miner. Abh. 109, 192 (1968).

Kitamura,K., S.Kimura, and K.Watanabe, J. Cryst. Growth 47, 475 (1982).

Kittel,C., "Introduction to Solid State Physics. 2nd.ed." John Wiley & Sons, Inc. New York (1956).

Kimura,S., E.Bannai, and I.Shindo, Mat. Res. Bull. 17, 209 (1982).

Kimura,S., in " Research Report of NIRIM. 37 ", pp.12-13, NIRIM (1983).

Kodama,K., and G.Muto, J.Solid State Chem. 17, 61 (1976a).

Kodama,K., and G.Muto, J.Solid State Chem. 17, 245 (1976b).

Kummer,J.T. in "Progress in Solid State Chemistry. Vol.7", (Reiss and McCaldin Eds.) p.141, Pergamon Press, New York (1972).

Liebertz,J., Zeit. fur Kristallogr. 166, 297 (1984).

Lindop,A.J., C.Matthews, and D.W.Goodwin, Acta Crystallogr. Sect. B31,

2940 (1975).

Mateika,D., and H.Lauden, J. Cryst. Growth 46, 85 (1979).

McWhan,D.B., P.D.Dernier, C.Vettier, A.S.Cooper, and J.P.Remeika, Phy. Rev. B 17 (1978).

Mizuno,M., R.Berjoan, J.P.Coutures, and M.Foex, Yogyo Kyokaishi 82, 631 (1974).

Mizuno,M., R.Berjoan, J.P.Coutures, and M.Foex, Yogyo Kyokaishi 83, 50 (1975).

Mizuno,M., T.Yamada, and T.Noguchi, Yogyo Kyokaishi 85, 91, (1977a).

Mizuno,M., T.Yamada, and T.Noguchi, Yogyo Kyokaishi 85, 374, (1977b).

Morgan,P.E.D., and E.H.Cirlin, J. Am. Ceram. Soc. 65, C114 (1982).

Morgan,P.E.D., and T.M.Shaw, Mat. Res. Bull. 18, 539 (1983).

Newsam,J.M., and B.C.Tofield, J.Phys. C: Solid State Phys., 14, 1545 (1981a).

Newsam,J.M., and B.C.Tofield, Solid State Ionics 5, 59 (1981b).

Newsam,J.M., Solid State Ionics, 6, 129 (1982).

Obradors,X., A.Collomb, M.Pernet, D.Samaras, and J.C.Joubert, J. Solid State Chem. 56, 171 (1985).

Pauling,L., "The Nature of the Chemical Bond," 3rd ed., Cornell Univ. Press, Ithaca, New York (1960).

Peters,C.R., M.Bettman, J.W.Moore, and M.D.Glick, Acta Crystallogr. Sect. B 27, 1826 (1971).

Reidinger,F., Ph.D. Thesis (1979) cited by Roth et al.(1977).

Rolin,M., and P.H.Thanh, Rev. Int. Hautes Temp. Refract. 2, 175 (1965).

Ropp,R.C., and G.G.Libowitz, J. Amer. Ceram. Soc. 61, 11 (1978).

Roth,R.S., and S.Hasko, J. Amer. Ceram. Soc. 41, 146 (1958).

Roth,W.L., Trans. Am. Cryst. Assoc. 11, 51 (1975).

Roth,W.L., J. Solid State Chem. 4, 60 (1972).

Roth,W.L., F.Reidinger, and S.LaPlaca, in "Superionic Conductors" (G.D.Mahan and W.L.Roth, Eds.), p.223, Plenum, New York (1977).

Sakurai,T., K.Nakatsu, H.Iwasaki, and M.Fukuhara, RSFLS-4, UNICS II. The Crystallographic Society of Japan (1967).

Sakurai,T., RSSFR-5, UNICS II. The Crystallographic Society of Japan (1967).

Shannon,R.D., and C.T.Prewitt, Acta Crystallogr. Sect.B 25, 925 (1969).

Shannon,R.D., Acta Crystallogr. Sect.A 32, 751 (1976).

Shindo,I., J. Cryst. Growth 50, 839 (1980).

Stevels, A.L.N., and A.D.M.Schrama-de-Pauw, J. Electrochem. Soc. 123, 691 (1976).

Stevels,A.L.N., and J.M.P.J.Verstegen, J. Lumin. 14, 207 (1976).

Stevels,A.L.N., J. Lumin. 17 121 (1978).

Takano,Y., " Classification of Twins ", p.57, Kokon Shoin, Tokyo (1973).

Takekawa,S., in " Research Report of NIRIM. 37 ", pp.15 - 17, NIRIM (1983).

Takekawa,S., unpublished data (1984).

Tessman,J., K.Kahn, and W.Schockley, Phys. Rev. 92, 890 (1953).

Toropov,N.A., Dokl. Akad. Nauk SSSR 6, 147 (1935).

Toropov,N.A., M.M.Stukalova, C.R.Acad.Sci.SSSR. 24, 459 (1939).

Toropov,N.A., M.M.Stukalova, C.R.Acad.Sci.SSSR. 27, 974 (1940).

Toropov,N.A., V.P.Barzakovskii, V.V.Lapin, and N.N.Kurtseva, " Handbook of Phase Diagrams of Silicate Systems," Vol.1, 2nd ed., Jerusalem (1972).

Verstegen,J.M.P.J., and A.L.N.Stevels, J. Lumin. 9, 406 (1974).

Wagner,T., and M.O'Keeffe, Acta Crystallogr. Sect.B41, 108 (1985).

Wang,J.C., M.Gaffari, and S.Choi, J.Chem. Phys. 63,772 (1975).

Wang,J.C., J. Chem. Phys. 73, 5786 (1980).

West,A.R., Mat. Res. Bull. 14, 441 (1979).

Williams,D., Acta Crystallogr. Sect.A27, 452 (1971).

Wolf,D., J. Phys. Chem. Solids, 40, 757 (1979).

Wycoff,R.W.G., "Crystal Structures," 2nd ed., Vol.3, p.497, Wiley-Interscience, New York (1965).

Yajima,Y., unpublished data.

Yamaguchi,G., and K.Suzuki, Bull. Chem. Soc. Japan 41, 93 (1968).

Yamamoto,N., and M.O'Keeffe, Acta Crystallogr. Sect.B40, 21 (1984).

Yao,Y.F.Y., and J.T.Kummer, J.Inorg.Nucl.Chem. 29, 2453 (1967).

Yuen,P.S., R.R.Murfitt, and R.L.Collin, J. Chem. Phys. 61 2383 (1974).

Yuen,P.S., M.W.Lister, and S.C.Nyburg, J. Chem. Phys. 68, 1936 (1978).

Zandbergen,H.W., F.C.Mijlhoff, D.J.W.Ijdo, and G.van Tendeloo, Mat. Res. Bull. 19, 1443 (1984).